

Consequences of ocean change for ecological function:
Observational and modeling case studies of larval echinoderms

Kit Yu Karen Chan

A dissertation

submitted in partial fulfillment of the
requirements for the degree of
Doctor of Philosophy

University of Washington

2012

Reading Committee:

Daniel Grünbaum, Chair

Evelyn J. Lessard

Richard R. Strathmann

Program Authorized to Offer Degree

Oceanography

University of Washington

Abstract

Consequences of ocean change for ecological function:

Observational and modeling case studies of larval echinoderms

Kit Yu Karen Chan

Chair of the Supervisory Committee:

Professor Daniel Grünbaum

School of Oceanography

Planktonic larvae of many marine invertebrates play important roles in connecting and sustaining disjunct adult populations. Most larvae are denser than seawater and rely on swimming to regulate their vertical positions. Because environmental variables including direction and strength of advective currents and prey and predator concentrations vary with depth, larval swimming behaviors can significantly impact larval survival and transport. Quantification of larval movement is therefore essential for understanding population dynamics, especially in the face of global climate change because of the need to predict possible shifts in ecosystems.

Larval swimming is physically constrained by their morphologies, which are often complex and highly variable. Behavioral responses to surrounding environmental variables modulate the actual swimming performance within physical limits. This study took a two-pronged approach to understand

larval swimming through 1) quantifying larval behaviors under changing environmental conditions and 2) modeling larval morphology-flow interactions.

This study applied novel non-invasive video motion analysis techniques to quantify effects of environmental variations. Ocean acidification is considered one of the major threats to marine ecosystems and larvae are suggested to be particularly vulnerable. When reared under elevated pCO₂ level, larval sand dollars *Dendraster excentricus* maintained their swimming performance but had lower feeding success. By combining feeding and respiration experiments with motion analysis, we observed similar tradeoffs among larval purple urchins, *Strongylocentrotus purpuratus*, and heart urchins, *Brissopsis lyrifera*. These two echinoids also underwent budding under acidified conditions, an asexual reproduction strategy that has not been previously reported. These results suggest that sublethal OA impacts could be carried over from planktonic stages to later development stages and affect population dynamics.

Previous studies suggest that larval swimming performance peaks within a tight morphospace. Larval sand dollars are phenotypically plastic and develop longer arms when starved. Starved individuals swam with higher oscillatory speeds than their fed counterpart. To distinguish the biomechanical constraints associated with morphological changes from behavioral adjustments, we developed a detailed 3-dimensional model of individual larvae using laser confocal microscopy and finite-element mesh generation. This novel modeling approach can easily be adapted for other taxa to help understand constraints that swimming imposes on the evolution of larval form.

TABLE OF CONTENTS

	Page
List of Figures	iii
List of Tables	v
Chapter 1: Biomechanics of larval morphology affect swimming: insights from the sand dollars, <i>Dendraster excentricus</i>	
1.1 Abstract	1
1.2 Larval swimming significantly impacts dispersal	2
1.3 Larval sand dollars as a model system for larval swimming	4
1.4 Hydrodynamic considerations when defining swimming performance	4
1.5 Larval morphology biomechanically constrains swimming	6
1.6 Modeling larval swimming in flow	8
1.7 Behavioral changes modulate swimming performance	9
1.8 Functional consequences of morphological variations: a case study in ocean acidification	10
1.9 Future directions for the study of mechanics of swimming and behaviors	13
Chapter 2: Temperature and diet modified larval swimming behaviors of the sand dollar, <i>Dendraster excentricus</i>	
2.1 Abstract	22
2.2 Introduction	23
2.3 Materials and Methods	25
2.4 Results	30
2.5 Discussion	31
Chapter 3: Effects of ocean acidification-induced morphological changes on larval swimming and feeding	
3.1 Abstract	44
3.2 Introduction	45
3.3 Materials and Methods	48
3.4 Results	53
3.5 Discussion	56

Chapter 4: Ocean acidification impacts physiological and behavioral performance of larval echinoderms	
4.1 Abstract	74
4.2 Introduction	75
4.3 Materials and Methods	78
4.4 Results	83
4.5 Discussion	87
Chapter 5: Advances in biomechanical analysis of functional morphology in planktonic larvae: a case study of starved and fed larval sand dollars	
5.1 Summary	103
5.2 Introduction	104
5.3 Materials and Methods	106
5.4 Model parameterization	109
5.5 Observational results and discussion	110
5.6 Modeling results and discussion	111
5.7 Conclusions	114
Chapter 6: Interdisciplinary guided inquiry on estuarine transport using a computer model in high school classrooms.	
6.1 Abstract	126
6.2 Project motivation	126
6.3 Module development and details	127
6.4 Module Evaluation	129
6.5 Results	130
6.6 Discussion	132
Bibliography	142

LIST OF FIGURES

Figure Number		Page
Figure 1.1	Survey of the number of articles in the Web of Science database with a title or abstract containing the phrase “marine larval dispersal model” and “swimming behaviors”	15
Figure 1.2	Schematic drawings illustrating larval movement in vertical shear	16
Figure 1.3	Schematic drawings illustrating two proposed physical mechanisms whereby larvae maintain stability	17
Figure 1.4	Vertical velocities of model larvae with different relative arm lengths, with the postoral arm representing 0.1 to 1.9 of total arm length (a) in still water and (b) in vertical shear	18
Figure 1.5	Procrustes superimpositions of the landmark coordinates of the present-day and acidified treatments suggest a change in overall shape	19
Figure 1.6	Trajectory of model larva in still water over 40 seconds	20
Figure 2.1	Morphometric characteristics of echinopluteus larva	37
Figure 2.2	Representative larval swimming trajectories at 20 and 12°C extracted from 6 min video clips of 4-arm larvae raised on <i>Dunaliella tertiolecta</i>	38
Figure 2.3	Swimming metrics of 4- and 8-arm larvae	39
Figure 2.4	PCA Axes 2 and 3 scores plotted against PCA Axis 1 scores	40
Figure 3.1	Representative larval swimming trajectories under acidified and present-day conditions from 3 min video clips of 8-arm larvae	63
Figure 3.2	Representative individuals from acidified and present-day treatments at 4-, 6- and 8- arm stage	64
Figure 3.3	Swimming metrics (means \pm SE) of larvae in acidified and present-day treatments at 4-, 6- and 8-arm stages	65
Figure 4.1	Micrographs of the representative larvae reared under present-day and elevated pCO ₂ levels.	93
Figure 4.2	Larval density (percentage of the initial density) over time for <i>Amphiura filiformis</i> , <i>Brissopsis lyrifera</i> and <i>Stronglyocentrotus purpuratus</i>	94
Figure 4.3	Ingestion rates of larval <i>Amphiura filiformis</i> , <i>Brissopsis lyrifera</i> , and <i>Stronglyocentrotus purpuratus</i> .	95
Figure 4.4	Oxygen consumption rates of larval <i>Amphiura filiformis</i> , <i>Brissopsis lyrifera</i> , and <i>Stronglyocentrotus purpuratus</i> .	96

Figure 4.5	Swimming metrics (means \pm SE) of larval echinoderms under control and elevated pCO ₂ treatments	97
Figure 5.1	Micrographs and swimming metrics of larval sand dollars in the two food treatments	114
Figure 5.2	Laser confocal micrographs of 8-arm larval sand dollar	115
Figure 5.3	Steps in extracting tissue outline based on confocal micrographs	116
Figure 5.4	Defining geometric elements for meshing using smoothing splines	117
Figure 5.5	Results of the finite element mesh generation for fed and starved larvae	118
Figure 5.6	Model representation of larval skeleton	119
Figure 5.7	Sequence of positions of model larva passively sinking in still water	120
Figure 5.8	Sequence of positions of model larva passively sinking in vertical shear	121
Figure 6.1	Physical model of an estuary	135
Figure 6.2	Key concepts introduced during the mini lecture	136
Figure 6.3	Computer model of an estuary	137
Figure 6.4	Examples of students' work on guided inquiry worksheets	138
Figure 6.5	Example of assessment questions	139
Figure 6.6	Students' learning gain	140

LIST OF TABLES

Table Number		Page
Table 1.1	Comparison of mid-line body and postoral arm length of four-arm larval sand dollars	21
Table 2.1	Means and standard errors of measured morphometrics in microns of 4- and 8-arm <i>Dendraster excentricus</i> larvae	41
Table 2.2	Summary of PCA and parallel analysis results	42
Table 2.3	Two-way ANOVA table for the effects of temperature and diet on PCA Axes 1-3 scores	43
Table 3.1	Morphometrics of 4-, 6- and 8-arm larval sand dollars	68
Table 3.2	Effects of OA on larval morphologies for 4-, 6- and 8-arm larval sand dollars	70
Table 3.3	Swimming metrics (means \pm SE) of 4-arm larvae reared under present-day conditions exposed to short-term change in ambient CO ₂	71
Table 3.4	Effects of CO ₂ , maternal lineage on swimming metrics	72
Table 4.1	Carbonate system speciation in the experimental treatments	98
Table 4.2	Linear Regression of larval density over time	99
Table 4.3	Analysis of covariance (ANCOVA) for larval density with pH as fixed factor and larval age as covariate	100
Table 4.4	Analysis of covariance (ANCOVA) of swimming metrics for larval <i>Amphiura filiformis</i> , <i>Brissopsis lyrifera</i> and <i>Strongylocentrotus purpuratus</i>	101
Table 5.1	2-way ANOVA on the effects of maternal lineages and food treatments on swimming metrics of larval sand dollars	122
Table 5.2	Parameters of larval skeleton used in the hydrodynamic model	123
Table 5.3	Morphometric measurements of starved and fed larval sand dollars	124
Table 6.1	List of National and Washington State Science Education Standards met by the estuary model module	141

ACKNOWLEDGEMENTS

First and foremost, I would like to thank my advisor Dr. Daniel Grünbaum for his guidance and support. Danny said graduate school is a place where one transforms into a true scientist. I am very grateful that he had faith in me and encouraged me throughout this long transformation process. Not only did my years in the Grünbaum lab change my thinking towards science, Danny has also inspired me outside of work including the use of duct tape, hot glue guns, and Dremels. I am extremely thankful to all of my committee members. Richard Strathmann not only has a wealth of knowledge on larval biology but is also the most approachable and supportive scientist I have ever met. When I lost sight of my research motivation, Richard's enthusiasm helped me see the big picture and kept me going. Evelyn Lessard taught me the true meaning of protists and generously made available her lab space and equipment. Carolyn Freidman took me into her lab group and introduced me to the world of shellfish growers and diseases. Julie Keister not only helped me better appreciate the biophysical interactions between the environment and zooplankton. She also shared valuable insights in teaching oceanography field courses. Rick Keil always brought interesting perspectives into very biologically-focused discussion during committee meetings. Rick also threw the best train and cookies parties for the holidays. Thank you to all the members of this "Super-super PAC".

Jody Bourgeois was an exceptional mentor outside oceanography. Gabrielle Rocard, Becca Price, Martha Groom, Sara Lindsay, Mark Warner, Steve Emersson, Jody Deming, Kathy Newell, Mary Pat Wenderoth, Karen Fresiman all contributed towards improving my teaching. I had the pleasure of taking and TA-ing the larval biology course in the Friday Harbor Labs. I thank the co-instructors Richard Strathmann, Danny Grünbaum, and Richard Emlet, and all the students for the incredible experience.

My research would not been possible without my resourceful and generous collaborators. Thank you, Sam Dupont and Michael Thorndyke for opening the door to the Sven Lovén Center for Marine

Sciences in Sweden. Michael O'Donnell taught me valuable lessons in ocean acidification, Ceri Lewis in fertilization ecology, Michael Brett in fatty acid analysis, and Colleen Durkin in diatoms. Both the Lovén Center and Friday Harbor Labs are supported by fabulous staff to whom I am very thankful. I also need to thank the amazing support I received from the staff of UW Oceanography, especially Megan Schatz, Mike Foy, Dave Thoreson, Tor Bjorklund, Randy Fabro, and Shelly Carpenter. I am also very lucky to have worked alongside intelligent and kind graduate students and postdocs, Tansy Clay, Owen Coyle, Mike Nish, Elizabeth Tobin, Marcela Ewerts, Sylvia Yang, and Raechel Waters.

Friends and family are my rock. I am extremely fortunate that the Beardsleys took me in as a member of their family, giving me a home away from home. Sarah Silvia, I am lucky to have you as my housemate. Members of the Flamenco Gitana studio and the Seattle Aquarium birds and mammal team kept me connected with the real-world outside academia. I am also grateful for friends who walked beside me. With the exception of Evelyne Kuo and Kevin Kwok, these friends are not scientists. Many of them live in Hong Kong and had accommodated the time difference. In particular, I want to thank Alfred Tse who always cheers me up and deserves a special mention for he was “brave” and kind enough to visit me during the thesis writing craze.

Last but not least, I need to thank my supportive and loving family. Being the youngest in the extended family, it has been incredible to have a village rallying behind me throughout graduate school. Though my parents may not fully comprehend my research nor will I learn how to explain larval biology in Cantonese, they have been my best champions. I love you mom and dad.

“How lucky I am to have something that makes saying goodbye so hard.”

— A.A. Mile, Winnie-the-Pooh

DEDICATION

給最疼我的爸爸媽媽和在天上的三舅父

For my loving parents and Uncle Tim

CHAPTER ONE: BIOMECHANICS OF LARVAL MORPHOLOGY AFFECT SWIMMING: INSIGHTS FROM THE SAND DOLLARS, *DENDRASTER EXCENTRICUS**

1.1 Abstract

Most planktonic larvae of marine invertebrates are denser than sea water, and rely on swimming to locate food, navigate advective currents, and avoid predators. Therefore, swimming behaviors play important roles in larval survival and dispersal. Larval bodies are often complex and highly variable across developmental stages and environmental conditions. These complex morphologies reflect compromises among multiple evolutionary pressures, including maintaining the ability to swim. Here, I highlight metrics of swimming performance, their relationships with morphology, and the roles of behavior in modulating larval swimming within biomechanical limits. Sand dollars have a representative larval morphology using long ciliated projections for swimming and feeding. Observed larval sand dollars fell within a narrow range of key morphological parameters that maximized their abilities to maintain directed upward movement over the most diverse flow fields, outperforming hypothetical alternatives in a numerical model. Ontogenetic changes in larval morphology also led to different vertical movements in simulated flow fields, implying stage-dependent vertical distributions and lateral transport. These model outcomes suggest a tight coupling between larval morphology and swimming. Environmental stressors, such as changes in temperature and pH, can therefore affect larval swimming through short-term behavioral adjustments and long-term changes in morphology. Larval sand dollars reared under elevated pCO₂ conditions had significantly different morphology, but not swimming speeds or trajectories. Geometric morphometric analysis showed a pH-dependent, size-mediated change in shape, suggesting a coordinated morphological adjustment to maintain swimming performance under acidified conditions. Quantification of the biomechanics and behavioral aspects of swimming improves predictions of larval survival and dispersal under present-day and future environmental conditions.

* Originally published in Integrative and Comparative Biology in August 2012, Volume 52, Issue 4

1.2 Larval swimming significantly impacts dispersal

Many marine invertebrates have adult life stages with limited mobility but disperse extensively as planktonic larvae (Cowen & Sponaugle, 2009). Larval transport and connectivity have been of increasing interest as a basis for formulating sound strategies for conservation and management, for example in understanding the spread of invasive species and for designing marine protected areas (Levin, 2006). Planktonic larvae were once assumed to undergo transport similar to that of passive particles. However, evidence suggests that larvae are retained near natal locations more often than would be expected for passive particles (Shanks, 2009). Larval behaviors are suggested to play important roles in causing this retention, and in modulating other aspects of dispersal (McManus & Woodson, 2012, Metaxas & Saunders, 2009).

Larval behaviors during selection of settlement sites have long been subjects of intense research (Young, 1990). Roles of various environmental (e.g., turbulence, presence of conspecific adults, prey items) and physiological (e.g., larval age) factors that affect larval choices of settlement sites are well-described (Botello & Krug, 2006, Hadfield *et al.*, 2006, Koehl, 2007). In contrast, pre-settlement behaviors in the plankton are less well-studied.

Most marine invertebrate larvae are denser than seawater and rely on swimming to regulate their vertical positions in the water column. Because environmental variables such as food concentration and advective currents are often vertically structured in nature, adjustments in vertical positions can significantly impact larval growth, survival, and dispersal (Fiksen *et al.*, 2007). Recent observations highlighted larval sensory abilities and documented behavioral responses to a wide array of environmental variables, e.g. food patches (Metaxas & Young, 1998), haloclines (Sameoto & Metaxas, 2008), and turbulence (Fuchs *et al.*, 2004). These behavioral responses can affect larval growth and survival by enabling larvae to avoid predators, and to locate food or warmer water masses (Naylor, 2006). The roles of larval behaviors in selective tidal transport in estuaries have been extensively studied (Forward & Tankersley, 2001). In addition to selective transport by temporally varying currents, like

flood and ebb tides, larval swimming can affect lateral transport wherever advective currents vary with depth. By including simple behavioral responses to the presence of a halocline in a bio-physically coupled model, North et al. (2008) demonstrated that swimming speeds of oyster veligers, though orders of magnitude smaller than the spatial scale of advective currents, significantly impacted dispersal distance, recruitment success, and exchange of individuals between populations within Chesapeake Bay. Therefore, incorporating realistic larval behaviors can significantly improve the accuracy of predictions of dispersal models.

High-resolution General Circulation Models (GCMs), like that in the study by North et al. (2008), have become increasingly important predictive tools in larval dispersal studies (Fig. 1.1). However, to date, most bio-physically coupled models exclude larval behaviors and include larvae as passive particles at the surface. For studies that include “swimming behaviors”, behaviors are often modeled as ontogenetic variations in the depth where larvae are found. Swimming statistics e.g., speeds and turning rate based on actual observations are rarely incorporated, particularly for weakly swimming larvae (see Broekhuizen *et al.*, 2011, Fisher, 2005 for examples on larval fishes). With recent improvements in physical and chemical dynamics in GCMs (Blackford *et al.*, 2010), remaining sources of error have greater impacts on the accuracy and efficiency of predicting patterns of dispersal. Lack of quantitative data about larval behaviors is one of these remaining sources of error. Therefore, there is a need to gather such information and to integrate behavioral ecology with oceanography to predict changes in structures of population and community.

Here, building upon the premise that larval swimming behaviors significantly impact dispersal (see reviews by Metaxas, 2001, Woodson and McManus, 2007), I focus on the roles of biomechanics and behaviors in shaping larval swimming, discuss some ecological and evolutionary implications, and highlight future directions of research on larval biomechanics and behaviors.

1.3 Larval sand dollars as a model system for larval swimming

The larval sand dollar, *Dendraster excentricus*, is a good model system for studying the relationships between larval morphology, behaviors, and swimming performance for several reasons. First, larval sand dollars propel themselves with ciliated bands (Strathmann, 1975). Ciliary swimming is a widespread propulsive mechanism among early life stages of marine invertebrates, including hemichordates, echinoids, molluscs and annelids (Chia *et al.*, 1984). However, when compared to other propulsive mechanisms used by larvae, such as muscular swimming in larval fish (Liao, 2007), cnidarians (Nawroth *et al.*, 2010), ascidians (McHenry *et al.*, 2003), and appendicular motion in larval crustaceans (Ford *et al.*, 2005), the hydrodynamics of larval ciliary motion is poorly studied.

Second, larval sand dollars represent two common larval morphologies – spheroidal in the early embryonic stages and the “armed morphology” in later pluteus stages. Swimming blastulae and gastrulae of many marine invertebrates are often spheroidal. Some taxa also have later stages that are spheroidal, e.g. trochophore larvae of annelids and molluscs, non-feeding larvae of echinoids. The pluteus larvae of sand dollars possess long, ciliated extensions used both for swimming and feeding. This larval form is referred as the “armed morphology” (Grünbaum & Strathmann, 2003). This morphology is also observed among the actinotroch larvae of phoronid worms, the feeding larvae of brachiopods, some larval gastropods, and some larval annelids. In addition to having a representative propulsive mechanism and morphology, larval sand dollars are easily cultured such that their growth and developmental ecology are well-described.

1.4 Hydrodynamic considerations when defining swimming performance

Quantitatively assessing the role of swimming in larval dispersal requires relevant metrics of performance. The most intuitive metric of swimming performance is perhaps swimming speed. However, the swimming trajectories of many planktonic organisms are non-linear and often are indicative of behavioral responses to environmental conditions, e.g. the tumbling of heterotrophic dinoflagellates in food patches (Bartumeus *et al.*, 2003). Turning angles and frequencies are examples of parameters that

can be used to describe the shape of non-linear trajectories. These statistics on individual movement collected in the laboratory can be used to parameterize advection-diffusion models that predict population distributions in the field (Menden-Deuer, 2008).

While speed is one metric of performance, the ability to maintain directed movement i.e., stability in flow is another. For example, in strata with strong hydrodynamic shear (i.e., where horizontal current velocities vary rapidly with depth), upwardly swimming phytoplankton can lose stability, start tumbling, and become “trapped” at a particular depth stratum with a critical shear level (Durham *et al.*, 2009). Directed movements of larvae have also been observed to be disrupted by shearing flow (Strathmann & Grünbaum, 2006). Vertical shearing flows i.e., a horizontal gradient of vertical flow, can tilt larvae, causing a component of what would otherwise be vertical velocity to be directed horizontally (Fig. 1.2). This redirected velocity can result in horizontal transport towards downwelling or upwelling water. When entrained by such downwelling or upwelling currents, individuals have net vertical velocities greatly exceeding those of swimming alone. Interactions between flow and larval swimming highlight the importance of studying larval swimming under diverse, realistic conditions of flow.

Despite the importance of maintaining stability, many planktonic larvae lack gravity-sensing organs such as statoliths and hence cannot actively regulate their orientation. However, there are two ways through which larvae can restore their default upward-pointing orientation passively. These physical models are referred to as the buoyancy-gravity model and the drag-gravity model (Mogami *et al.*, 2001). In the buoyancy-gravity model the center of mass (center of gravity) and the centroid of the organism (center of buoyancy) do not coincide (Fig. 1.3). The separation of these centers can be a result of heterogeneity in internal density. When the organism tilts, the centers of gravity and buoyancy are not aligned vertically, resulting in an orienting torque that returns the organism to its upright position (Machemer & Braucker, 1992). Many invertebrate larvae have this characteristic because they possess calcified structures that differ in density from the rest of their body tissues. Examples of calcified structures include shells of molluscan veligers, skeletal rods of echinoplutei, and posterior ossicles of

auricularia. Consistent with the prediction of this model, experimental removal of larval skeletons of echinoplutei compromised the ability of sinking larvae to reorient themselves with arms pointing upwards (Pennington & Strathmann, 1990).

In the drag-gravity model, the geometric asymmetry in body plan shifts the center of hydrodynamic force away from the center of gravity (Fig. 1.3). In an environment with low Reynolds' number, the thicker end of an individual with front-rear asymmetry sinks faster than the thinner end. This difference in sinking forces helps to create a righting moment to restore the tilted organism to its original position (Roberts, 1970). For invertebrate larvae that usually have some intrinsic asymmetry in density and geometry, both physical models are likely to be operative in generating the torque that reorients organisms.

1.5 Larval morphology biomechanically constrains swimming

Given the importance of swimming to larval survival in the plankton, maintaining swimming performance could constrain the evolution of larval morphology. If so, the observed complex and variable morphology would reflect the biomechanical requirements that swimming imposes. Development of specialized structures used in swimming is one of the ways that larvae can address these physical constraints. Some larval echinoderms develop epaulettes or vibratile lobes during development. These regions of the ciliated bands have longer cilia compared to other regions and are therefore believed to be associated with locomotion and ontogenetic increases in larval swimming speeds (Lacalli and Gilmour , 1990; Strathmann, pers. comm.).

Overall size affects stability and weight-carrying capacity of larvae. For ciliated swimmers, an isometric increase in size increases the length of ciliated bands, and hence provides more lift. Experimental and modeling comparisons of swimming embryos and blastulae suggest a negative scaling between size and density (McDonald & Grünbaum, 2010). This observed negative relationship offsets the increase in mass with sizes such that larger individuals can maintain their upward swimming speeds.

Because the orienting torque of an individual also scales with size, larger individuals that have a longer turning moment are also more stable (Grünbaum & Strathmann, 2003). Physical constraints that swimming imposes on larval size could therefore have evolutionary implications for egg size and for maternal investment per embryo.

In addition to size, shape of an individual also affects the mechanics of swimming. The common spheroidal larval form reflects physical requirements of swimming. Emlet (1994) surveyed non-feeding echinoid larvae, many of which are prolate spheroids with a length to width ratio of 2:1, a shape that minimizes drag. Often non-feeding larvae rearrange their cilia into rings along their axes. These transverse ciliated bands provide more propulsive force per unit area than that of uniformly distributed cilia. There is a positive relationship between larval size and the number of ciliated bands amongst the 51 species studied. These observations suggest that generation of propulsive force could be a possible physical constraint on the transition from feeding to non-feeding forms.

The “armed morphology” also reflects the functional constraints imposed by swimming on larvae. An increase in the number or length of arms increases drag and hence reduces sinking speed (Emlet, 1991). However, long extensions experience larger bending force with increasing drag. Larval echinoids have two types of skeletal rods supporting these ciliated extensions, simple cylindrical and fenestrated. Fenestrated rods are stiffer (Emlet, 1982). These stiffer arm rods are found in longer arms and can provide more resistance to the bending force. The fenestration may add even greater stiffness than required for the forces produced by swimming (Emlet, 1983). Dense larval skeletons in echinoids, and mucous strands in some veligers, can act as tethers that impede motion by increasing the excess density of the larva or the drag that an individual experiences (Strathmann & Grünbaum, 2006). Although tethering compromises swimming speeds, filter feeding efficiency increases with a tether that opposes forward motion (Emlet, 1990). This observation on tethering highlights functional tradeoffs between swimming and other ecologically important functions such as feeding, suggesting that larval morphology reflects a compromise between these selective pressures.

1.6 Modeling larval swimming in flow

Previous studies on the hydrodynamics of larval morphology were often conducted in still water. However, larvae encounter moving water in nature. Therefore, their morphology likely reflects the physical requirements of swimming both in still water and in flow. Clay and Grünbaum (2011) tested this hypothesis by simulating movements of pluteus-like larvae in still water and in shear flows. The model larva was parameterized with geometries of the sand dollar *Dendraster excentricus*, and was approximated by ciliated rods representing arms and by non-ciliated rods extending to the base of the larva representing the body. The buoyancy and gravitational forces were computed based on the density and distribution of tissue and calcite skeleton in Stokes' flow. Three morphological families were created by incrementally altering one morphological characteristic from observed morphologies. The three morphological variables investigated were larval body skeleton volume, relative arm lengths, and arm elevation angle (Fig. 1. 4). Swimming performance of these model larvae were measured by net vertical velocities and comparisons were made between still water and shear flows.

Considering realistic flow field is important when studying larval movement because swimming performance of model larvae with identical morphologies differed between levels of shear. Observed morphologies of larval sand dollars fell within the morphospace in which model larvae were able to swim upward in still water. However, the observed larval morphology did not maximize upward swimming speed and was outperformed by a subset of alternative morphologies in still water (Fig. 1. 4). Variability in vertical velocities across flow fields was smallest for the observed morphology, suggesting individuals maximize the ability to maintain upward swimming across the most diverse conditions of flow. This modeling experiment suggests that 1) slight changes in morphological characteristics can compromise swimming performance and 2) observed larval morphologies represent a reasonable tradeoff between the differing requirements for swimming in still as opposed to moving water.

Ontogenetic changes in morphology are common among invertebrate larvae. Larval sand dollars add pairs of arms during development. Stage-dependent depth distribution has been reported from both

laboratory experiments (Pennington & Emlet, 1986) and field observations (Emlet, 1986). Both modeling and video tracking of four-armed, six-armed, and eight-armed larval sand dollars suggested that the developmental changes in larval morphology lead to quantitative and qualitative differences in larval movement in shear flow between stages: four-armed and eight-armed larvae are more prone than are six-armed larvae to move into downwelling water. Changes in larval morphology over the course of development could allow individuals to move selectively to different depths within the water column and hence affect dispersal (Clay & Grünbaum, 2010).

1.7 Behavioral changes modulate swimming performance

Understanding the biomechanics of larval form provides an estimate of the capability of larvae to move, and their behavioral responses to environmental variables fine-tune their actual swimming. Traditionally, behavioral observations have focused on describing depth distribution with respect to the presence of environmental cues (e.g. Metaxas and Young, 1998) or ciliary motion (Podolsky & Emlet, 1993). The latter often utilizes video microscopy and deduces swimming speed based on the rate at which tracer particles pass by an individual. These approaches have provided important information on larval sensory capabilities (Chia *et al.*, 1984, Morgan, 1995, Naylor, 2006). Videography has improved over the past decades and one can now use video motion analysis to simultaneously observe hundreds of freely-swimming individuals with minimal wall effects, and compare between treatments (e.g. ambient temperature, pH). This approach has been applied to quantifying larval responses to environmental variables in the laboratory, e.g. settlement cues (Hadfield *et al.*, 2006) and turbulence (Fuchs *et al.*, 2004). *In-situ* devices such as the OWNFOR (Orientation With No Frame Of Reference) apparatus have been developed to study orientation of larval fish in the pelagic environment using video motion analysis (Irisson *et al.*, 2009).

Video motion analysis can also be used to quantify behaviors under changing conditions that reflect conditions in the flow. Field observations suggest that some larval invertebrates aggregate in thermoclines (Boudreau *et al.*, 1992). Low temperatures reduce swimming speeds of many planktonic

ectotherms, compromising their abilities to regulate depth. Swimming speeds of larval sand dollars, calculated on the basis of ciliary motion were lowered by 40% when experiencing a 10°C decrease in temperature (Podolsky & Emler, 1993). Using video motion analysis, Chan and Grünbaum (2010) found that larval sand dollars behaviorally alter their characteristic helical swimming when subjected to a decrease in temperature from 20°C to 12°C (Fig. 2.3 & 2.4). Even as swimming speeds are reduced, these larvae maintained net vertical velocities by reducing the widths of helical trajectories, which had the effect of reducing the total distance traveled for a given vertical excursion. Maintaining vertical velocities under lower temperature suggests a behavioral compensation that enables larvae to preserve their ability to navigate their vertically structured environment (Chan & Grünbaum, 2010). Blastulae of red urchins, *Strongylocentrotus franciscanus*, also appeared to adjust their helical trajectories when experiencing a temperature change (McDonald, 2004). These observations highlight larval abilities to rapidly adjust behavior in ways that circumvent temperature-induced physiological and biomechanical constraints on swimming.

1.8 Functional consequences of morphological variations: a case study in ocean acidification

Because larval morphologies and behaviors affect swimming, processes that have morphological or physiological impacts are likely to have functional implications for swimming. Many invertebrate larvae display phenotypic plasticity. For example, echinoplutei grow longer arms and smaller stomachs when starved and these changes in arm length were suggested to increase maximum clearance rates, i.e., the volume of water cleared of food particles per time (Hart & Strathmann, 1994). However, the impacts of these naturally-induced morphological changes on swimming are not well-understood.

Ocean acidification (OA) refers to the process whereby excess carbon dioxide in the atmosphere hydrates with sea water, altering the carbonate chemistry and releasing protons. Global emission levels are predicted to continue rising, with atmospheric pCO₂ reaching >700 ppm by 2100 (Caldeira & Wickett, 2003). This rapid change in chemistry is suggested to threaten marine ecosystems. Previous studies have demonstrated that OA has sub-lethal impacts on various marine invertebrate larvae, including reduced

developmental rate, changes in morphology, and reduced calcification (Byrne, 2011b, Dupont *et al.*, 2010). The functional impacts of these sub-lethal changes on larval swimming have not been quantified.

When exposed to an elevated pCO₂ level of 1000 ppm, representing the “business as usual” prediction for 2100 (IPCC, 2007), larval sand dollars developed significantly narrower bodies and smaller stomachs at the four-armed stage. Morphological changes also varied between four maternal lineages, suggesting within-population variation in sensitivity to changes in pCO₂ level. Despite these morphological changes, pCO₂ level alone had no significant effect on swimming speeds or on the shape of swimming trajectories (Fig. 1.5 a-c). However, acidified larvae had reduced feeding performance, as indicated by significantly smaller larval stomachs and body volume due to narrower bodies (Chan *et al.*, 2011). Acidified, four-armed larvae from some maternal lineages also had longer arms (Table 1.1). Development of smaller stomach and longer arms in the acidified treatment resembled the effect of limited food but not other stressors such as low salinity (George and Walker, 2007). Acidification negatively affect feeding despite the longer arms that could indicate a greater maximum clearance rate. One hypothesis is that acidification reduced the capture of particles passing the ciliary band or the ingestion or assimilation of captured particles. If this is the case, the acidified and starved larvae maybe retaining swimming performance while adjusting clearing rate. Prioritization of swimming over feeding is perhaps because the inability to swim incurs high immediate costs, e.g. failure to escape predators or locate food patches. The implication of this tradeoff is that that negative effects of ocean acidification are carried over to subsequent developmental stages (Chan *et al.*, 2011).

Maintenance of swimming performance despite morphological changes led to two hypotheses regarding larval motion under changing oceanic conditions. The first hypothesis is that when exposed to elevated pCO₂ levels, larval sand dollars alter their ciliary beat patterns such that swimming performance is maintained. Larval sand dollars adjusted their swimming trajectories over hours when exposed to lowered temperature (Chan & Grünbaum, 2010) . Because morphological adjustment is unlikely during this time frame, it is likely that there are mechanisms of rapid adjustment, such as shifts in ciliary beat

that maintain vertical velocities. Ciliary motion and reversals are associated with ionic pumps (Hart, 1990) and their functions are likely to be affected by pH. If the number of ciliary reversals decreases under acidified conditions due to the change in availability of calcium ion, it is possible that more force is directed towards swimming at the cost of less efficient feeding.

The second hypothesis is that the observed changes in morphology are well-coordinated such that the physical requirements for swimming are met. The impact of OA on each morphological characteristic was not identical as indicated by different loadings in a principle component analysis (Chan *et al.*, 2011). For instance, acidified four-armed larvae had narrower bodies but did not have shorter arms nor body heights. Therefore, acidified larval sand dollars were isometrically shrinking. Such overall change in shape can affect the mechanics of swimming. Given larval sand dollars have pyramid-shaped bodies, narrowing of the body width without a complementary change in body height implies higher arm elevation angle (Fig. 1.6a). Higher arm elevation angles increases stability, possibly by reducing the width exposed to shear or increasing the distance between the centers of buoyancy and gravity (Clay & Grünbaum, 2011). This coordinated morphological change could compensate for the reduced stability caused by smaller body size and reduced calcification under OA conditions.

Landmark analysis can be used to test the second hypothesis of coordinated change in morphology. To compare the differences in shape, landmarks of the objects of interest are uniformly scaled, rotated, and translated into a common superimposition. Such approach is referred to as Procrustes analysis and has been widely used to compare observed morphologies of various organisms, e.g. insect wings, mammalian skull, and fish fins (Bookstein, 1997). However, this approach has not been applied to marine invertebrate larvae. I selected 60 individuals from the same maternal lineage and investigated how changes in pCO₂ affected larval morphology (Fig. 1.6d). I identified and digitalized 13 landmarks, representing the tip of the body, tip of each arm, mid-points along the postoral arms, and points at which arms intersect with the body using the tps2DIG program (Rohlf, 2010.). Using the canonical variance analysis in morphoJ, I compared the distances between the normal and acidified treatments from a

common Procrustes superimposition (Klingenberg, 2011). Based on the comparisons of single morphological measurement (mid-line body length and length of postoral arms), acidification had a significant effect on body length but not arm length (Table. 1.1). However, the landmark analysis suggested acidification affected the overall shape of the larvae but not size at the four-armed stage ($F_{1,22} = 6.93$, $p = 0.001$). This result supports the hypothesis that changes in larval morphology under acidified condition were coordinated. Therefore, multiple morphological characteristics should be considered when studying the effects of environmental variables on invertebrate larvae. Single morphological measurements may lead to incorrect conclusions that morphological changes are isometric and that individuals are experiencing developmental delays.

1.9 Future directions for the study of mechanics of swimming and behaviors

Observations on larval sand dollars suggest that the swimming performance of larvae peaks in a restricted morphospace and that there are potential behavioral and developmental adjustments that maintain swimming performance. These observations reinforce the notion that physical requirements for swimming help shape the evolution of larval morphology. If so, other naturally observed morphological variations in larval morphology, such as asymmetry (Collin, 1997) and plastic responses to feeding conditions (Hart & Strathmann, 1994) would be under selection pressure favoring good swimmers. One approach to assess the impacts of these morphological variations is to create hydrodynamic models using detailed morphological reconstructions that reflect the coordinated changes, e.g. confocal micrographs (Fig. 1.6). These micrographs provide an accurate outline for finite element mesh generation, and the mesh can then be used to obtain discretized flow-field solution using Stokelets (Grünbaum & Strathmann, 2003). This solution will allow us to evaluate swimming performances of model larvae with realistic morphologies in different flow regimes and can be adapted to study different taxonomic groups.

Helical swimming is observed in a wide variety of marine plankton suggesting that such movement provides some ecological advantages, e.g. reducing the area in which predators can detect larvae (Kiorboe & Visser, 1999). Yet, benefits and mechanics of helical swimming have not been

explored in depth for invertebrate larvae. There are reports that early life history stages (blastulae and larvae) adjust their helical trajectories when experiencing temperature changes on the time scale of minutes to hours (Chan & Grünbaum, 2010, McDonald, 2004). These observations suggest that one benefit of helical swimming is the provision of a fast, energetically inexpensive means to adjust vertical velocity. Video observations of larval sand dollars in vertical shear suggest that helical movement may also affect horizontal transport by enabling individuals to sample a broader range of flow lines and move away from downwelling water or towards upwelling water (Clay and Chan, pers. obs.). Asymmetry in larval bodies and in metachronal waves of ciliated bands could contribute towards helical movement. The new modeling approach can be combined with immuno-staining techniques to visualize and to model ciliary bands, allowing for the investigation of the role of fine-scale ciliary beats in overall individual movements.

In the face of global climate change, understanding connectivity of marine populations is essential for formulating sound strategies for conservation and management. Larval swimming is one of the biological factors that should be considered in the parameterization of bio-physically coupled models. Quantitative data of larval behavior currently focus on several taxonomic groups such as molluscs and echinoderms and should be extended to other groups. Small-scale fluid dynamics have been more extensively studied in other marine plankton such as calanoid copepods and dinoflagellates. Similar computational and experimental techniques could be used to study the biological-physical-chemical interactions between invertebrate larvae and their environments, such that we can better predict larval dispersal and the population dynamics of marine organisms.

Figure 1.1

Survey of the number of articles in the Web of Science database with a title or abstract containing the phrase “marine larval dispersal model” (light gray bar) and “swimming behaviors” (dark gray bar) published between 1990 and 2010.

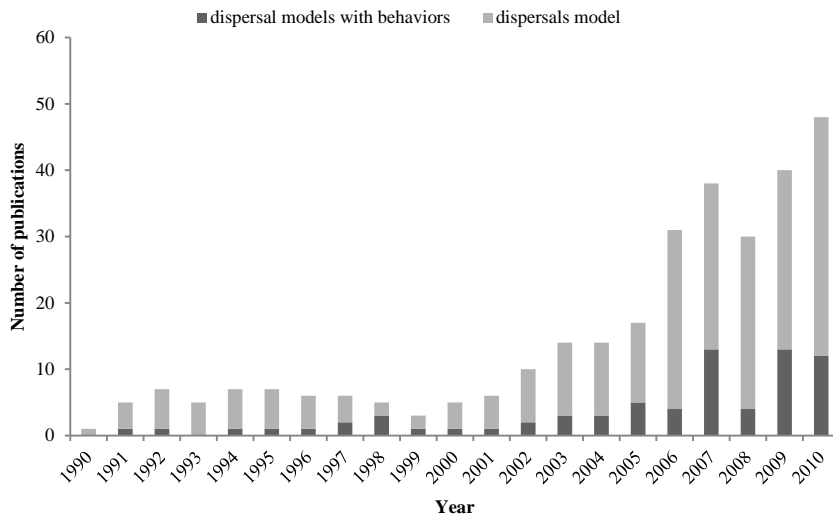


Figure 1.2

Schematic drawings illustrating larval movement (thick grey arrow) in vertical shear (i.e. a horizontal gradient of vertical flow) with upwelling on one side (right) and downwelling (left) on the other. We assume the larva swims upwards in still water (lower right). When the individual is tilted by shearing fluid forces, a component of its velocity is then directed horizontally towards the downwelling side. As a result of the horizontal swimming component, the individual moves into the downwelling current and is transported downwards, despite its upwards swimming.

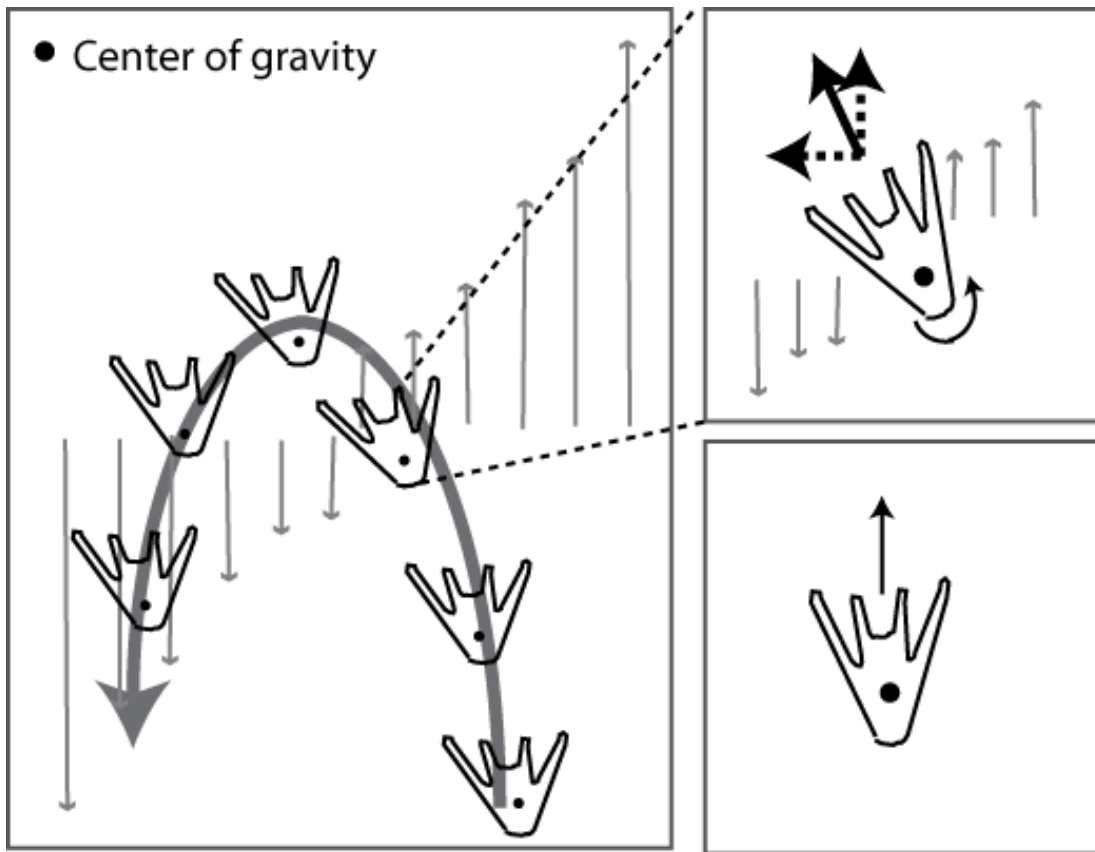


Figure 1.3

Schematic drawings illustrating two proposed physical mechanisms whereby larvae maintain stability (Mogami et al., 2001). Three forces are balanced on these individuals: gravity (F_G), buoyancy (F_B) and hydrodynamic (F_H). (a) For a hypothetical individual with uniform density and symmetry, F_G , F_B and F_H act at the same point. Thus, no torque is generated when the individual is tilted. (b) For an individual with heterogeneity in density (e.g. density differs between tissue and skeleton), F_G and F_B act on different points of the body. An orienting torque is generated when the individual is tilted. This mechanism is referred to as the “buoyancy-gravity model” or simply “bottom heaviness”. (c) For an individual with geometric asymmetry, F_G and F_H act on different points of the body. An orienting torque is generated when the individual is tilted. This mechanism is referred to as the “gravity-drag model” (d) For a real larva with heterogeneity in density and geometric asymmetry, both physical models apply.

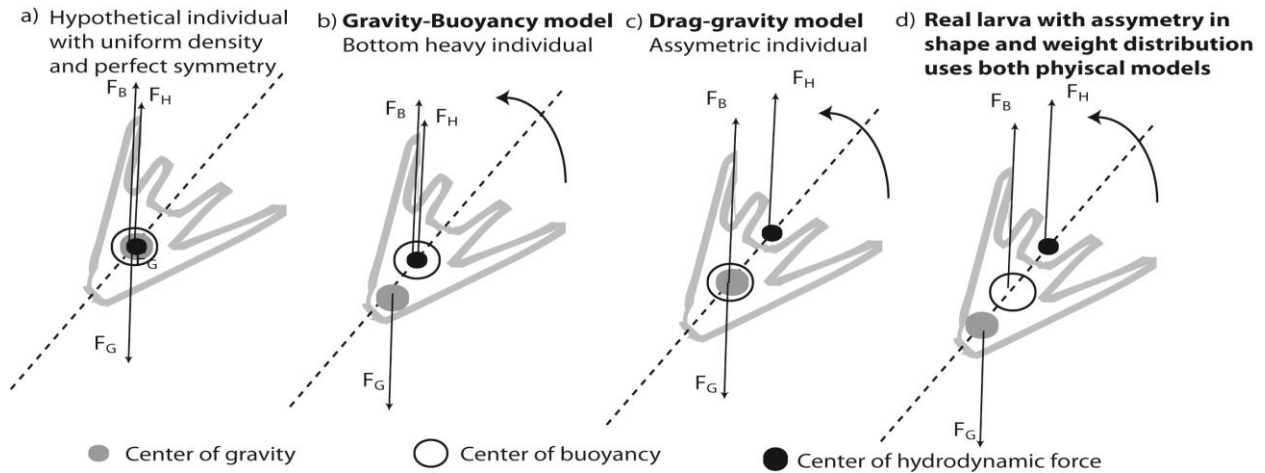


Figure 1.4

Vertical velocities of model larvae with different relative arm lengths, with the postoral arm representing 0.1 to 1.9 of total arm length (a) in still water and (b) in vertical shear (ranging from 0-10 s^{-1}). Vertical velocities are reported as the median (gray line) of 128 runs for each morphological type. The area between the 10th and 90th percentiles is shaded in gray. Each run was initiated with a different random orientation. Variability in velocity, when present, results from larvae tumbling and/or having multiple stable orientations. The morphology marked with a star corresponds to morphological measurements of real larvae. Modified from Clay and Grünbaum, 2011.

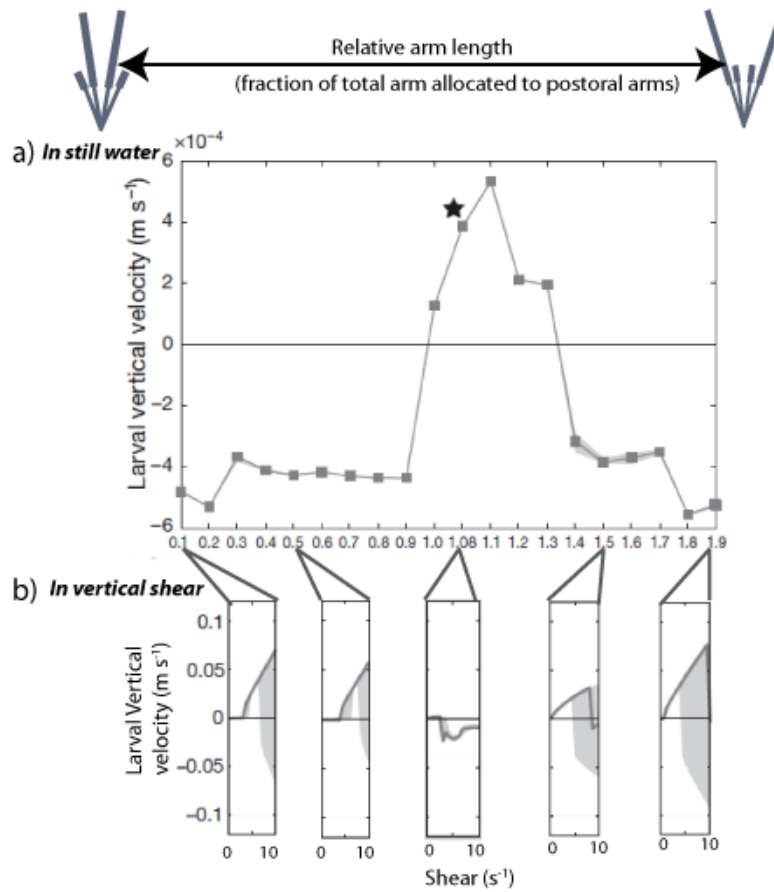


Figure 1.5

Representative individual larval sand dollars (*Dendraster excentricus*) from (a) present-day conditions and (b) elevated (acidified) pCO₂ treatments. Morphometric measurements are labeled in (a) and landmarks used in the geometric morphometric analysis are labeled in (b). Total speeds of larval sand dollars did not differ significantly between the two pCO₂ treatments across developmental stages (c). However, Procrustes superimpositions of the landmark coordinates of the present-day and acidified treatments suggest a change in overall shape (d). (a-c) are modified from Chan et al., 2011.

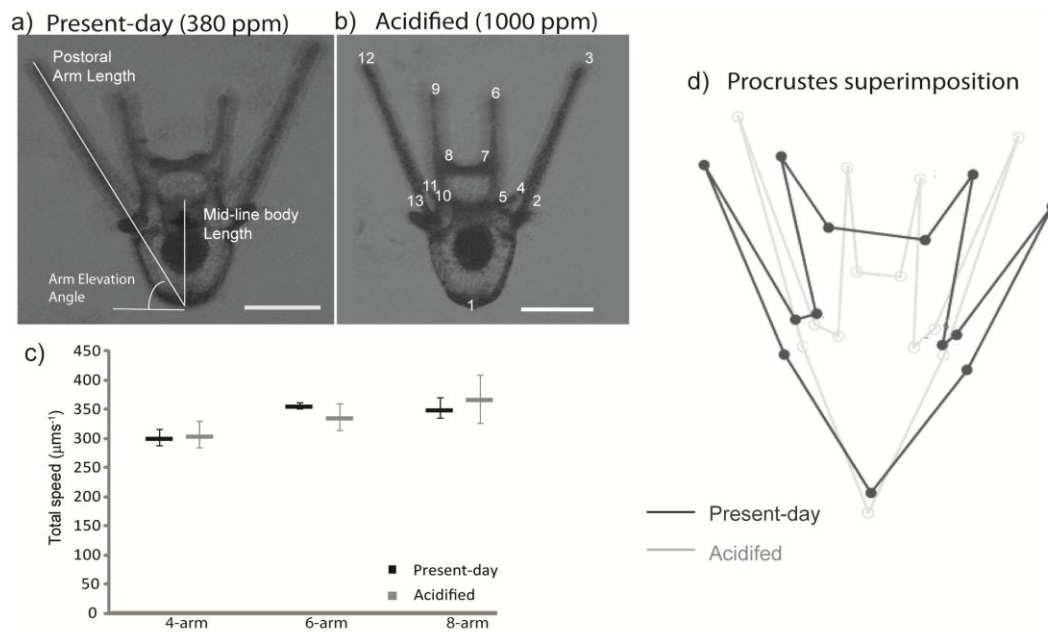


Figure 1.6

Trajectory of model larva in still water over 40 seconds (a). Model larva (b) was reconstructed based on confocal micrograph of the four-armed larval sand dollar *Dendraster excentricus* labeled with propidium iodide shown in (c).

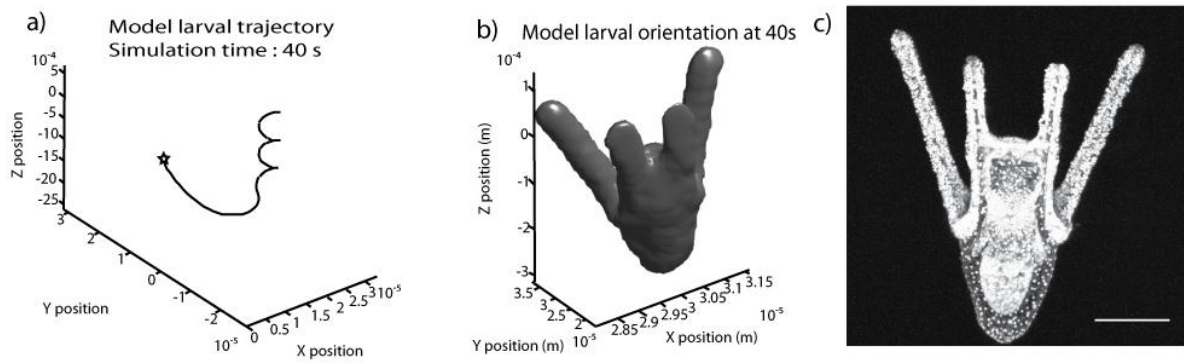


Table 1. 1

Comparison of mid-line body and postoral arm length of four-arm larval sand dollars, *Dendraster excentricus*, mean and standard deviation using 1-way ANOVA.

	Present-day (380 ppm)	Acidified (1000 ppm)	1-way ANOVA
Mid-line body length	182.5 $\mu\text{m} \pm 2.7 \mu\text{m}$	190.3 $\mu\text{m} \pm 2.5 \mu\text{m}$	$F_{1,59} = 4.48, p = 0.039$
Postoral arm length	458.5 $\mu\text{m} \pm 10.4 \mu\text{m}$	484.5 $\mu\text{m} \pm 7.2 \mu\text{m}$	$F_{1,59} = 3.55, p = 0.066$

**CHAPTER TWO. EFFECTS OF TEMPERATURE AND DIET ON LARVAL SWIMMING
BEHAVIORS OF THE SAND DOLLAR *DENDRASTER EXCENTRICUS****

2.1 Abstract

Swimming behaviors of marine invertebrate larvae play key roles in larval dispersal and survival and, hence, have important consequences for adult population dynamics. However, to date, insufficient quantitative information exists on larval swimming to understand and predict swimming movements in most marine invertebrate species. Previous work suggests that larvae swim more slowly at lower temperatures and, consequently, might have difficulty regulating depth when experiencing temperature changes. Improved diet quality in terms of essential fatty acid composition has been suggested to increase cold tolerance in many organisms. We used non-invasive video-tracking techniques to quantify swimming in larvae of the sand dollar *Dendraster excentricus*, raised on 4 algal diets differing in their fatty acid profiles and then exposed to an ecologically relevant temperature decrease from 20 to 12°C. Differences in diet quality led to significant morphological differences by the 8-arm larval stage, and there were significant diet–temperature interaction effects on swimming patterns. While larval swimming speeds decreased as temperature decreased across all diet treatments, net vertical velocities of larvae did not decrease. Changes in helical geometries of larval swimming trajectories suggest that larvae compensate for reduced swimming speeds by reducing horizontal movement, thus preserving their ability to regulate depth. The observed compensatory mechanism effectively circumvents constraints on swimming due to lowered temperatures. More generally, video-tracking of free-swimming larvae can yield quantitative data to inform biophysically coupled models that better predict consequences of larval dispersal for adult population dynamics under current and future environmental conditions.

* Originally published in Marine Ecology Progress Series, September 2010, volume 415, pp 49-59

2.2 Introduction

The planktonic larvae of marine organisms play important roles in shaping the distribution and abundance of populations. Particularly for organisms with a sessile benthic adult stage, this mobile, transitional phase is the major vehicle for colonizing unoccupied habitats, and for connecting and sustaining existing populations (Cowen *et al.*, 2007, Gaines & Roughgarden, 1985, Underwood & Fairweather, 1989). Biophysically coupled models have been increasingly used to understand and predict larval dispersal patterns due to the challenges of sampling planktonic larvae in the field, and have been used to determine connectivity patterns between disjunct populations and to inform sustainable management strategies (Metaxas & Saunders, 2009).

Recent field and numerical studies have shown that planktonic larvae are not passive drifters for which dispersal outcomes are determined solely by physical mechanisms. Through vertical swimming, larvae can affect the direction and distance they travel by exploiting variations in the strength and direction of advective currents with depth (Dekshenieks *et al.*, 1996, North *et al.*, 2008). In addition to larval transport, swimming behaviors affect larval survival, because other environmental characteristics, such as temperature and abundance of predators and food, are also vertically structured (Metaxas, 2001).

In spite of its importance, there is to date relatively little quantitative information on larval swimming behavior (Chia *et al.*, 1984, Young, 1995). Studies of the biomechanics of the ciliary motion of invertebrate larvae have provided estimates of individual swimming capabilities based on ciliary speeds and beating frequencies (e.g. Strathmann 1971, Hart & Strathmann 1994). Experimental and field studies have demonstrated that invertebrate larvae aggregate along thermoclines and haloclines or in food patches, and avoid water masses with predator cues (Metaxas *et al.*, 2009, Metaxas & Young, 1998, Sameoto & Metaxas, 2008). These observations are revealing population-level distributions of larvae. However, these studies do not provide a strong basis for predicting larval distribution in the field, because they do not quantify the underlying behaviors that lead to the observed aggregations. Additional

quantitative descriptions of larval swimming behaviors and of how swimming movements change in response to the environmental variability that larvae are likely to encounter would enable us to better parameterize predictive biophysical model (Metaxas, 2001).

To provide these quantitative descriptions of larval behavioral responses, we have developed a non-invasive computerized video-tracking technique that enables us to quantify the characteristics of 100s of freely swimming individual larvae in the laboratory at relatively large spatial scales (10s of centimeters) over relatively long periods of time (hours). Similar techniques have been used to study protists (e.g. Mayali *et al.*, 2008, Menden-Deuer & Grunbaum, 2006, Sheng *et al.*, 2007) or other larvae (e.g. Clay & Grünbaum, 2010, Fuchs *et al.*, 2004, McDonald, 2004, Strathmann & Grünbaum, 2006) . Video-tracking is desirable for behavioral studies because it does not require tethering, and because it allows for relatively large observation chambers in which wall effects are minimal. This approach accurately quantifies specific elements of organism-level movement behaviors, such as turning and reversals between swimming and sinking, that are crucial for predicting long-term water-column distributions.

In the present study, we used video-tracking to quantify responses of larval *Dendraster excentricus* to variations in temperature and diet quality. *D. excentricus* is a good model organism for larval swimming studies, because effects of food quantity and quality on its growth and morphology are well characterized (Hart & Strathmann, 1994), effects of low temperature on its ciliary motion have been measured (Podolsky & Emlet, 1993), and effects of larval morphology on its swimming mechanics have been modeled (Clay & Grünbaum, 2010, Grünbaum & Strathmann, 2003).

Temperature and diet are of particular importance to larval behaviors. Sand dollars are found in shallow fjords that experience surface heating and large temperature variations (Emlet, 1986). McEdward (1985) showed that electron transport activity in larval sand dollars increases 93% with a temperature increase from 12 to 22°C that occurs frequently in sand dollar habitats. Kinematic viscosity of seawater decreases by ~10% with this 10°C increase, implying a greater resistance to swimming at low

temperatures (Sleigh & Blake, 1977). Consistent with this, Podolsky & Emlet (1993) reported that swimming speeds of larval sand dollar were reduced by 40% when larvae were subjected to this 10°C temperature decrease.

Diet, especially food quality in terms of fatty acid profiles, may modulate the behavioral responses of larval *Dendraster excentricus* to temperature decreases. Fatty acids, particularly long-chain polyunsaturated fatty acids (PUFAs), such as eicosapentaenoic acid [EPA, 20:5(n-3)] and docosahexaenoic acid [DHA, 22:6(n-3)], have been suggested to aid in cold stress tolerance in *Daphnia* sp. and fish larvae (Brett *et al.*, 2006, Logue *et al.*, 2000).

With respect to *Dendraster excentricus*, these earlier studies suggest that larval swimming ability and hence larval survival can be severely affected by temperature decreases commonly experienced in temperate coastal waters, but that sufficiently high diet quality can mitigate or eliminate these deleterious temperature-induced impacts. To test these hypotheses, we raised larval sand dollars on 4 algal diets with different fatty acid profiles. We applied video-tracking techniques to quantify and compare swimming behaviors of larvae from different dietary treatments across an 8°C temperature decrease from 20 to 12°C.

2.3 Materials and methods

Spawning and fertilization

Adult sand dollars *Dendraster excentricus* were collected from Crescent Beach, East Sound, Orcas Island, Washington, USA, in early summer 2008 and maintained in flow-through sea tables at the Friday Harbor Laboratories until use. Spawning was induced by injecting 0.5 to 1 ml of 0.55 M KCl into the coelomic cavity (Strathmann, 1987). Eggs collected were washed through a 200 µm sieve, placed in a beaker with 1000 ml of <10 µm filtered seawater, and fertilized with 5 drops of sperm. Ten minutes after fertilization, the eggs were examined under a microscope for the presence of fertilization envelopes to confirm fertilization success. By fertilizing eggs from 3 females with a mixture of sperm from 2 males, 3 maternal lineages were created. Fertilized embryos from different maternal lineages were raised

separately. Results from different maternal lineages were later pooled by stage to increase sample size after confirming that their morphology showed no statistical differences (data not shown).

Diet treatments

Larvae were fed 2 species of microalga, *Isochrysis galbana* and *Dunaliella tertiolecta*. The prymnesiophyte *I. galbana* is a common larval food in aquaculture and contains large amounts of EPA and DHA. The chlorophyte *D. tertiolecta*, a commonly used echinoplutei food, lacks those long-chain PUFAs (Tang & Taal 2005). Other larvae were fed the heterotrophic dinoflagellate *Oxyrrhis marina* preying on *I. galbana* or *D. tertiolecta*. *I. galbana* and *D. tertiolecta* were cultured in enriched *f/2* medium, while *O. marina* (~50 ml) was first inoculated into 200 ml of *I. galbana* or *D. tertiolecta* culture and later transferred to 1000 ml *f/2* medium. All cultures were maintained at 13°C on a 14 h light:10 h dark cycle. Heterotrophic protists can ‘trophically upgrade’ their prey and increase their EPA and DHA content through elongation of shorter chains fatty acids (Klein Breteler *et al.*, 1999). We designated these 4 dietary treatments as *Iso*, *Dun*, *OxyI*, and *OxyD*, respectively.

Larval culture

Larvae were reared under continuous stirring at $16 \pm 1.5^\circ\text{C}$ in 600 ml glass jars in $0.45 \mu\text{m}$ filtered seawater at a density of $\sim 2 \text{ ind. ml}^{-1}$. Each dietary treatment had 4 replicate jars, arranged in a Latin square. Water was changed and food was added every other day. Algal concentration was determined with a hemocytometer, and biovolumes were estimated according to cell diameter assuming spherical cells. Larvae were fed an equal biovolume of cells (40000, 5000, and 320 cells ml^{-1} for *Iso*, *Dun*, and *Oxyrrhis marina* culture) to ensure the effect was from food quality and not quantity. In the *Iso* and *Dun* treatments, algal cells were centrifuged and the *f/2* medium was discarded. Cells were then resuspended in filtered seawater and added to larval cultures. For *OxyI* and *OxyD*, the cultures were filtered through a $15 \mu\text{m}$ membrane filter to remove algal prey cells, so that only the *O. marina* cells were presented to the larvae.

To assess the effectiveness of the dietary treatments, 25 ml of each algal food and 1000 8-arm larvae were frozen at -80°C for further chemical analyses. Lipids were extracted and analyzed by gas chromatography using the protocol detailed in Ravet et al.(2003). The presence and relative amount of fatty acids detected matched closely with the results published by Tang & Taal (2005) and Schiopu et al. (2006) (data not shown).

Behavioral observations and video-acquisition

Swimming behaviors of 4- and 8-arm larvae were quantified at 20 and 12°C (a 4°C temperature excursion in both directions from the rearing temperature of 16°C) in 4 Plexiglas chambers of $3.5 \times 3.5 \times 30$ cm, which was filled with $0.45 \mu\text{m}$ filtered seawater. These 4 chambers were submerged into a common water bath in which temperature was maintained by an immersion circulator (Lauda Ecoline RE-105). This enabled simultaneous observation of larvae from the different dietary treatments. At the beginning of each replicate trial, we pipetted ~ 300 larvae from each treatment into a randomly assigned chamber, and the larvae were allowed to acclimate for 30 min. At this density of <1 ind. ml^{-1} , interactions between individuals were negligible. Five minutes prior to filming, a Plexiglas stirrer was used to gently re-disperse larvae.

Video clips of larvae were captured at 15 frames s^{-1} in the dark under infrared illumination, using 2 Panasonic DS400 digital camcorders mounted side by side on a computer-controlled motorized platform such that each camcorder focused on 2 of the 4 chambers without overlap. Video was captured in a series of vertical ‘casts’ that sequentially imaged lower (0 to 14.4 cm) and upper (11.6 to 25 cm) regions of the tank. Each cast required 15 min and consisted of 6 min videos captured in each region of the tank, plus 3 min to reposition cameras. Six casts were performed at the initial temperature of 20°C . Temperature in the chambers was then lowered to 12°C in 2°C increments with 30 min of equilibration time between each increment. Then, 6 casts were performed at 12°C . Observations were repeated 8 times for each developmental stage.

Larval morphometrics

The 4- and 8-arm larvae were pipetted out of each chamber at the end of each observation and fixed in 90% sodium bicarbonate-buffered ethanol. Individuals were photographed within 3 wk of preservation under a microscope at 16× using a Nikon E4500 digital camera. Arm lengths, distances between pairs of arms, body widths, and heights of 10 individuals from each treatment in each observation were measured (total n = 640) with ImageJ (Rasband 2008) and calibrated with photographs of a stage micrometer (Fig. 2.1).

Video-processing and analysis

Video clips were analyzed by equalizing lighting, removing background variations, selecting moving particles (larvae) based on brightness and size, and extracting the pixel coordinates of larvae in a modified version of the video-editing package avidemux2.4. Videos were calibrated using a grid of 2 mm squares with 4 mm spacing. Pixel co-ordinates were converted to physical positions and assembled into larval swimming trajectories by associating points in successive video frames that represented the same organism over time using Tracker3D, an in-house Matlab program.

Statistical analyses

Effects of diet on larval morphometrics were assessed with Kruskal-Wallis tests, as data were not normally distributed. Post hoc Dunn's tests were performed when significant differences were detected (Zar, 1996).

Because larval *Dendraster excentricus* swim in a helical manner, their trajectories resemble sine waves when viewed as 2-dimensional (2D) projections (Fig. 2.2a). Only individual trajectories longer than 30 s that had above-threshold horizontal acceleration ($>0.06 \text{ mm s}^{-2}$) were included in the statistical analyses, to exclude remaining passive particles. We defined the 'path' of a larva using a cubic smoothing spline with short knot spacing, such that the curve followed the actual trajectory while removing frame

rate noise (Fig.2.2b). We defined the 'axis of travel' analogously, but with long knot spacing such that the resulting curve approximated the overall direction of travel of the trajectory.

We computed total swimming speed of each path by taking its time derivative. We calculated the net displacement of larvae as the distance between the starting and ending points of the axis of travel. We computed net vertical and horizontal velocities by dividing the net displacement by path duration. We applied a correction factor of $\pi/2$ to horizontal components to estimate true horizontal velocities from 2D projections.

We characterized helical larval trajectories using 3 geometric parameters. We defined 'zero crossings' as points at which the path and the axis of travel intersected (Fig. 2.2b). We computed the oscillatory parameters for trajectories that had at least 5 zero crossings, such that the trajectories had at least 2 complete oscillations. We defined 'oscillatory speed' as the time derivative of the distance between the path and the axis of travel. We also calculated the mean distance between zero crossings, representing the helical pitch, and the maximum distance between the path and the axis of travel, representing helical width.

We computed weighted means of swimming metrics for each vertical cast by sampling at 10 s time points and averaging trajectories intersecting each time point. This scheme gave equal statistical weight to each frame in which each larva was tracked, avoiding bias towards shorter or longer trajectories.

We performed a principal component analysis (PCA) on the correlation matrix of mean swimming metrics for both 4- and 8-arm larvae with Varimax rotation using Kaiser normalization for data reduction (Harris 1975). We determined the number of factors to retain in further analyses with parallel analysis (PA). We used scores of PCA axes (can we undo this for consistency) to assess the effect of temperature and diet by comparing the Anderson-Rubin component scores for each treatment using 2-way ANOVA with Bonferroni corrections for each developmental stage. This factorial design consisted of 4 dietary treatments and 2 temperatures, where each treatment had 8 replicates and within each treatment

there were 6 representative weighted means for each vertical cast. We performed post hoc Tukey's tests with Bonferroni corrections when significant differences ($p < 0.05$) in component scores were detected (Zar, 1996). All statistical analyses were performed in SPSS.

2.4 Results

Larval morphometrics

There were no significant differences in morphometrics of 4-arm larvae between dietary treatments (Table 2.1). In contrast, among 8-arm larvae there were significant differences ($p < 0.05$) between dietary treatments in 8 of the 10 morphometric characteristics. The general trend of morphometric variation was that larvae fed with Dun were largest, followed by larvae fed with Iso, then larvae fed with *OxyI*, and finally those fed with *OxyD*. Exceptions to this trend were mean lengths of preoral and posterodorsal arms, in which the rank of *OxyI* and *OxyD* were reversed (i.e. *OxyI* had the shortest preoral and posterodorsal arms). A post hoc Dunn's test did not yield consistent grouping across morphometric variables.

Principal component analysis

Loadings of the original variables on PCA Axes 1 to 3 and the percentage of variance these axes explain are listed in Table 2. PCA Axis 1 was heavily loaded with total and oscillatory speeds, with a higher PCA Axis 1 score denoting faster total speeds. PCA Axis 2 was heavily loaded with helical width, with a higher PCA Axis 2 score denoting wider helices. PCA Axis 3 was heavily loaded with vertical swimming velocity, with a higher PCA Axis 3 score denoting faster upward swimming. Parallel analysis (PA) suggested the PCA Axes 1 and 2 be retained because the eigenvalues for these factors were higher than the average eigenvalues for the random factors in PA. This analysis was ambiguous for PCA Axis 3, for which the eigenvalue was close to that of the random factor. We included this PCA axis (undo for consistency) in further analyses because it is most highly correlated to vertical swimming velocity, which is the most essential variable in controlling larval depth (Table 2.2).

Effects of temperature, diet, and their interactions on swimming

For 4-arm larvae, reducing temperature from 20 to 12°C significantly reduced total swimming speeds (PCA Axis 1 scores) across all dietary treatments ($p < 0.0001$; Table 2.3, Fig. 2.3). Helical width (PCA Axis 2 scores) significantly decreased with temperature ($p < 0.0001$); however, vertical swimming velocities (PCA Axis 3 scores) were not affected by such a decrease ($p = 0.994$). Dietary treatments had no significant effect on any of the 3 PCA axis scores (consistency), and there was no significant effect of temperature–diet interaction either ($p > 0.3$).

For 8-arm larvae, reducing the temperature from 20 to 12°C significantly reduced total swimming speeds (PCA Axis 1 scores) across all dietary treatments ($p < 0.0001$). Temperature alone did not have a significant effect on either helical widths (PCA Axis 2 scores, $p = 0.601$) or vertical velocities (PCA Axis 3 scores, $p = 0.111$). Dietary treatments had a significant effect on helical widths (PCA Axis 2 scores, $p < 0.001$), but not on total swimming speeds or vertical velocities. Post hoc tests suggest that larvae raised on *OxyI* have significantly larger helical widths than those fed on *OxyD*, while there was overlap with the other dietary treatments. There were also significant temperature/diet interaction effects on helical width ($p = 0.047$; Table 2.3, Fig. 2.4). This interaction was driven mainly by larvae fed with *OxyI*, in which helical width increased with decreasing temperature, while the remaining dietary treatments showed decreased helical widths (Fig. 2.3).

2.5 Discussion

Swimming behaviors of invertebrate larvae can significantly impact larval survival and dispersal outcomes. Quantitative analysis of larval *Dendraster excentricus* swimming trajectories showed that swimming capability, as measured by total swimming speed, was compromised when subjected to a significant, environmentally relevant temperature decrease. However, there was a surprising consistency in their upward vertical velocities between temperatures. This suggests a strong compensatory mechanism, which enables larval *D. excentricus* to retain their depth-regulating abilities in spite of reduced swimming

capabilities. This compensatory mechanism appears to involve behavioral choices that may effectively circumvent the physiological and biomechanical limitations imposed by low temperature on larval abilities to swim. Diet quality modulated larval responses to decreased temperature.

Temperature compensation in swimming behaviors

For both 4- and 8-arm larvae, total swimming speed significantly decreased from 20 to 12°C (Figs. 2.3 & 2.4). Total swimming speeds of 4-arm larvae, combining all dietary treatments, dropped from $349.9 \pm 10.3 \mu\text{m s}^{-1}$ at 20°C to $317.2 \pm 7.36 \mu\text{m s}^{-1}$ at 12°C. The 8-arm larvae had a greater between-temperature difference in their total swimming speeds, which dropped from $325.3 \pm 6.96 \mu\text{m s}^{-1}$ at 20°C to $293.5 \pm 4.92 \mu\text{m s}^{-1}$ at 12°C. These observed total swimming speeds are consistent with a previous prediction, based on physiological and biomechanical constraints, that larvae swim more slowly at lower temperatures (Podolsky & Emlet, 1993). However, in our observations, larval net vertical velocities at both 4- and 8-arm stages were unaffected by the temperature decrease. The 4-arm larvae had an average net vertical speed of $40.5 \pm 5.63 \mu\text{m s}^{-1}$ at 20°C and $47.5 \pm 6.45 \mu\text{m s}^{-1}$ at 12°C, whereas 8-arm larvae had an average net vertical speed of $66.0 \pm 7.01 \mu\text{m s}^{-1}$ at 20°C and $56.7 \pm 5.59 \mu\text{m s}^{-1}$ at 12°C. Thus, despite the constraints imposed by an 8°C temperature decrease, larval *Dendraster excentricus* maintained their net vertical velocities, implying that their ability to regulate depth through up-swimming was not affected.

The disproportional changes in total and vertical speeds might be explained by the shape of the helical swimming trajectories of larval *Dendraster excentricus* (Fig. 2a). In both developmental stages, only small portions of larval movements were vertically directed. If the helical geometries of swimming trajectories are behavioral choices rather than fixed physiological or biomechanical properties, larvae may selectively reduce either the horizontal or vertical components of their movement. In that case, changes in total speed would not proportionately translate into changes in net vertical displacement.

In our experiments, larval *Dendraster excentricus* selectivity reduced the horizontal components of their helical movement so as to minimize the effects of temperature decrease on their vertical

movement. Across all dietary treatments, 4-arm larvae swam in narrower helices at 12°C than at 20°C, as evidenced by the decrease in PCA Axis 2 scores. At the 8-arm stage, similar trends were observed in 3 out of 4 dietary treatments, but the differences in helical widths were not statistically significant. It is possible that the changes in helical width for 8-arm larvae were relatively smaller than those of 4-arm larvae because they had extra lifting force provided by the additional pairs of arms, because their reduced densities were reduced by increased lipid storage (Pennington & Strathmann, 1990), or because 8-arm larvae were able to behaviorally adjust their morphologies through the flexing of posterodorsal arms (Burke, 1983).

We suggest that maintaining vertical speed and depth-regulating ability through the observed behavioral adjustments is an adaptive response to temperature decrease. Lower temperatures usually reduce larval feeding rates and delay growth (Pechenik, 1987). Planktonic mortality rates are often high, especially in cold viscous water where hydrodynamic signals to predators may be magnified and larval escape responses to predator attacks could be compromised (Gallager, 1993, Rumrill, 1990). Hence, an inability to escape cold water is likely to delay larval development and decrease recruitment success.

The compensatory behavior we observed implies that larval *Dendraster excentricus* were not maximizing their vertical speeds, at least at the higher temperature we observed, because they did not exercise their abilities to swim in narrower helices. This suggests that intermediate vertical velocities may better satisfy ecological requirements than either slower or faster speeds. However, tradeoffs leading to some advantages for intermediate vertical speeds are at present unclear. Some potential tradeoffs include up-swimming to escape cold water masses, maintaining a helical path to limit the exposure volume and thus predation risk (Visser, 2007), movement towards phytoplankton-rich surface waters, and avoidance of deleterious UV radiation.

Temperature-dependent changes in helical swimming geometries are not limited to the plutei of sand dollars. Embryos of the red urchin *Strongylocentrotus franciscanus* swam in helices with higher

pitch to slow overall rates of ascent when experiencing a temperature increase from 10 to 14°C (McDonald, 2004). More generally, many planktonic organisms are known to adjust their helical trajectories, most commonly (as far as is known) in response to food concentration (e.g. Menden-Deuer & Grunbaum, 2006). Our observations suggest that temperature-driven behavioral adjustments, like those found in sand dollar plutei, may be a widespread mechanism among small marine ectotherms to cope with thermal limitations on swimming.

Effects of diet on larval morphologies and swimming behaviors

For 4-arm larvae, dietary treatments did not affect larval morphologies. This lack of morphological differences is consistent with the findings of Schioppa *et al.* (2006), who found that significant differences in larval morphologies among dietary treatments started to emerge only 4 d post-fertilization. This might reflect a time lag during which ingested food is converted into body tissues and maternal reserves are used for growth. Biomechanical modeling studies have suggested that larval *Dendraster excentricus* exist in a narrow ‘morphospace’ such that a slight perturbation to a single morphological parameter could significantly compromise swimming (Clay & Grünbaum, 2010, Grünbaum & Strathmann, 2003). The lack of morphological differences amongst 4-arm larvae from different dietary treatments suggests that swimming metrics should not differ between them, and that expectation is consistent with our observations.

In contrast, morphologies of 8-arm larvae varied significantly between dietary treatments (Table 2.1). According to the model, larvae with different morphologies are likely to swim differently. However, diet alone did not have a significant effect on either total or net vertical swimming speeds. If the model results are to be believed, this suggests diet-dependent morphological changes in 8-arm larvae were highly coordinated so as to conserve swimming capability as measured by swimming speed.

While all 8-arm larvae were able to maintain their net vertical velocities during the temperature decrease, larvae from 1 of the dietary treatments accomplished this without swimming in narrower helices.

Diet and diet/temperature interactions had significant effects on the PCA Axis 2 scores, i.e. helical width (Table 2.3). Larvae fed *Oxyrrhis marina* preying on *Isochrysis galbana* (*OxyI*) swam in significantly wider helices when temperature was decreased, a trend opposite that seen in the other dietary treatments (Fig. 2.3). Larvae in the *OxyI* treatment may have maintained their vertical velocities by increasing helical pitches with decreasing temperature. However, due to the great variability in helical pitch, we were not able to resolve the presence or absence of this potential change in swimming trajectories. Interestingly, *OxyI* was also the food that had the highest content of EPA, which has been hypothesized to play an important role in cold tolerance (Hall *et al.*, 2002). Further investigations are needed to test whether EPA concentrations could explain why larvae fed *OxyI* responded differently to temperature than larvae in the other dietary treatments.

In addition to swimming behaviors, essential fatty acids (PUFAs) may also explain the differences in larval morphologies between dietary treatments. In our experiment, the sizes of 8-arm larvae were negatively correlated to the amount of PUFAs available in the diet (Table 2.1). This decoupling between PUFAs availability and larval size was hypothesized by George *et al.* (2008) to be a result of larval *Dendraster excentricus* desaturating and elongating shorter chain PUFAs into long-chain PUFAs, e.g. steric acid, which are abundant in *Dunaliella tertiolecta*, into EPA. However, it is also possible that other biochemical differences between dietary treatments (e.g. caloric value, protein, and carbohydrate content) are responsible for the observed differences in growth and behaviors (Brown *et al.*, 1997). Larvae may also have responded to differences in food quality as they would have to differences in food quantity, by growing longer ciliated arms to increase clearance rates when starved (Hart & Strathmann, 1994).

The observed differences in larval morphologies and responses to temperature changes between dietary treatments have implications for larval transport in the field. In temperate regions, succession in phytoplankton communities corresponds to changes in fatty acid concentrations and compositions of larval food (Hayakawa *et al.*, 1996, Parrish *et al.*, 2005). Spawning seasons of *Dendraster excentricus* and

many other marine organisms span the succession of phytoplankton communities (Strathmann, 1987). Larvae released at different times during the spawning season would encounter prey items of different qualities. Our results suggested that dietary treatments had little effect on swimming speeds and that larvae were able to maintain their depth-regulating abilities when temperature changed. An implication of reduced sensitivity to diet and temperature may be less variability in water-column position, and, hence, in long-range larval transport, across long spawning seasons than might otherwise be expected.

Using video-tracking techniques, we obtained detailed quantitative information on larval swimming behaviors and complex responses to environmental conditions that can be used to inform biophysically coupled larval dispersal models. Global climate change is expected to intensify ocean stratification and magnify the temperature changes routinely encountered by small marine ectotherms in estuarine and other marine environments (Cox *et al.*, 2000). Behavioral compensation in helical trajectories suggests marine ectotherms might be better able to regulate their vertical positions in future variable temperature environments than implied by physiology and biomechanics alone.

Figure 2.1

Morphometric characteristics of echinopluteus larva. Solid black lines: body width (BW) and height (BH); dark gray lines: lengths of anterolateral arms (AL), postoral arms (PO), preoral arms (PR), and posterodorsal arms (PD); dotted lines represent the distance between pairs of arms. Note that PR and PD arm pairs are not present in 4-arm larvae

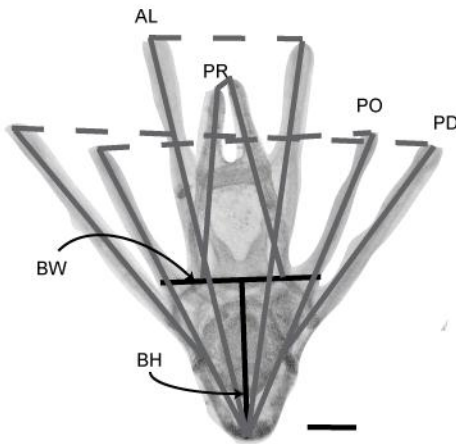


Figure 2.2

- (a) Representative larval swimming trajectories at 20 and 12°C extracted from 6 min video clips of 4-arm larvae raised on *Dunaliella tertiolecta*. Field of view is 30 × 40 mm. Helical widths were significantly smaller after temperature reduction from 20 to 12°C. (b) Relationships of swimming metrics to a 3-dimensional helix

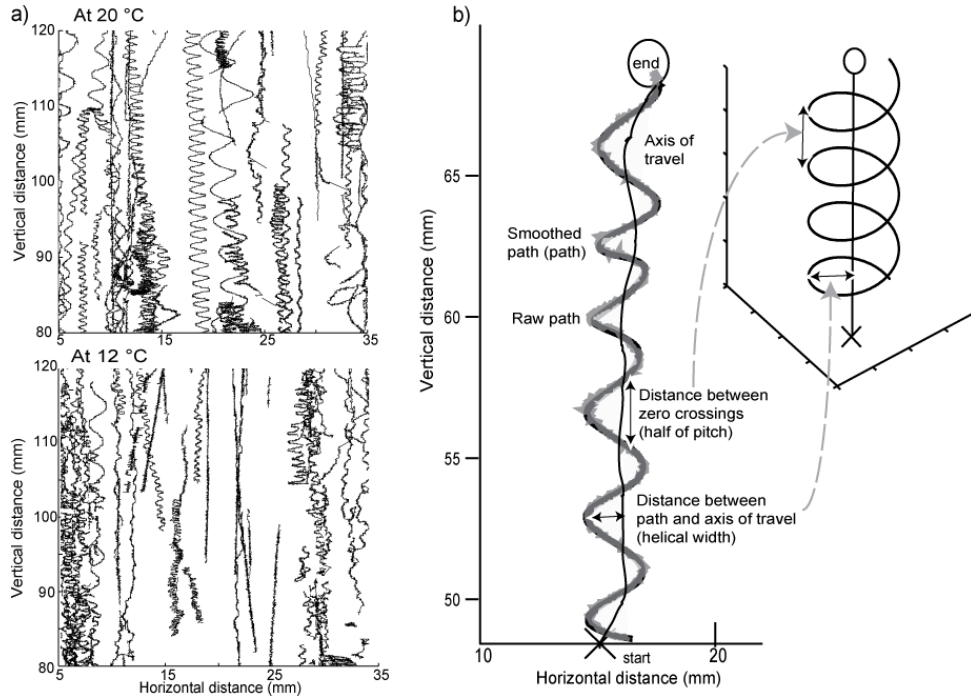


Figure 2.3

Swimming metrics of 4- and 8-arm larvae. Treatments see Table 2.1. Open symbols: means of observations at 12°C; filled symbols: means of observations at 20°C. Error bars: SE of means multiplied by 5

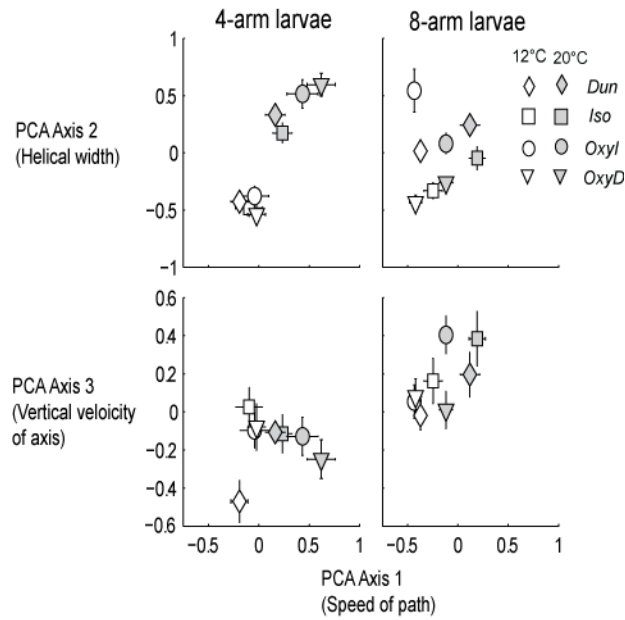


Figure 2.4

PCA Axes 2 and 3 scores plotted against PCA Axis 1 scores. Treatments see Table 2.1. Symbols: means of the scores for each dietary treatment, open: observations at 12°C; filled: observations at 20°C. Error bars: SE of means multiplied by 5.

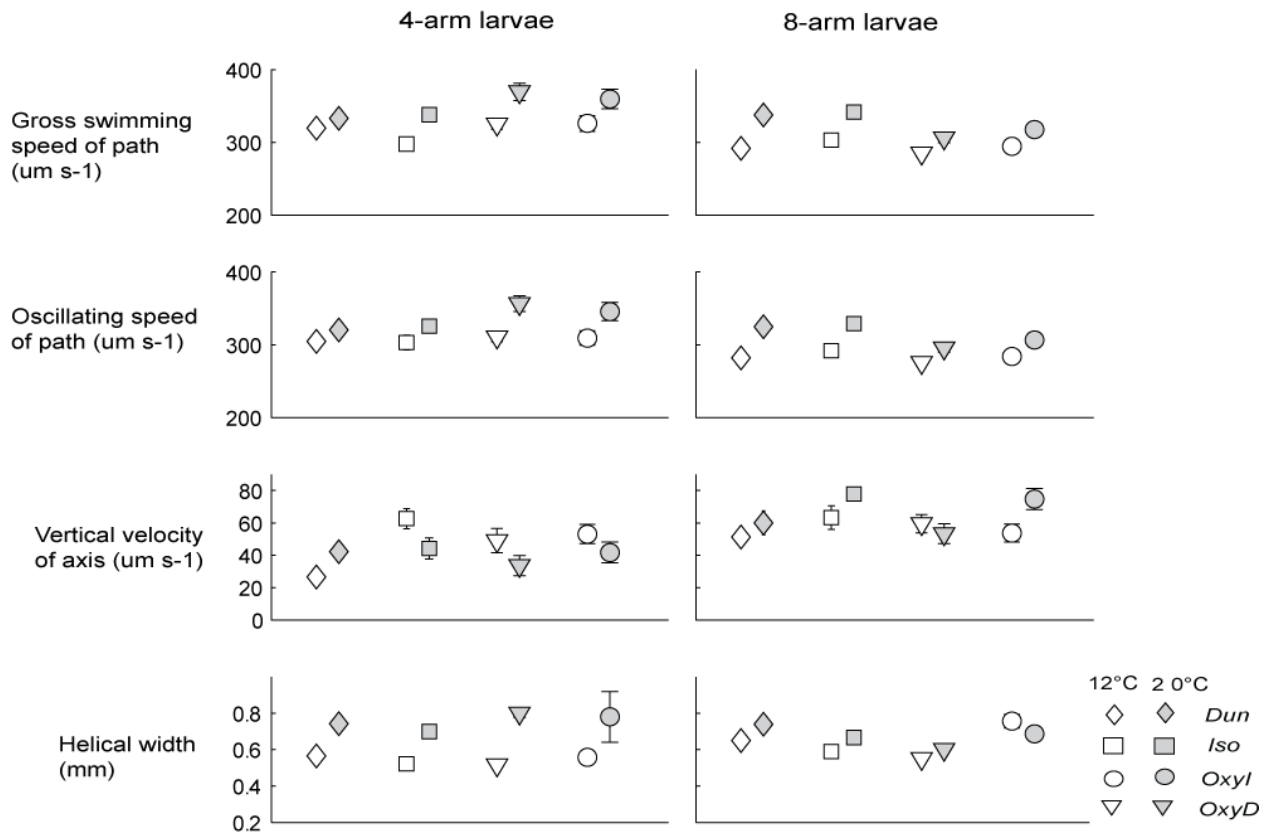


Table 2.1

Means and standard errors of measured morphometrics in microns of 4- and 8-arm *D. excentricus* larvae. Dietary treatments of *Isochrysis galbana*, *Dunaliella tertiolecta*, *Oxyrrhis marina* fed with *I. galbana* and *O. marina* fed with *D. tertiolecta* were abbreviated as *Dun*, *Iso*, *OxyI* and *OxyD*. Bold type indicates significance by a Kruskal-Wallis' test ($p < 0.05$). Underlines show groupings based on Dunn's test.

	<i>Dun</i>	<i>Iso</i>	<i>OxyI</i>	<i>OxyD</i>
4- arm larvae				
Body width	184.3 ± 2.5	186.6 ± 2.0	185.3 ± 2.0	185.7 ± 1.8
Body Height	202.3 ± 1.5	201.5 ± 2.1	200.8 ± 1.6	200.5 ± 1.1
Distance between arms				
anterolateral arm	109.7 ± 2.7	113.3 ± 2.8	114.6 ± 2.7	113.6 ± 2.8
postoral arm	303.4 ± 6.1	304.9 ± 4.4	306.7 ± 4.5	310.1 ± 4.4
Mean arm length				
anterolateral arm	387.9 ± 4.6	379.0 ± 4.5	375.2 ± 5.1	375.5 ± 5.3
postoral arm	425.1 ± 4.2	410.9 ± 5.4	411.9 ± 5.3	418.1 ± 5.3
8- arm larvae				
Body width	209.9 ± 3.3	205.5 ± 3.5	191.9 ± 2.7	187.6 ± 2.2
Body Height	219.2 ± 2.1	214.3 ± 2.0	213.9 ± 2.4	213.3 ± 2.1
Distance between arms				
anterolateral arm	146.6 ± 3.7	141.7 ± 2.9	120.4 ± 3.5	116.9 ± 2.3
postoral arm	376.1 ± 10.9	353.8 ± 9.5	319.6 ± 6.8	300.1 ± 5.5
preoral arm	51.7 ± 1.9	47.4 ± 2.3	47.5 ± 1.5	48.4 ± 1.4
posterodorsal arm	522.2 ± 13.6	580.6 ± 49.4	400.3 ± 11.2	352.5 ± 10.1
Mean arm length				
anterolateral arm	458.8 ± 7.8	454.7 ± 6.8	420.6 ± 6.3	413.8 ± 5.5
postoral arm	443.9 ± 9.3	427.6 ± 8.6	421.1 ± 7.4	406.4 ± 6.7
preoral arm	192.3 ± 8.9	181.8 ± 6.7	115.8 ± 4.5	131.2 ± 7.2
posterodorsal arm	310.2 ± 7.9	314.8 ± 7.7	214.3 ± 6.8	238.9 ± 7.2

unit = μm

Table 2.2

Summary of PCA and parallel analysis results. Rotated component matrix after varimax rotation with Kaiser Normalization was applied. The variables with high loading (> 0.7) for each component are in bold type. Relative variance, cumulative percent, and eigenvalue variance of the correlation are shown for principal components 1 to 3.

	Components		
	1	2	3
	<i>Speed of</i>		
	<i>path</i>	<i>Helical width</i>	<i>Vertical velocity of axis</i>
Total swimming speed	0.960	0.048	0.021
Oscillatory speed	0.960	0.069	0.013
Horizontal velocity of axis of travel	0.217	0.312	- 0.103
Vertical velocity of axis of travel	0.027	-0.075	0.993
Distance between zero crossings	0.568	0.055	0.052
Distance between path and axis of travel	0.065	0.956	-0.082
% of variance explained	49.353	24.398	14.138
Cumulative % of variance explained	49.353	73.751	87.889
Eigenvalue	2.961	1.464	0.848
Parallel analysis for principal components	1.190	1.098	1.030

Table 2.3

Two-way ANOVA table for the effects of temperature and diet on PCA Axes 1 -3 scores. The principal component axes were most significantly affected by speed of path, helical width and vertical speed of axis respectively. Bold type indicates significant difference ($p < 0.05$).

		4-arm larvae				8-arm larvae			
Source		SS	df	f	p	SS	df	f	p
PCA	Temperature	18.39	1	13.31	<0.001	12.29	1	25.54	<0.001
Axis 1	Diet	4.30	3	1.04	0.38	3.48	3	2.41	0.067
	Temperature								
<i>Speed</i>	x Diet	0.91	3	0.21	0.88	0.54	3	0.38	0.77
<i>of path</i>	Error	446.23	323	-	-	155.38	323	-	-
PCA	Temperature	61.01	1	74.45	<0.001	0.255	1	0.27	0.60
Axis 2	Diet	2.26	3	0.92	0.43	22.21	3	7.96	<0.001
	Temperature								
<i>Helical</i>	x Diet	2.53	3	1.03	0.38	7.49	3	2.69	0.047
<i>width</i>	Error	264.70	323	-	-	300.53	323	-	-
PCA		4.81 x 10 ⁻⁵							
Axis 3	Temperature	⁵	1	0.000	0.994	2.63	1	2.55	0.11
	Diet	2.44	3	0.88	0.45	2.92	3	0.95	0.42
	Temperature								
<i>Vertical</i>	x Diet	3.92	3	1.42	0.24	1.97	3	0.64	0.59
<i>velocity</i>	Error	297.92	323	-	-	332.92	323	-	-
<i>of axis</i>									

CHAPTER THREE: EFFECTS OF OCEAN ACIDIFICATION-INDUCED MORPHOLOGICAL CHANGES ON LARVAL SWIMMING AND FEEDING*

3.1 Abstract

Reduction in global ocean pH due to the uptake of increased atmospheric CO₂ is expected to negatively affect calcifying organisms, including the planktonic larval stages of many marine invertebrates. Planktonic larvae play crucial roles in the benthic-pelagic life cycle of marine organisms by connecting and sustaining existing populations and colonizing new habitats. Calcified larvae are typically denser than sea water and rely on swimming to navigate vertically structured water columns. Larval sand dollars *Dendraster excentricus* have calcified skeletal rods supporting their bodies, and propel themselves with ciliated bands looped around calcified projections called “arms”. Ciliated bands are also used in food capture, and filtration rate is correlated with band length. As a result, swimming and feeding performance are highly sensitive to morphological changes. When reared at an elevated pCO₂ level (1000 ppm), larval sand dollars developed significantly narrower bodies at 4- and 6-arm stages. Morphological changes also varied between four observed maternal lineages, suggesting within-population variation in sensitivity to changes in pCO₂ level. Despite these morphological changes, pCO₂ concentration alone had no significant effect on swimming performance. However, acidified larvae had reduced feeding performance, as indicated by significantly smaller larval stomachs and bodies. Adjustments to larval morphologies in response to OA may prioritize swimming over feeding, implying that negative consequences of ocean acidification are carried over to later developmental stages.

* Originally published in Journal of Experimental Biology in November 2011, in Volume 214, pp 3857-3867.

3.2 Introduction

Atmospheric partial pressure of carbon dioxide ($p\text{CO}_2$) has increased by 36% since the 18th century, and over one-third of the anthropogenic CO_2 released to the atmosphere has been absorbed by the surface oceans (Sabine *et al.*, 2004). The $p\text{CO}_2$ level in surface waters has increased by 100 parts per million (ppm) over the past century, and is predicted to continue rising at a faster rate than has been observed in the last 300 million years (Caldeira & Wickett, 2003). Ocean acidification (OA) is the reduction of ocean pH as this CO_2 is hydrated into seawater. Modeling studies suggest that pH levels in the surface ocean will drop by 0.3-0.4 pH units by 2100 (Orr *et al.*, 2005).

A growing body of research suggests this pH drop will affect the physiologies of marine organisms (Pörtner, 2008) and, subsequently, their ecological functions and interactions with other organisms (Widdicombe & Spicer, 2008). In particular, OA is expected to negatively impact calcifying organisms such as reef-building corals (Kleypas *et al.*, 1999), coralline algae (Hall-Spencer *et al.*, 2008), coccolithophores (Riebesell *et al.*, 2000), pteropods (Fabry *et al.*, 2008), molluscs (Gazeau *et al.*, 2007) and echinoids (Wood *et al.*, 2008). These studies have demonstrated that OA could have negative impacts on growth, reproduction, and development in a broad spectrum of calcifying marine organisms (Doney *et al.*, 2009).

Planktonic larvae of many marine invertebrates also possess calcified structures, including shells of molluscan veligers, skeletal rods of echinoplutei and posterior ossicles of auricularia. These calcifying larval stages are likely to be susceptible to changes in ocean pH, and some species are known to be highly (Dupont *et al.*, 2010, Kurihara, 2008). For example, a 0.4 pH unit decrease caused 100% mortality in a larval brittle star, *Ophiothris fragilis* (Dupont *et al.*, 2008). Experimental observations of larvae of other species suggest that reduced pH often has sublethal effects, including decreased larval growth and calcification rates and changes in gene expression patterns (Clark *et al.*, 2009, Kurihara & Shirayama, 2004, O'Donnell *et al.*, 2010). Future environmental stresses, including shifts in ocean pH, are likely to be expressed in many species initially as sublethal effects rather than outright mortality. Predicting

ecological responses for marine communities to environmental changes therefore requires understanding the functional significance of these sublethal responses of larval stages.

Planktonic larvae of sessile marine invertebrates are the primary dispersal mechanism that connects and sustains disjunct populations, and colonizes new habitats (Cowen & Sponaugle, 2009, Gaines & Roughgarden, 1985, Underwood & Fairweather, 1989). Most planktonic larvae are not passive drifters; instead, they use active swimming to regulate their vertical positions in the water column (Chia *et al.*, 1984, Metaxas, 2001, Young, 1995). Because environmental variables such as temperature, direction and strength of advective currents, and concentrations of prey and predators are vertically structured in most marine environments, larval swimming behaviors can significantly affect larval survival and dispersal (North *et al.*, 2008).

Larval swimming behaviors are constrained by morphological characteristics, such as size, shape and propulsive mechanism (Emler, 1990, Emler, 1991). For “armed larvae” – larvae such as echinoplutei that use slender ciliated body extensions for swimming and/or feeding – the length and arrangement of ciliated extensions significantly affects both the weight distribution and the propulsive force generation, and hence important aspects of swimming performance (Grünbaum & Strathmann, 2003).

One key metric of larval swimming performance is stability, i.e., the ability to maintain swimming orientation in spite of perturbations from ambient flows. By experimentally removing the calcite skeleton of echinoplutei, Pennington and Strathmann (1990) demonstrated that larval weight distribution depends strongly on calcite, and that larval skeletons enhance larval stability by acting as counter-weights. Hydrodynamic models have been used to argue that adjustments in arm number, length and elevation angle also strongly affect larval stability (Clay & Grünbaum, 2010, Clay & Grünbaum, 2011, Grünbaum & Strathmann, 2003). Arm elevation angle is a measure of rotation between an arm rod and its projection on the horizontal plane. Hence, a shorter distance between tips of paired arms implies a higher arm elevation angle (Grünbaum & Strathmann, 2003). Their model predicted that higher arm

elevation angles improve stability, minimizing movement towards downwelling water when larvae are exposed to vertical shear. Motion analysis of echinoderm larvae from different taxa conformed to these predictions about larval stability (Strathmann & Grünbaum, 2006). These studies suggest that, although impacts of morphological changes on swimming performance are sublethal, they can nonetheless strongly impact adult population dynamics by altering larval dispersal and survival.

In addition to swimming, morphological changes have implications for other ecological functions. In echinoplutei, ciliated bands looped around larval arms are used both for generating propulsive forces and for filtering food particles. Maximum clearance rate in these larvae increases with the length of the ciliated bands (Hart, 1991). Echinoplutei are known to be phenotypically plastic: larvae develop longer arms when food is limited than when food is abundant (Hart & Strathmann, 1994, Miner, 2005). However, there is a morphological tradeoff including arm length: although longer larval arms increase ciliated band length and enhance feeding efficiency, longer larval arms can also incur the cost of reduced stability in moving water. This is because longer arms cut across more flow lines and increase the destabilizing torque larva experiences, potentially causing it to move into downwelling water or to tumble (Strathmann & Grünbaum, 2006).

In addition to arm lengths, food concentration also affects stomach sizes among echinoids. Under food-limited conditions, larvae develop smaller stomachs and juvenile rudiments. Rudiments are united structures from the amniotic invagination and hydrocoel that give rise to future adults (Hart & Strathmann, 1994). Plasticity in larval stomach size is unlikely caused by food distending the stomach because larval urchins that larvae develop bigger stomachs when reared under high food concentration even before they are capable of particle capture (Miner, 2005). This observation suggests that cues of food availabilities induce changes in morphogenesis of both larval arms and stomachs. Heyland and Hodin (2004) further hypothesized that the thyroid hormone from algal food serves as a signaling cue to accelerate development and initiate metamorphosis. Collectively, these studies strongly suggest that larval nutrition and morphogenesis are tightly coupled.

The functional relationships between arm morphology, swimming performance and feeding success suggests the hypothesis that sublethal changes in larval morphologies observed in OA experiments negatively affect swimming performance, feeding success, or both. Both swimming and feeding have implications for larval survival; degradation of performance in either function may be a mechanism through which effects of OA on larval morphology that are sublethal in the laboratory may nonetheless have significant consequences for wild populations.

In this study, we assessed the functional impacts of OA on swimming and feeding performance of larval sand dollars, *Dendraster excentricus*. Swimming mechanics and behavior of this species have been previously described (Chan & Grünbaum, 2010, Clay & Grünbaum, 2010) Length of ciliated bands of larval sand dollars have also been shown to positively correlate with clearance rates (Hart & Strathmann, 1994, Miner, 2005). Because within-population variation in sensitivity to changes in pH has been suggested for other echinoids (Byrne *et al.*, 2010), we compared the sublethal responses of larvae from four maternal lineages. For each of these lineages, we reared the larvae under two pCO₂ concentrations, documented the corresponding larval morphologies, and quantified swimming performance with non-invasive video tracking techniques.

3.3 Materials and methods

CO₂ incubations

Larval *Dendraster excentricus* Eschscholtz 1831 were raised under two different concentrations of pCO₂, chosen to reflect CO₂ emission scenarios predicted by the Intergovernmental Panel on Climate Change: 380 ppm (present-day atmospheric CO₂ level) and 1000 ppm (A1FI “business as usual scenario”) (IPCC, 2007). Seawater was 0.22 µm-filtered and batch-equilibrated with gas blends, prepared by combining pure CO₂ and CO₂-free air to reach 380 and 1000 ppm. Hereafter, we refer to these two treatments as “present-day” and “acidified”, respectively. We measured the pH of each culture vessel twice a day using an Orion 720A meter and a ROSS Ultra combination electrode calibrated with Nation

Bureau of Standards buffers (Thermo Scientific Corp., Beverly, MA, USA). Water samples from the batch equilibration buckets were collected and fixed in accordance with SOP1 of Dickson et al. (2007) at the beginning and middle of the experiment. Samples were analyzed for total alkalinity (A_T) and total dissolved inorganic carbon (DIC) by NOAA's Pacific Marine Environmental Laboratory. Analysis of these samples showed that the experimental conditions matched the expected values closely, with mean pH values of 8.06 and 7.75, respectively. The present-day treatment at the beginning and middle of the experiment had A_T values of 2124.68 and 2113.63 $\mu\text{mol kg}^{-1}$ and DIC values of 1892.3 and 1889.5 $\mu\text{mol kg}^{-1}$, respectively. The acidified treatment at the beginning and middle of the experiment had A_T values of 2126.95 and 2108.57 $\mu\text{mol kg}^{-1}$ and DIC values of 2030.8 and 2023.6 $\mu\text{mol kg}^{-1}$, respectively.

Larval cultures

Adult sand dollars, *D. excentricus*, were collected from Crescent Beach, East Sound, Orcas Island, WA, USA in early summer 2009 and maintained in sea tables at the Friday Harbor Laboratories until use. Spawning was induced by injecting 0.5-1 mL of 0.55 M KCl into the coelomic cavity (Strathmann, 1987). Collected eggs were washed through a 200 μm sieve placed in a beaker with 1000 mL of 0.22 μm -filtered seawater and fertilized with 5 drops of sperm. Ten minutes after fertilization, the eggs were examined under a microscope for the presence of fertilization envelopes to confirm fertilization success. Four maternal lineages were created by fertilizing eggs from 4 females with sperm from a single male, and were labeled as females 1 to 4. Egg sizes did not differ significantly between females (mean diameter \pm s.e. = $123.8 \pm 8.1 \mu\text{m}$, $n = 40$, ANOVA, $F_{3,36} = 1.73$, $p = 0.177$).

Ten hours post-fertilization, gastrulae were transferred into 24 glass jars, each 3.7 L, providing 3 replicates for each maternal lineage within each of the two CO_2 treatments. Because movement of meshchyme cells occur after hatching (Decker & Lennarz, 1988), exposure at hatching enabled us to assess the effects of CO_2 treatment on larval development and swimming throughout spicule and endoskeleton formation. Our experimental protocol implies that our study may underestimate the overall

functional impact of OA, because other developmental processes such as fertilization and cleavage took place at the present-day pCO₂ level.

Larvae were reared under gentle bubbling with the respective pre-mixed CO₂ gases at 20°C ± 1°C in 0.22 µm-filtered seawater at a density of approximately 2 individual mL⁻¹. Water was changed every other day with present-day and acidified seawater. Larvae were fed with an equal mixture of the algae *Rhodomonas lens* and *Dunaliella tertiolecta* at 5000 cells mL⁻¹. After algal concentration was determined with a haemocytometer, cells were concentrated by centrifugation and subsequently resuspended in filtered seawater from the respective CO₂ treatments. Food was added 12 hours prior to water changes to minimize the effect of photosynthesis by algal food on carbonate chemistry.

Behavioral observations and video processing

To assess the functional impact of exposure to elevated pCO₂ through larval development, we observed swimming behaviors of 4-, 6- and 8-arm larvae from the two pH treatments and four maternal lineages using video tracking analysis, following the methods of Chan and Grünbaum (2010). In brief, approximately 300 larvae from each treatment (~100 larvae from each replicated culturing jar) were pipetted into one of four Plexiglas® chambers (3.5 cm x 3.5 cm x 30 cm) submerged in a common water bath at a constant temperature (20°C). Larvae from different pH treatments were observed in filtered seawater equilibrated to their respective rearing pCO₂ levels. Larvae were allowed to acclimate for ten minutes, and then were gently stirred. After five additional minutes for transient water movement to dissipate prior to filming, movements of individuals were recorded under infrared illumination with digital camcorders (Panasonic DS400) at 15 frames per second. Video clips were captured in a series of vertical “casts” that sequentially imaged lower (0– 14.4 cm) and upper (11.6 – 25 cm) regions of each chamber. Each cast took 10 min: 3 min videos captured in each region of each chamber, 3 min to move cameras, plus 1 min pause. Six casts were performed in each observation. Observations were replicated three times for each developmental stage (4-, 6- and 8- arm stages). Under this sampling scheme, larvae from each maternal lineage in each pH treatment had a total of 18 casts at each developmental stage.

We also tested for swimming responses to short-term changes in pCO₂ in 4-arm larvae from two of the maternal lineages reared under present day conditions. We exposed these larvae to either present-day or acidified seawater for 60 minutes, while observing their swimming behaviors using the video protocol described above.

Video clips were analyzed by equalizing lighting, removing background variations, distinguishing moving larvae based on brightness and size, and extracting the pixel coordinates of larvae with a customized version of the video editing package avidemux2.4. Videos were calibrated with a grid of 2 mm x 2 mm squares, with 4 mm distances between each of their centers. Pixel coordinates were converted to physical positions and assembled into larval swimming trajectories using Tracker3D, an in-house MATLAB program (Fig. 3.1; see Clay and Grünbaum, 2010 for details).

Morphometric analysis

At the end of each observation, larvae were relaxed in MgCl₂ and fixed in buffered 2% formaldehyde. Individuals were photographed under a microscope at 16x using a Nikon E4500 digital camera. Arm lengths, distances between pairs of arms, body lengths and widths, and stomach lengths and widths of 10 individuals from each observation chamber were measured with ImageJ (Abramoff *et al.*, 2004); 2 pH treatments x 4 maternal lineages x 3 replicated observations x 3 stages x 10 individuals, total n = 720), using photographs of a stage micrometer for calibration (Fig. 2). Projected stomach size was computed by assuming the stomach is an ellipsoid (Heyland & Hodin, 2004).

Because the observed morphological characteristics are correlated, we performed a Principal Component Analysis (PCA) on the correlation matrix of morphological characteristics at each stage with varimax rotation using Kaiser Normalization to identify key components (Harris, 1975). The number of factors to retain was determined by eigenvalues and the shape of the scree plot. Because larval *Dendraster excentricus* add arms as they develop, the number of observed morphological characteristics increased with time. Though larvae were reared in separate jars, they were pooled prior to their video

observation and fixation. Therefore, we could not assess jar effects, which are instead subsumed into the error term. We assessed the effect of the main factors, pH and maternal lineage, on larval morphology using a 2-way analysis of variance (ANOVA) for each stage (Zar, 1996).

Swimming performance analysis

Our analysis of swimming metrics followed the methodology of Chan and Grübaum (2010). To avoid including passive particles in our analysis, only larval trajectories longer than 15 s and having horizontal acceleration $> 0.06 \text{ mm s}^{-2}$ in magnitude were included in the statistics. Individual trajectories were further subdivided into net up-swimmers and down-swimmers based on their net vertical displacement. Limited by the resolution of our video observation, we were not able to distinguish if down-swimmers were swimming with their arms pointing downwards, reversing their ciliary beat, or passively sinking with ciliary arrest. We applied cubic smoothing splines with different knot spacings to remove frame rate noise while defining each larval swimming trajectory (hereafter, *path*) and to identify the overall direction of travel (hereafter, *vertical axis of travel*).

For each trajectory, we computed the larva's total swimming speed by taking the first time derivative of the path, and the net vertical and horizontal velocities by dividing the displacement between the start and end points of the axis of travel by the path duration. Larval sand dollars typically swim in a helical manner. Two dimensional (2D) projections of helical paths, which appear as sinusoids, underestimate horizontal movement. To compensate for this underestimate, we applied a correction factor of $\pi/2$ to mean horizontal speed components. The vertical axes of the helices represent the overall direction of travel and the actual larval paths oscillated along these axes. To quantify the oscillating nature of the path, we also computed *oscillatory speed* as the time derivative of the distance between the path and the vertical axis. We used the maximum horizontal distance between the path and the axis as a measure of helical width. We further characterized the shapes of swimming trajectories by quantifying *zero crossings*, defined as points at which the path and the axis intersect. The distance between zero crossings is a measure of helical pitch (see Fig. 2 in Chan and Grünbaum, 2010).

We computed weighted means of swimming metrics for each vertical cast by sampling at 5 s intervals and taking the mean of swimming metrics of all larval trajectories observed at those time points. This scheme gives equal statistical weight to each frame in which each larva was tracked, avoiding bias towards shorter or longer trajectories. Initial analysis showed that the mean swimming speeds of larval sand dollars in both treatments were approximately 0.3 mm s^{-1} , similar to the value reported by Podolsky and Emler (1993). Assuming an even distribution at the beginning of the experiment, we estimated that most larvae would have left the field of view (0-25 cm) within the first fifteen to twenty minutes of observation. To avoid a bias towards slow-swimming individuals, we subsequently used only data collected from the first two casts (i.e., the first 20 minutes of the experiment) in the statistical comparisons.

The effects of CO₂ treatment, maternal lineages and their interactions on larval swimming performance were tested with a 2-way analysis of covariance (ANCOVA) with developmental stage as a covariate. In the experiment on 4-arm larval responses to short-term changes in pCO₂ level, a 2-way ANOVA was used to test for effects of CO₂ treatment and maternal lineages. We performed post-hoc Tukey's tests when significant differences ($p < 0.05$) in component scores were detected (Zar, 1996). All statistical analyses were conducted in PASW 18.0.

3.4 Results

Morphometric analysis

Across all observed developmental stages, acidified larvae had narrower larval bodies than those reared in present-day treatments. In the 6- and 8- arm stages, acidified larvae also had smaller larval stomachs. Maternal lineage and the interaction of CO₂ treatment with maternal lineage also had significant effects on morphologies in 6- and 8-arm larvae (Tables 3.1 & 3.2, Fig. 3.2). In particular, larval arms were shorter in the acidified treatments for 6- and 8- arm offspring of females 1 and 2, but not offspring of females 3 and 4 (Table 3.1).

In 4-arm larvae, PCA Axis 1 was most correlated to the width of the larval body and distance between tips of pairs of arms (Table 3.2). PCA Axis 2 was most correlated to stomach size. PCA Axis 3 was most correlated to lengths of arms. 2-way ANOVA of the PCA component scores showed that acidified larvae had narrower body widths (PCA Axis 1 score, $p = 0.03$), but there were no significant differences between the two CO₂ treatments in stomach size or arm lengths (PCA Axis 2 & 3 score). Maternal lineage alone did not have a significant effect on any of the PCA Axis scores. However, there was a significant interactive effect of CO₂ treatment and maternal lineage on larval body width (PCA Axis 1 score, $p < 0.001$).

In 6-arm larvae, PCA Axis 1 was most correlated with larval body width, body length:width ratio, and distances between tips of each pair of anterolateral and postoral arms. PCA Axis 2 was most correlated to stomach size. PCA Axis 3 was most correlated to the lengths of anterolateral and posterodorsal arms (Table 3.2). 2-way ANOVA of PCA component scores showed that acidified larvae had narrower larval bodies (PCA Axis 1 scores; $p < 0.001$) and smaller larval stomachs (PCA Axis 2 scores; $p = 0.006$), and had significantly shorter anterolateral and posterodorsal arm lengths (PCA Axis 3 scores; $p = 0.009$). Maternal lineage had significant effects on all 3 PCA component scores (Tables 3.1 & 3.2): *a*) larval body widths were wider in offspring of female 4 than in offspring of the other 3 females (PCA Axis 1 scores; $p < 0.001$); *b*) stomach sizes of offspring of females 1 and 3 were smaller than those of the offspring of female 4 (PCA Axis 2 scores; $p = 0.002$); and *c*) arm lengths of offspring of female 1 were shorter than those of female 4 (PCA Axis 3 scores; $p < 0.001$). There were also significant interactive effects of CO₂ treatment and maternal lineage on all three PCA Axis scores (Table 3.2).

In 8-arm larvae, PCA Axis 1 was most correlated with larval body width; distances between anterolateral, postoral and posterodorsal arms; and lengths of anterolateral, posterodorsal and preoral arms. PCA Axis 2 was most correlated to stomach size. PCA Axis 3 was most correlated to length of larval body and body length:width ratio (Table 3.2). 2-way ANOVA of PCA component scores showed that acidified larvae had significantly smaller larval stomachs (PCA Axis 2 score; $p < 0.001$). However, CO₂

treatments did not significantly affect PCA Axes 1 and 3 scores. To further investigate the effect of CO₂ treatments, we performed a 2-way ANOVA on the raw measurements of individual morphological characteristics, after confirming that the data were normally distributed and had equal variance. Comparing morphological characteristics individually suggested that acidified larvae had significantly narrower bodies ($F_{1,233} = 23.569$, $p < 0.001$), shorter distances between tips of anterolateral and postoral arms ($F_{1,233} \geq 6.33$, $p < 0.01$), and shorter preoral, postoral and posterodorsal arms ($F_{1,233} \geq 11.8$, $p < 0.001$). Non-significance of differences between the two CO₂ treatments in PCA Axis 1 scores was most likely driven by the lack of significant differences across treatments in anterolateral arm lengths and in distances between tips of posterodorsal and preoral arms. Maternal lineage had significant effects on all 3 PCA component scores: *a*) larval body widths were wider and arm lengths were longer in offspring of female 4 than in offspring of females 1 and 3 (PCA Axis 1 scores; $p = 0.001$); *b*) offspring of female 4 had the largest stomach, and offspring of female 2 had larger stomachs than offspring of females 1 and 3 (PCA Axis 2 scores; $p < 0.001$); and *c*) offspring of females 1 and 3 had longer body lengths than offspring of female 4 (PCA Axis 3 scores; $p = 0.003$). There were significant interactive effects of CO₂ treatment and maternal lineage on larval body width (PCA Axis 1 scores; $p < 0.001$), stomach size (PCA Axis 2 scores; $p = 0.04$) and larval body length (PCA Axis 3 scores, $p < 0.001$).

Swimming performance analysis

Larval developmental stage had a significant effect on total speed, oscillatory speed, and net vertical and horizontal velocities of both up- and down-swimming individuals, such that swimming speeds increased with larval stage (Fig. 3, Table S1, $F_{1,129} \geq 5.32$, $p \leq 0.02$). Developmental stage also affected the shape of swimming trajectories for up-swimming individuals: older larvae swam in wider helices (Table 3.4, $F_{1,129} = 4.32$, $p = 0.04$). However, CO₂ treatment alone did not have a significant impact on any swimming metrics. Maternal lineage significantly affected net horizontal velocity ($F_{3,129} = 4.32$, $p = 0.01$) and helical pitch ($F_{3,129} = 7.12$, $p < 0.001$) among up-swimming individuals, but there was no significant maternal effect on any swimming metrics of down-swimming individuals. There were no

significant interaction effects between CO₂ treatment and maternal lineage on any swimming metrics (Fig. 3.2, Table 3.4).

Short-term changes in the pCO₂ level in the surrounding water had no effect on swimming speeds or helical parameters (Table 3). Maternal lineage had a significant effect on the helical geometry of the swimming trajectories of down-swimming individuals, both in pitch ($p = 0.02$) and width ($p < 0.001$), despite there being no significant morphological differences between the two observed lineages. There were no significant interaction effects between CO₂ treatment and maternal lineage on any swimming metrics (Table 3.3).

3.5 Discussion

Ocean acidification (OA) negatively affects many calcifying organisms, including many planktonic marine invertebrate larvae that are believed to be highly vulnerable to environmental changes (Kurihara, 2008). In our experiments, growth under acidified conditions induced morphological changes in larval *D. excentricus*: when reared in a pCO₂ concentration of 1000 ppm, larvae had narrower bodies and smaller stomachs and, in the last observed stage, shorter arms. Previous modeling and experimental observations have suggested that such changes in larval morphology are likely to alter swimming performance (Clay & Grünbaum, 2010). However, the morphological changes observed in our study were not associated with negative impacts on the measured swimming performance metrics. There were also no observable changes in swimming metrics during short-term (1 hour) exposure to changes in ambient pCO₂ concentration. Both our video observations and hydrodynamic modeling suggest that the morphological changes were coordinated to preserve swimming performance, an ecologically important function. However, the fact that acidified larvae in our study had smaller stomachs, coupled with previous observations that stomach size reflects larval nutrition, suggests that the negative effects of OA on early stages were carried over to later stages.

OA-induced morphological changes may compensate for stability loss

The morphological effects we observed are consistent with previous studies in which OA negatively impacted growth and physiology of other larval urchins (Clark *et al.*, 2009, Kurihara, 2008, O'Donnell *et al.*, 2010). However, those studies on larval urchins were short (2-4 days) and the larvae were not fed. We monitored growth of fed larval sand dollars for 10 days, over 60% of their approximately 14-16 day larval duration at 20°C (Strathmann, 1987). Our observations showed consistent differences in larval morphologies between pH treatments at all three developmental stages. Though feeding provided additional resources to potentially compensate for OA impacts, the acidified larval sand dollars we observed remained smaller throughout their development than their siblings reared under present-day pCO₂ conditions (Fig. 3. 2, Table 3.2).

Under high pCO₂ level, larval urchins showed significantly reduced calcification (Clark *et al.*, 2009). Similarly, our acidified sand dollars were smaller and showed no sign of increased skeletal rod thickness or decreased fenestration under polarized light (Chan, pers. obs.), suggesting an overall reduction in calcification. A number of possible mechanisms could have led to reduced calcification under OA, including decreased carbonate ion availability, increased metabolic cost to deposit calcite, and increased dissolution rate (Doney *et al.*, 2009). Regardless of the underlying mechanisms, one implication of reduced calcification is that, under acidification, the total amount of skeletal material that an individual can possess is limited.

Smaller size and reduced calcification has at least two biomechanical consequences for larval swimming performance. First, hydrodynamic models indicate that isometric shrinking of “armed larvae” reduces their stability (Grünbaum & Strathmann, 2003). Second, because larval weight distribution is strongly dependent on calcite, reduced calcification (e.g. reduction or elimination of counterweights) further compromises larval stability (Pennington & Strathmann, 1990). Hence, through both mechanisms, a likely consequence of OA is a decreased ability to maintain oriented, directional swimming in moving water.

Hydrodynamic models suggest two hypothetical morphological adjustments that could at least partially restore stability to larvae with limited calcification (Grünbaum & Strathmann, 2003). The first possible adjustment is shortening skeletal arm rods, which would reduce the destabilizing torque imposed on larvae by shearing flows. The second possible adjustment is increasing arm elevation angles, which would increase the stabilizing torque by increasing the separation distance between the centers of buoyancy and gravity. This first adjustment is likely to negatively impact feeding, because particle capture rate is dependent on the total length of the ciliated band around the larval arms. There is no known strong relationship between feeding performance and the second adjustment, i.e. increasing arm elevation angles (though other swimming performance metrics, such as weight-bearing capacity, may be compromised). If both swimming and feeding performance are to be preserved under OA, the tradeoff between swimming stability and feeding efficiency suggests that growth leading to high arm elevation angles would be favored, and shortening arms would be disfavored.

The 4-, 6- and 8-arm acidified larvae we observed had narrower bodies than those reared under present-day conditions. There was no significant difference in arm lengths or body heights between pH treatments at the 4- and 6-arm stages. These observed morphological changes are consistent with the second hypothetical morphological adjustment to increase stability. Arm elevation angles in plutei are determined by the attachment points of transverse body rods, determined by body width and height, and by the lengths of arm rods (Fig. 3.2). Shortening transverse rods without commensurate movement of their attachment points narrows the larval body, elevates larval arms to increased angles, and hence increases stability in shear.

The 8-arm acidified larvae we observed, in addition to narrower bodies, also had shorter larval arms than their siblings reared under present-day conditions. A possible explanation may be that limitation on calcification became so extreme at this larval stage that preserving arm lengths was no longer physiologically possible. Because larval sand dollars develop juvenile rudiments at the 8-arm stage, it is also possible that acidified 8-arm larvae had shorter arms because the energy provided by feeding

could not support concurrent growth of larval body and rudiment, or that the relative payoff for investment in juvenile structures becomes more favorable at this stage than investment in a larval body that will soon be discarded.

Swimming performance was maintained despite morphological changes

In contrast to stage-dependent morphological changes, which are known to impact swimming (Clay & Grünbaum, 2010), the OA-induced morphological changes in our experiments were not associated with significant effects on larval swimming performance metrics (total speed, oscillatory speed, and net vertical velocity; Table 3.4, Fig. 3.2).

In addition to coordinated morphological changes, another possible mechanism through which larval sand dollars may have maintained consistent swimming is by modulating ciliary beat patterns. Reversals in ciliary beat during particle capture have been described in detail (Strathmann, 1975), but more subtle shifts such as those potentially involved in swimming adjustments have not been explored. Previous observations suggesting that facultative changes in ciliary beat pattern may be possible were reported by Chan and Grünbaum (2010), who observed apparent behavioral compensation for temperature decreases that maintained vertical swimming speeds despite reductions in total swimming speed. This compensation was reflected in reduced widths of helical trajectories, which had the effect of reducing the total distance traveled for a given vertical excursion. Because changes in trajectory characteristics occurred over short timescales (minutes), morphological adjustments are a less likely mechanism for compensation than rapid behavioral adjustments such as shifts in ciliary beat.

Impact of OA carried over to later stages by reducing feeding performance

Our acidified larvae, though fed, had reduced stomach sizes. Several possible explanations may account for this observation. Each of these interpretations suggests that OA negatively impacts larval nutrition.

One possible explanation for smaller stomachs for acidified larvae is that acidification affects ciliary beat pattern and reduces particle capture efficiency. Ciliary reversals, and hence, particle capture, in echinoplutei are associated with the opening and closing of calcium ion channels (Hart, 1990). It is possible that changes in pH affect ionic exchanges such that ciliary reversal and hence particle captures occur less frequently. Consistent with this hypothesis, Stumpp et al. (2011b) reported that the number of algal particles ingested by acidified larval purple urchins decreased with a 0.4 unit drop in pH. A likely byproduct of fewer ciliary reversals is more propulsive force generated per unit time. If this interpretation is true, it opens up a promising avenue of research on the tradeoff between feeding and swimming at the ciliary level.

A second hypothesis for small larval stomach size in acidified larvae is that acidification elevates larval metabolism, increasing the digestion rate, and therefore decreasing stomach distention. If so, an implication is that the elevated metabolic demands of acidified larvae were not met in our experiment. This is consistent with smaller overall sizes we observed in acidified larvae. A third hypothesis is that larval sand dollars may be responding to OA stress in a way similar to starvation, i.e. by growing longer arms and smaller stomachs. However, observed arm lengths of acidified larvae were not significantly longer than their siblings across all stages, this differs from the standard starvation response, and suggest that larvae were not able to compensate for food limitation stress by growing longer arms.

Regardless of the underlying mechanism that led to the observed smaller stomach sizes, our data and that of other studies consistently suggest that acidification has negative impacts on larval nutrition. It has long been established that larval nutritional conditions have significant impacts on the success of post-settlement stages (Pechenik *et al.*, 1998). These impacts suggest that the negative effects of OA on feeding, though sublethal in the laboratory at early larval stages, are likely to carry over to subsequent developmental stages and have significant population-level consequences under natural conditions.

Putting our experimental observations into an ecological context, our experimental sand dollars were collected in East Sound, a shallow embayment in Washington, USA. Intertidal areas experience large diurnal fluctuations in pH (Wootton *et al.*, 2008) and in upwelling areas, such as the Washington Coast, pH of the surface water is influenced by acidic deep waters (Feely *et al.*, 2008). It is therefore possible that sand dollars are acclimated to variations in pH level, at least within our experimental range. In the face of an apparent tradeoff between swimming and feeding performance, preserving swimming over feeding performance under acidified conditions might have been less deleterious than its converse. Larval sand dollars are known to uptake dissolved organic matter (Davis & Stephens, 1984) and to complete metamorphosis even under low food concentrations (Boidron-Metairon, 1988). This ability to cope with low feeding rates suggests that the immediate negative consequences of failure to swim (e.g., an inability to avoid predators and/or locate settlement sites) may outweigh the long term cost of smaller juveniles. If that were the case, larval morphologies that result in good swimmers but poor eaters could be beneficial for larval survival (Strathmann & Grünbaum, 2006).

Sensitivity to OA varied between families within a population

Both maternal lineage and its interaction with CO₂ treatment had significant effects on larval morphology (Table 1, 2), suggesting that there is among-family variability in sensitivity to changes in pCO₂. The differences we observed between offspring of different females probably did not result from variations in maternal provision, because egg size did not differ between females and because larvae were fed throughout the experiment (Bertram & Strathmann, 1998). Byrne *et al.* (2010) hypothesized that there is substantial within-population variation in OA sensitivity. Byrne *et al.* (2010) also suggested that polyandry vs. single male-female crossing could explain the contradiction between their results and those of Havenhand *et al.* (2008) concerning effects of OA on fertilization success in the urchin *Heliocidaris erythrogramma*. Our results show that there is indeed substantial within-population variation in OA sensitivity, at least in sand dollars. For example, had we made observations only on offspring of female 4 at the 8-arm stage, we would have concluded that acidified larvae were bigger and had a higher total swimming speed. However, our conclusion would have been the opposite had we observed only offspring

of female 1 (Table 3.1, Fig. 3.3). Variation of this kind reinforces the importance of including multiple parental lineages in future OA experiments, to reduce variability between experimental runs (Evans & Marshall, 2005), to make population-level generalizations more reliable, and to better predict community-level responses to changing environments.

Figure 3.1

Representative larval swimming trajectories under acidified and present-day conditions from 3 min video clips of 8-arm larval *Dendraster excentricus*. Size of the field of view is 25 × 35 mm. The bottom left hand corner of each chamber is considered the origin.

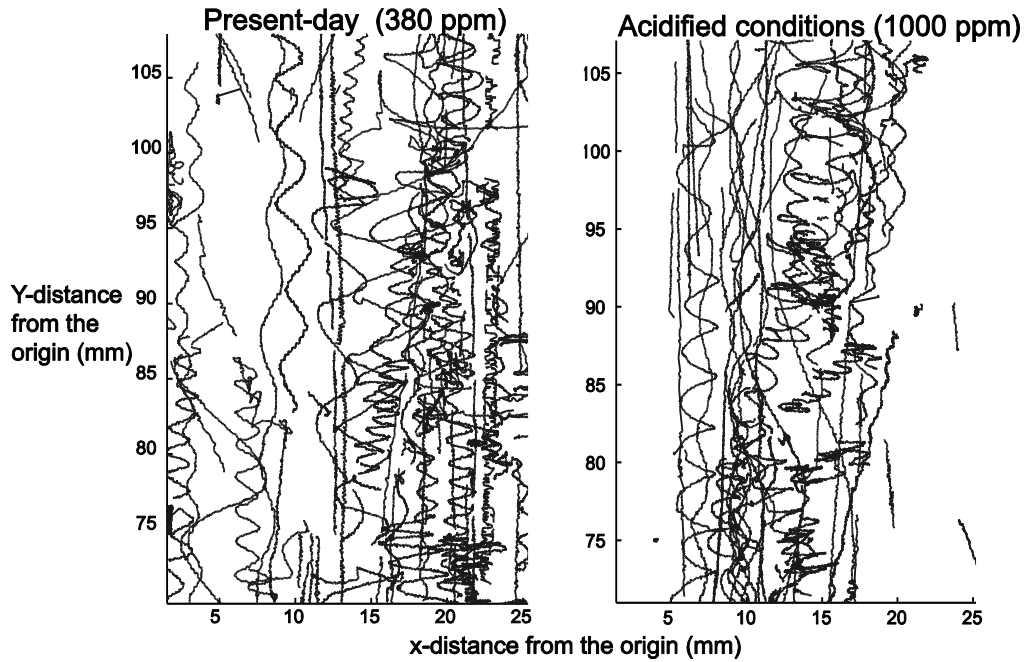


Figure 3.2

Representative *D. excentricus* from acidified and present-day treatments at 4-, 6- and 8- arm stage (top three rows). Measured morphological characteristics include body width (BW), body length (BL), stomach width, stomach length, lengths of anterolateral arms (AL), postoral arms (PO), preoral arms (PR) and posterodorsal arms (PD) and the distances between arm tips. Note that 4-arm larvae have not developed PR and PD and 6-arm larvae had not development PR fully. Scale bars represent 100 μ m. The last row illustrates the geometric relationship between larval body width, arm length and arm elevation angle.

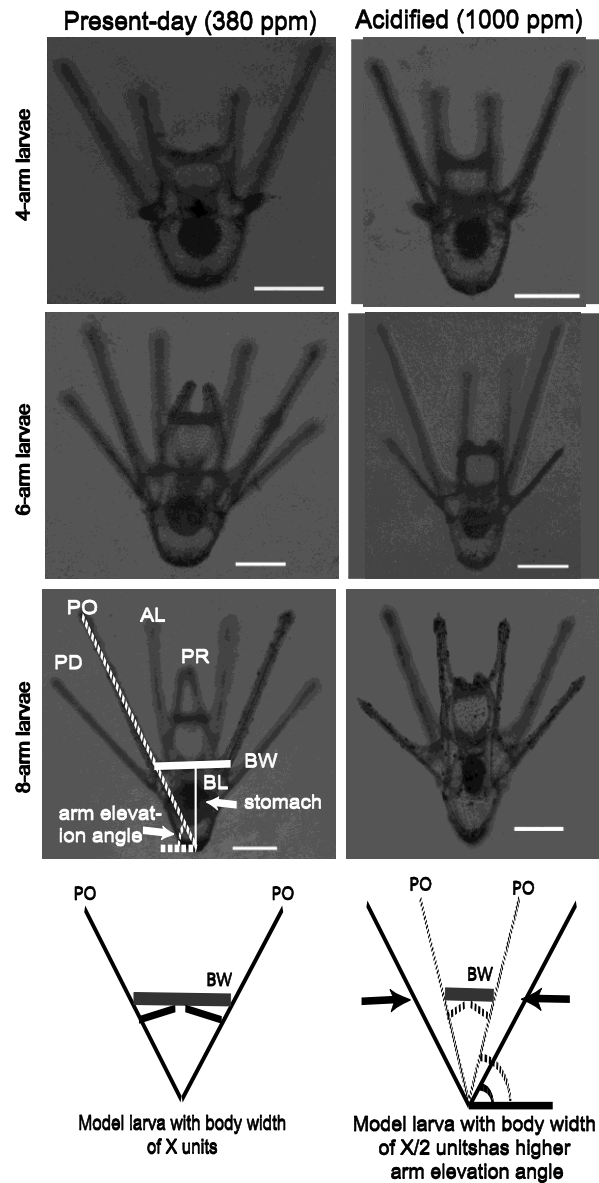
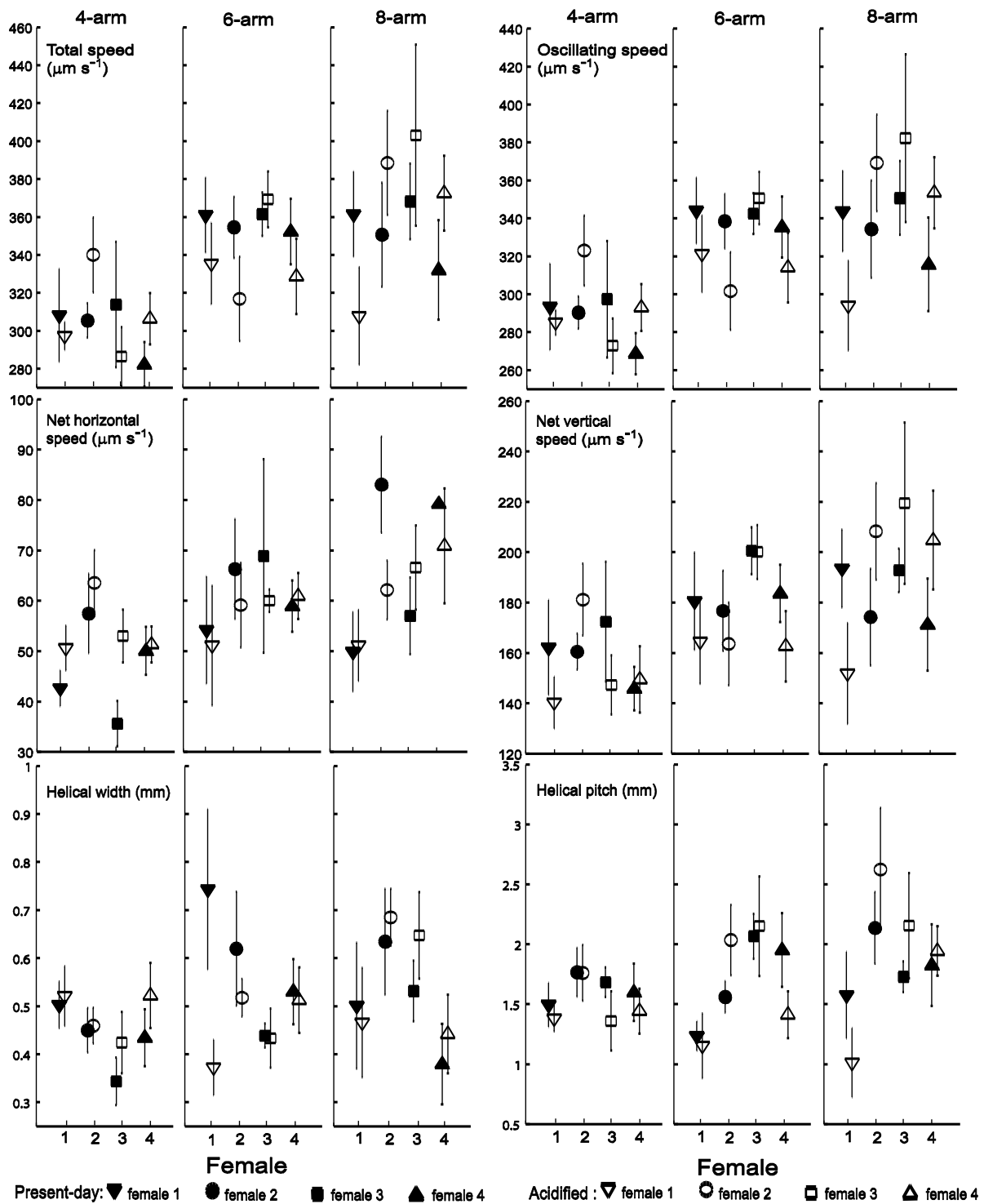


Figure 3.3

Swimming metrics (means \pm s.e.m.) of larval *Dendraster excentricus* in acidified and present-day treatments at 4-, 6- and 8-arm stages: (a) net up-swimming and (b) net down-swimming. Symbols denote different maternal lineages. Closed symbols represent larvae in the present-day treatment (380 ppm) and open symbols indicate larvae in the acidified treatment (1000 ppm).

Swimming metrics of up-swimming individuals



Swimming metrics of down-swimming individuals

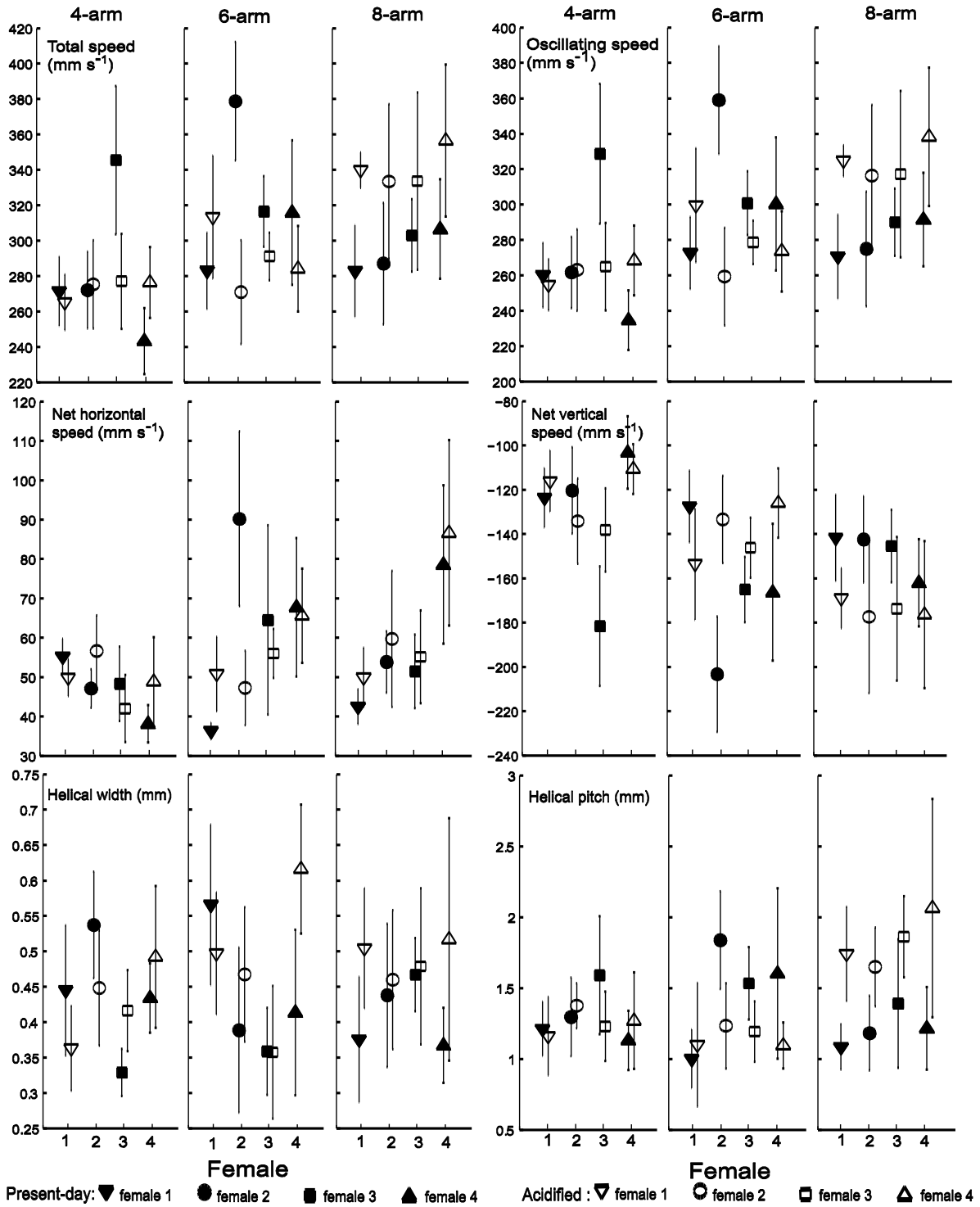


Table 3.1

Morphometrics of 4-, 6- and 8-arm larval *Dendroaster excentricus* (means \pm s.e.m.; units are in μm , except $\times 1000 \mu\text{m}^3$ for stomach volume) from four maternal lineages and two CO_2 treatments (present-day at 380ppm and acidified at 1000 ppm). Abbreviations for arms are AL for anterolateral arm, PO for postoral arm, PD for posterodorsal arm, and PR for preoral arm.

Female CO2 treatment	#1		#2		#3		#4	
	380	1000	380	1000	380	1000	380	1000
4- arm stage								
Width	172.4 \pm 3.5	157.9 \pm 4.1	167.0 \pm 4.2	158.0 \pm 3.6	164.1 \pm 2.6	150.3 \pm 3.6	162.2 \pm 3.8	176.5 \pm 3.1
Height	185.6 \pm 2.6	188.5 \pm 3.1	187.7 \pm 2.1	196.2 \pm 6.9	182.5 \pm 2.7	190.3 \pm 2.5	190.8 \pm 3.3	186.1 \pm 2.6
AL distance	124.7 \pm 9.5	96.3 \pm 6.5	101.3 \pm 7.4	91.9 \pm 6.5	108.3 \pm 6.6	78.3 \pm 7.8	86.5 \pm 5.4	102.6 \pm 4.8
PO distance	360.1 \pm 10.2	314.7 \pm 13.5	356.4 \pm 13.9	330.9 \pm 16.5	326.2 \pm 7.5	299.8 \pm 10.0	320.4 \pm 8.5	353.1 \pm 8.8
AL length	385.5 \pm 8.5	397.4 \pm 9.2	403.2 \pm 8.7	400.4 \pm 5.4	392.2 \pm 7.2	403.4 \pm 6.3	390.5 \pm 9.0	397.3 \pm 7.8
PO length	482.3 \pm 9.4	485.2 \pm 9.6	486.7 \pm 6.0	486.3 \pm 9.7	458.4 \pm 10.4	484.5 \pm 7.2	473.7 \pm 8.7	460.9 \pm 8.7
Stomach length	82.0 \pm 1.5	79.8 \pm 2.2	81.3 \pm 4.1	83.6 \pm 2.2	84.8 \pm 1.8	79.2 \pm 3.9	83.9 \pm 2.0	80.8 \pm 1.5
Stomach height	62.5 \pm 1.2	55.5 \pm 1.4	56.6 \pm 2.6	56.6 \pm 1.5	60.6 \pm 1.0	52.8 \pm 1.1	58.4 \pm 1.3	62.5 \pm 2.1
Stomach volume	16.2 \pm 0.50	14.02 \pm 0.62	14.85 \pm 1.42	15.02 \pm 0.42	16.24 \pm 0.54	13.21 \pm 0.73	15.53 \pm 0.62	15.96 \pm 0.22
6- arm stage								
Width	168.9 \pm 3.3	152.3 \pm 3.3	182.9 \pm 4.5	146.4 \pm 4.4	178.6 \pm 2.2	161.6 \pm 2.6	181.0 \pm 2.5	172.9 \pm 3.8
Height	197.7 \pm 3.1	202.6 \pm 3.1	200.5 \pm 4.3	204.7 \pm 3.0	201.3 \pm 2.5	212.8 \pm 3.4	202.8 \pm 2.7	197.9 \pm 2.7
AL distance	110.1 \pm 5.0	94.9 \pm 6.1	134.1 \pm 7.7	92.5 \pm 6.5	122.2 \pm 5.5	113.9 \pm 5.9	125.4 \pm 3.7	132.5 \pm 5.3
PO distance	387.5 \pm 10.1	332.7 \pm 8.8	420.9 \pm 11.2	342.8 \pm 12.9	403.5 \pm 6.7	355.4 \pm 10.4	428.0 \pm 8.8	411.5 \pm 11.7
PD distance	340.8 \pm 13.1	321.5 \pm 14.1	389.5 \pm 16.0	303.6 \pm 11.2	336.8 \pm 8.4	388.0 \pm 11.2	415.8 \pm 12.4	426.9 \pm 10.9
AL length	433.7 \pm 9.2	460.1 \pm 8.2	470.9 \pm 11.7	459.4 \pm 11.1	466.7 \pm 7.0	498.6 \pm 8.6	475.1 \pm 9.5	477.9 \pm 7.6
PO length	554.8 \pm 10.4	531.4 \pm 15.1	566.3 \pm 13.5	592.7 \pm 9.0	558.5 \pm 6.4	580.7 \pm 12.2	591.8 \pm 9.1	565.6 \pm 10.1
PD length	211.4 \pm 7.1	203.8 \pm 8.8	248.6 \pm 13.9	214.6 \pm 8.9	224.3 \pm 8.1	240.1 \pm 6.5	258.3 \pm 6.3	265.7 \pm 5.4
Stomach length	84.6 \pm 2.7	72.4 \pm 1.9	88.4 \pm 2.7	77.2 \pm 1.8	80.2 \pm 1.6	87.0 \pm 1.9	89.8 \pm 2.2	93.6 \pm 3.6
Stomach height	65.2 \pm 2.5	51.7 \pm 1.3	77.3 \pm 5.7	58.8 \pm 2.1	65.2 \pm 2.7	62.9 \pm 2.0	69.0 \pm 2.2	69.6 \pm 2.9
Stomach volume	17.64 \pm 1.08	11.87 \pm 0.53	22.33 \pm 2.15	14.31 \pm 0.62	16.41 \pm 0.66	17.37 \pm 0.77	19.76 \pm 0.99	20.93 \pm 1.35

Female	#1		#2		#3		#4	
	380	1000	380	1000	380	1000	380	1000
CO2 treatment								
<i>8- arm stage</i>								
Width	193.9± 3.5	182.7±3.9	208.8±5.5	181.3±3.9	196.5±3.4	174.4±2.9	197.5±3.5	205.3±4.0
Height	228.3± 6.8	210.0±2.5	214.0±2.7	203.1±2.5	208.7±3.0	213.7±2.4	215.5±2.7	199.2±3.3
AL distance	172.1± 3.7	151.8±5.9	187.2±6.6	150.7±4.8	161.2±4.9	157.2±5.2	163.1±4.0	188.5±5.0
PO distance	453.4± 17.7	401.0±12.0	480.7±13.1	431.5±13.8	446.5±7.9	410.1±8.2	471.6±12.1	487.9±20.6
PR distance	42.8± 11.9	38.7±1.9	36.0±2.7	29.2±1.9	29.8±2.5	28.3±1.9	33.5±3.1	45.2±11.0
PD distance	561.9± 20.6	473.0±18.8	566.3±18.0	514.1±15.4	509.7±9.2	544.6±14.5	572.4±12.5	621.3±14.7
AL length	529.4± 6.9	478.1±10.5	527.9±10.5	505.9±12.4	502.1±9.4	519.8±6.7	523.9±7.9	538.6±10.1
PO length	598.0± 9.7	543.8±11.9	595.6±10.2	567.1±12.2	584.0±8.7	585.2±6.3	599.8±6.5	571.0±9.9
PR length	239.4± 9.9	161.0±11.2	268.4±15.4	208.5±11.4	218.6±7.6	207.7±7.5	261.5±10.1	302.5±8.5
PD length	351.3± 7.3	283.3±12.3	359.7±10.3	314.0±10.9	335.7±6.9	332.7±7.5	358.8±6.3	395.0±9.0
Stomach length	100.9± 2.0	80.5±2.3	111.3±3.5	89.0±2.8	97.3±1.7	88.9±1.7	115.8±2.6	100.9±2.3
Stomach height	69.6± 2.4	57.1±1.8	82.7±2.5	64.4±2.6	67.6±2.9	58.2±1.8	84.2±2.7	70.2±2.1
Stomach volume	22.38± 1.13	14.66±0.78	29.48±1.64	18.38±1.12	20.92±1.14	16.40±0.7	31.07±1.59	22.49±1.07

Table 3.2

Effects of OA on larval morphologies for 4-, 6- and 8-arm larval sand dollars. Because morphological characteristics measured are correlated, Principal Component Analysis was used for data reduction.

Rotated component matrix after varimax rotation with Kaiser Normalization was applied to this PCA.

Statistical significance of the effects of elevated pCO₂, maternal lineage and their interactions on the component scores were tested with 2-way ANOVA. Bold phase indicates significant difference (p < 0.05).

See Table 3.1 for list of abbreviations.

	PCA 1	PCA 2	PCA 3	
	38.23	19.13	13.85	
Cum. % of variance	38.23	57.36	71.21	
Eigenvalue	3.82	1.913	1.385	
4-arm larvae	Highest loading Factors (component score)	distance between AL (0.823) body width (0.860)	stomach volume (0.975) stomach width (0.822)	PO length (0.885) AL length (0.669)
	ANOVA	distance between PO (0.734)	stomach length (0.768)	---
	pCO ₂	F _{1,229} = 4.78, p = 0.03	F _{3,229} = 2.96, p = 0.08	F _{3,229} = 1.67, p = 0.197
	Female	F _{3,229} = 1.89, p = 0.13	F _{3,229} = 0.78, p = 0.51	F _{3,229} = 2.06, p = 0.11
	pCO ₂ x female	F _{3,229} = 7.30, p < 0.001	F _{3,229} = 2.18, p = 0.09	F _{3,229} = 1.30, p = 0.27
		42.49	19.02	10.81
	Cum. % of variance	42.49	61.51	72.33
Eigenvalue	5.10	2.28	1.30	
6-arm larvae	Highest loading Factors (component score)	body width (0.904) distance between PO (0.873) body length :width (0.868)	stomach volume (0.941) stomach length (0.864) stomach width (0.765)	AL length (0.861) PD length (0.799) --
	ANOVA			
	pCO ₂	F _{1,233} = 63.3, p < 0.001	F _{3,233} = 7.90, p < 0.001	F _{3,233} = 4.79, p = 0.003
	Female	F _{3,233} = 7.56, p = 0.006	F _{3,233} = 5.04, p = 0.002	F _{3,233} = 7.32, p < 0.001
	pCO ₂ x female	F _{3,233} = 6.95, p = 0.009	F _{3,233} = 8.61, p < 0.001	F _{3,233} = 3.26, p = 0.022
	49.464	13.699	9.803	
Cum. % of variance	49.464	63.163	72.966	
Eigenvalue	6.925	1.918	1.372	
8-arm larvae	Highest loading Factors (component score)	distance between PD,AL,PO (0.80,0.77,0.64) PD, PO, AL length (0.85,0.81,0.80) body width (0.61)	stomach volume (0.94) stomach width (0.91) stomach length (0.82)	body length (0.79) body length: width ratio (-0.83)
	ANOVA			
	pCO ₂	F _{1,232} = 1.78, p = 0.67	F _{3,232} = 107.10, p < 0.001	F _{3,232} = 2.63, p = 0.11
	Female	F _{3,232} = 6.16, p < 0.001	F _{3,232} = 18.98, p < 0.001	F _{3,232} = 4.75, p = 0.003
	pCO ₂ x female	F _{3,232} = 16.04, p < 0.001	F _{3,232} = 2.81, p = 0.04	F _{3,232} = 11.40, p < 0.001

Table 3.3

Swimming metrics (means \pm s.e.m) of 4-arm larval *D. excentricus* reared under present-day conditions exposed to short-term change in ambient CO₂.

pCO ₂ of surrounding water		380 ppm		1000ppm	
Female		3	4	3	4
Up-swimmers	Total speed (μms^{-1})	256.80 \pm 27.10	289.59 \pm 16.43	282.46 \pm 4.67	309.54 \pm 21.33
	Oscillating speed (μms^{-1})	246.71 \pm 25.43	276.27 \pm 15.26	269.45 \pm 14.35	294.33 \pm 19.61
	Net horizontal speed (μms^{-1})	33.24 \pm 2.80	46.56 \pm 6.66	31.78 \pm 23.51	31.22 \pm 4.61
	Net vertical speed (μms^{-1})	119.67 \pm 19.53	146.87 \pm 12.00	147.60 \pm 22.02	166.15 \pm 16.24
	Helical pitch (mm)	1.61 \pm 0.48	2.14 \pm 0.76	1.78 \pm 0.35	2.00 \pm 0.44
	Helical width (mm)	0.40 \pm 0.06	0.34 \pm 0.04	0.40 \pm 0.04	0.34 \pm 0.04
Down-swimmers	Total speed (μms^{-1})	259.22 \pm 22.97	256.39 \pm 24.59	185.70 \pm 34.35	241.76 \pm 20.46
	Oscillating speed (μms^{-1})	248.16 \pm 21.12	245.05 \pm 22.71	176.99 \pm 31.81	230.06 \pm 19.00
	Net horizontal speed (μms^{-1})	30.30 \pm 6.71	31.26 \pm 4.34	29.07 \pm 7.48	47.92 \pm 10.83
	Net vertical speed (μms^{-1})	-127.9 \pm 19.00	-128.38 \pm 18.21	-93.91 \pm 24.15	-124.60 \pm 14.85
	Helical pitch (mm)	0.45 \pm 0.13	0.93 \pm 0.23	0.24 \pm 0.08	0.99 \pm 0.22
	Helical width (mm)	0.26 \pm 0.09	0.37 \pm 0.03	0.11 \pm 0.03	0.24 \pm 0.04

Table 3.4

Effects of CO₂, maternal lineage on swimming metrics. Bold phase indicates significant difference (p< 0.05, 2-way ANCOVA).

	df	Total speed		Oscillating speed		Net horizontal speed		Net vertical speed		Helical pitch		Helical width		
		F	P	F	p	F	p	F	P	F	P	F	P	
Up-swimmer	Stage	1	25.99	<0.001	26.92	<0.001	5.319	0.023	16.24	<0.001	3.781	0.054	4.32	0.040
	pCO ₂	1	0.132	0.717	0.175	0.676	0.004	0.951	0.0002	0.990	0.107	0.744	0.337	0.563
	Female	3	1.09	0.353	0.974	0.407	4.32	0.006	2.17	0.090	7.12	<0.001	1.95	0.125
	pCO ₂ x female	3	1.54	0.207	1.502	0.217	0.824	0.483	2	0.117	1.153	0.330	1.54	0.206
	Error	129												
Down-swimmer	Stage	1	8.57	0.004	8.34	0.005	4.39	0.038	9.69	0.002	2.01	0.158	0.004	0.950
	pCO ₂	1	0.135	0.714	0.155	0.695	0.791	0.375	0.001	0.979	0.912	0.341	0.923	0.339
	Female	3	0.955	0.416	0.905	0.441	2.511	0.060	1.632	0.185	1.378	0.252	4.32	0.006
	pCO ₂ x Female	3	0.601	0.616	0.656	0.581	0.912	0.437	0.375	0.771	0.316	0.814	0.875	0.456
	Error	129												

CHAPTER FOUR: OCEAN ACIDIFICATION IMPACTS PHYSIOLOGICAL AND BEHAVIORAL PERFORMANCE OF LARVAL ECHINODERMS

4.1 Abstract

Ocean acidification (OA), the reduction in oceanic pH due to the hydration of excess atmospheric carbon dioxide, is an increasing threat to marine ecosystems. Many marine invertebrates have benthic-pelagic life cycles in which planktonic larvae connect and sustain disjunct adult populations but are vulnerable to stresses. Previous studies have focused on OA-induced larval mortality and calcification of a single species. However, sublethal effects observed in the laboratory could have significant population-level impacts by affecting larval survival and dispersal. Understanding interspecific variations in OA sensitivity is crucial to predicting future community compositions and ecological interactions. Using feeding and respiration experiments and non-invasive video tracking techniques, we quantified physiological and behavioral impacts of OA on three ecologically important echinoderms (brittlestar *Amphiura filiformis*, heart urchin *Brissopsis lyrifera*, and urchin *Strongylocentrotus purpuratus*). Larval *A. filiformis* was the most sensitive and experienced over 80% mortality after 7 days exposure to 1000 μatm pCO_2 level. Larval *B. lyrifera* and *S. purpuratus* underwent budding (release of blastula-like particles) under acidified conditions. OA reduced feeding in all three species. Acidified larval *B. lyrifera* and *S. purpuratus* had higher swimming speeds. Because larval echinoids use their ciliated bands for both feeding and swimming, our results suggest a tradeoff between feeding and swimming under OA stress. I hypothesize that increased swimming speeds and larval budding each provide short-term benefits, e.g., escaping less favorable depth strata and reducing metabolic costs. An implication is that larval echinoids have the potential to cope with acute exposure to elevated pCO_2 . However, these physiological and behavioral responses came at the cost of reduced larval sizes and delayed development, suggesting long-term deleterious impacts carried over to later developmental stages.

4.2 Introduction

Dissolution of anthropogenic carbon dioxide from the atmosphere into the global ocean has altered its carbonate chemistry and reduced pH. This process of ocean acidification (OA) is occurring at an unprecedented rate: atmospheric carbon dioxide levels ($p\text{CO}_2$) have increased from an average of 270 μatm in 1850s to 390 μatm in 2011, and are associated with a 0.2 unit drop in surface ocean pH. $p\text{CO}_2$ level is predicted to continue rising, reaching 1000 μatm at the end of this century (Sabine *et al.*, 2004). At this rate of increase, average surface ocean pH will drop to 7.7 units by 2100 (Caldeira & Wickett, 2003). A growing body of evidence suggests that exposure to elevated $p\text{CO}_2$ levels can significantly impact survival, growth, behavior, and physiology of various marine organisms (Byrne, 2011a, Doney *et al.*, 2009, Dupont *et al.*, 2010). Calcifying organisms, in particular, are known to be susceptible to changes in pH and carbonate chemistry (Fabry *et al.*, 2008). OA is therefore considered one of the major threats to marine ecosystems in the 21st century.

Many marine invertebrates have complex life histories that include a planktonic larval stage. This planktonic stage plays important roles in the exchange of individuals between disjunct populations, particularly for species whose adults have limited mobility (Cowen & Sponaugle, 2009). However, the planktonic larval stage is considered the most vulnerable life history stage under acidification stress (Kurihara, 2008, Rumrill, 1990). To successfully recruit, planktonic larvae need to perform multiple ecological functions which include feeding, assimilation, growth, and swimming to locate suitable settlements sites and to avoid predators. Negative impacts on any of these ecological functions can have significant implications for population dynamics of marine invertebrates.

Impacts of OA vary among species but appear to be negative overall (Dupont *et al.*, 2010). Certain species are extremely sensitive. For example, the brittlestar *Ophiothrix fragilis* experienced 100% larval mortality under elevated $p\text{CO}_2$ conditions at 1000 μatm (Dupont *et al.*, 2008). Larvae of other species such as some urchins, mussels, and oysters, seem to experience only sub-lethal impacts. These

impacts include increased metabolic costs, reduced feeding, delays in growth and development, and changes in gene expression patterns (Doo *et al.*, 2011, Hammond & Hofmann, 2012, Stumpp *et al.*, 2011b). Negative impacts in the planktonic larval stage can be “carried over” to later development stages (Hettinger *et al.*, 2012). For example, long-term exposure (4 months) of adult green urchins *Strongylocentrotus droebachiensis* to elevated pCO₂ levels reduces the settlement success of their offspring (Dupont *et al.*, 2012). In addition to ecological impacts, negative impacts of OA on larvae also have significant economic implications such as reduced oyster seed production (Barton *et al.*, 2012). However, few studies to date have assessed multiple functional impacts of OA on larvae simultaneously with a view to assess tradeoffs between key functions and their ecological implications.

Echinoderms play important roles in coastal ecosystems through grazing and bioturbation. Therefore, it is important to understand their performances in the face of global climate change. Among echinoderms, echinoids and ophiuroids are ideal for studying tradeoffs in ecological functions because they have planktonic larvae which have complex morphologies. These larvae, known as plutei, have long ciliated projections (arms) attached to a pyramid-shaped larval body. Larvae add pairs of arms throughout larval growth and development. These arms are supported by calcified structures, and are used for both feeding and swimming (Strathmann, 1975). Modeling and experimental studies have shown that slight changes in larval morphology significantly impact larval feeding and swimming, and suggest tradeoffs between the two functions (Chan, 2012, Clay & Grünbaum, 2011, Strathmann & Grünbaum, 2006). For example, when starved, plutei develop longer arms. This change in growth pattern increases particle clearance rates (Hart & Strathmann, 1994) but compromises individuals’ abilities to maintain directed swimming in moving water (Grünbaum & Strathmann, 2003, Pennington & Strathmann, 1990). When reared under elevated pCO₂ conditions, the larval sand dollar, *Dendraster excentricus*, showed morphological changes, including reduced stomach size but showed no reduction in swimming speeds (Chan *et al.*, 2011). This suggests that OA could impact ecological functions differently and that tradeoffs occur under stressful conditions. Because larval growth, morphology, and physiological and behavioral

performance influence and interact with each other, larval echinoids are good candidates to study the tradeoffs in ecological functions under OA stress.

In addition to describing the biological impacts of elevated pCO₂ levels, understanding the ability of marine organisms to adapt to changes in oceanic conditions is needed to formulate sound conservation and management strategies (Melzner *et al.*, 2009). Many coastal organisms, including echinoderms, experience large diurnal and seasonal variations in carbonate chemistry at present (Dai *et al.*, 2009, Wootton *et al.*, 2008). Along the Northern California coast, surface ocean pH can reach 7.7 units during upwelling, as low as global surface ocean pH predicted for 2100 (Feely *et al.*, 2008, Yu *et al.*, 2011). Benthic infauna, such as brittlestars, also routinely experience low pH. For instance, in coastal sediment from San Diego Bay, pH decreased from 7.90 to 7.15 units (equivalent to pCO₂ level of 3000 µatm) within the first centimeter (Cai & Reimers, 1993). Exposure to low pH in native habitats may pre-adapt these organisms to cope with oceanic changes. Comparing the responses among echinoderm classes found in different coastal habitats allows us to investigate effects of evolutionary history on stress responses.

Taking an integrative and comparative approach, we studied the larval performance of three echinoderms under acidified conditions representing “business as usual” predictions for 2100 and 2300 (IPCC, 2007). The three echinoderm species studied are the purple urchin (*Strongylocentrotus purpuratus*), the brittlestar (*Amphiura filiformis*), and the heart urchin (*Brissopsis lyrifera*). Purple urchins are key grazers of macrophyte found in upwelling regions (Pearse, 2006). Larval purple urchins were the focus of several OA studies and have been shown to experience developmental delay, reduced scope of growth, and changes in gene expressions (Hammond & Hofmann, 2012, Stumpp *et al.*, 2011a). Recently, larval purple urchins were also observed to undergo budding (release of blastula-like particles) under low pH, suggesting the possibility of larval cloning as a mechanism to cope with OA stress (Chan *et al.*, in review). However, the impacts of OA on larval purple urchins’ behaviors have not been described. Adult *A. filiformis* increase calcification but have increased muscle wastage under acidified conditions (Wood *et al.*, 2008). However, little is known about the impacts of OA on larval *A. filiformis*. *B. lyrifera* co-occur

with *A. filiformis* in soft sediments and are suggested to play important roles in maintaining biodiversity of the benthos (Widdicombe & Spicer, 2008). However, the larval ecology, including stress responses, of this heart urchin are not well described, probably due to their low larval survivorship in the laboratory (Vasseur & Carlsen, 1949). Therefore, our study not only provides baseline data on responses of key echinoderms to OA but also an opportunity to assess the inter-specific variations in OA resilience.

By quantifying five aspects of larval performance -- larval survivorship, growth (size and shape), oxygen consumption, ingestion rates, and swimming speeds, we aim to: 1) describe the functional impacts of OA on a key life history stage; 2) explore tradeoffs between ecological functions under OA stresses; and 3) compare interspecific sensitivity.

4.3 Materials and Methods

Animal collection and spawning

Adult *S. purpuratus* were collected from the California coast (Kerckhoff Marine Laboratory, California Institute of Technology, USA) and transferred to the Sven Lovén Centre for Marine Sciences (Kristineberg, Sweden) in June 2011. Adults of *A. filiformis* and *B. lyrifera* were collected using an Agassiz trawl in the Gullmars fjord near the Sven Lovén Centre between July and August 2011 when they were sexually mature. All animals were maintained in a flow-through system at 14°C. *S. purpuratus* adults were fed on a diet of *Ulva lactuca*.

Spawning of *S. purpuratus* and *B. lyrifera* was induced by injecting 0.5-1 ml of 0.5 M KCl into the coelomic cavity (Strathmann, 1987). In the first experiment, *S. purpuratus* gametes from two females and one male were used to create two half-sib groups (hereafter, female 1 and 2). In the second experiment with *S. purpuratus*, gametes from two males and two females were used to create one common garden culture (hereafter, mixed population). For *B. lyrifera*, gametes from two females and two males were used to create common garden cultures and the experiments were repeated with a different set of parents (hereafter, population 1 and 2). *A. filiformis* were sexed based on gonad appearance (white

sperm and orange eggs) and exposed to temperature shock in groups of 10 – 15 to induce spawning (i.e., placing individuals in sea water of $\sim 28^{\circ}\text{C}$ for 15 minutes and returning them to 14°C in the dark). Because spawning occurred *en mass*, gametes from multiple individuals were mixed to create common garden cultures. All fertilization were performed in present-day pCO_2 level.

To ensure fertilization success, 2-cell stage embryos of all three species were transferred at the density of approximately 5 individuals ml^{-1} to aerated 5L culturing vessels containing filtered seawater. Duplicate or triplicate cultures were set up for each pCO_2 treatment.

Larval rearing

Larvae were reared at 14°C . pH in each culturing vessel that was maintained with a computerized feedback system (AquaMedic) that regulated pH by bubbling pure gaseous CO_2 directly into the seawater (± 0.02 pH units). Both larval *S. purpuratus* and *B. lyrifera* were reared at three nominal pCO_2 levels: 380, 1000, and 2000 μatm , which represent the atmospheric pCO_2 concentration at present and that predicted for the years 2100 and 2300. Based on preliminary experiments, larval *A. filiformis* were reared only in 380 and 1000 μatm due to high larval mortality under acidified conditions (Dupont et al., pers. obs.). pH was measured with a Metrohm 827 pH lab pH electrode calibrated with total scale (T) buffers (Dickson *et al.*, 2007). Alkalinity was measured with a spectroscopic method (Sarazin et al. 1999). Salinity of the culture vessels was maintained at 32 psu. Carbonate system speciation (pCO_2 , Ω_{Ca} and Ω_{Ar}) was calculated from pH_T and alkalinity using CO2SYS (Pierrot *et al.*, 2006) with dissociation constants from Mehrbach et al. (1973) refitted by Dickson and Millero (1987) (Table 4.1).

Larvae were fed *Rhodomonas* sp. at $150 \mu\text{g C L}^{-1}$, approximately 4000-5000 cells ml^{-1} starting from 5 days post-fertilization. The carbon content of the algae was estimated based on biovolume measurements as equivalent spherical diameter (ESD) with an electronic particle analyzer (Elzone 5380, Micrometrics, Aachen, Germany, (Mullin *et al.*, 1966)).

Larval density (individual ml⁻¹) was monitored daily by taking duplicate 10 ml subsamples from the culturing vessels and counting the number of individuals under a microscope. Individuals were subsequently fixed in buffered 4% paraformaldehyde (PFA) and 10 individuals from each replicate jar were photographed. Landmark analysis was used to assess the change in larval size and shape over time. We identified and digitized landmarks (Fig. 4.1), representing the tip of the body, tip of each arm, mid-points along the postoral arms, and points at which arms intersect with the body using the tps2DIG program (Rohlf, 2010.).

Quantifying physiological and behavioral performance

Given that larval duration and survivorship differed between the three species, the feeding, respiration, and swimming experiments were conducted approximately every 3 days post-fertilization and within 24 hours of each other.

Ingestion experiments

To assess the impact of elevated pCO₂ on larval feeding, we measured ingestion rate of larvae as the amount of algal cells consumed over a 12 or 24 hour period (ng C individual⁻¹h⁻¹). 25 larvae from each culturing vessel were transferred to 100 mL glass bottles (3-4 replicates) containing a known concentration of *Rhodomonas* cells (150 µg C L⁻¹, approximately 5000 cells ml⁻¹) in filtered seawater equilibrated to the respective experimental pCO₂ level. Control bottles without larvae were also prepared to account for algal growth during incubation. These bottles were incubated at 14⁰C. At the end of the incubation period, the larvae were filtered out using a 50µm sieve and the algal concentration was determined with a particle analyzer (Elzone 5380, Micrometrics, Aachen, Germany).

Respiration experiments

We measured oxygen consumption over time using a modified protocol of Marsh and Manahan (1999) (see Stumpp et al (2011) for details). Briefly, individuals (50 or 100 larvae, depending on larval size) were picked, rinsed, and transferred into respiration vials filled with filtered seawater equilibrated to

the respective pCO₂ levels. Three methodological replicates were prepared for each culture jar at each time point. Three vials for each pCO₂ treatment without larvae were prepared as bacterial respiration control. We used micro-optodes (PreSens, 4-OXY Micro, Germany) to measure pO₂ in each vial before and after incubation to estimate oxygen consumption over time. Incubations were conducted with the respiration vial closed and placed in a circulating water bath set at 14⁰C for 8 to 12 hours. To ensure oxygen consumption rates did not change during incubation, continuous pO₂ measurements (n = 4) were conducted to demonstrate a linearity of pO₂ decline (data not shown). To avoid respiration stresses due to oxygen depletion, we ensured that the pO₂ in the vials did not drop below 80% air saturation. We then corrected for bacterial respiration rate using the blank samples. We also fixed and counted larvae in each vial to obtain an accurate respiration rate in pmol O₂ individual⁻¹ hour⁻¹.

Video motion analysis

Larval behaviors were quantified using video motion analysis detailed in Chan and Grünbaum (2010). Briefly, 50-100 individuals were selected to avoid inclusion of buds (see results for details) and gently injected into a 2.5cm x 2.5cm x 30cm plexiglass chamber containing filtered seawater equilibrated to the respective pCO₂ levels. All six chambers were submerged in a water bath maintained at 14⁰C. Two-minute long videos clips were collected at 15 frames per sec (fps) with two modified webcams (Logitech webcam Pro9000) equipped with 7.5mm CCTV lens (Rainbow Tech. Inc., Alabama, USA). Cameras were mounted on an automated platform to capture video from two fields of view 0-13 cm and 13-25 cm. Video clips were collected every 6 minutes for a total of 37 minutes. Two more sets of observations were made on the same group of larvae by gently mixing the chambers to redistribute individuals. We analyzed the video clips with customized software Avidemux2.4 to subtract background, threshold for size and brightness, and extract pixel coordinates. We then used the in-house Matlab program Tracker3D to calibrate and to assemble individual tracks over time.

We computed swimming statistics only for individuals tracked for ≥ 5 s. Because larval echinoderms typically travel in a helical manner and we only had 2-D projections of the tracks, we applied a correction factor of $\pi/2$ to the horizontal components of the movements. Using cubic smoothing splines of different knot spacings, we removed frame rate noise and differentiated the overall direction of travel (axis) from the oscillatory components of the tracks. We computed total speed as the time derivative of the smoothed track. We computed the net horizontal and vertical velocities as the displacement between the starting and ending point of the track divided by the track duration. We computed the oscillatory speed as the time derivative of the distance between the axis and smoothed track. To describe the helical paths, we identified points where the oscillatory component and the axis intersect (zero-crossings). Helical pitch is the distance between two consecutive zero crossings. Helical width is the maximum distance between the actual path and the axis within the bounds of two consecutive zero crossings. Taking into account that individuals were tracked for different durations, we computed weighted means of all the swimming metrics by sampling at 5 s time intervals and averaging trajectories intersecting each time point (see Chan et al., 2011 for more details of the statistics).

Statistical analysis

Larval densities were normalized to initial densities. Larval densities were compared between pCO₂ levels with larval age (days post fertilization) with an ANCOVA with age as a covariate after logarithmic transformation. To examine potential differences between lineages, data from different lineages were not pooled. For the multiple lineages of larval *S. purpuratus*, we assessed effects of lineage on larval density over time using an ANOVA with pCO₂ and populations as fixed factors.

For ingestion rate, after confirming homogeneity of variance with a Levene's test, we compared the mean of the methodological replicates to test for effects of pCO₂ treatments on larval ingestion rate of *A. filiformis* and *B. lyrifera*. We also conducted a post-hoc Tukey's test to compare effects of pCO₂ treatments for larval *B. lyrifera*. Repeated measurements were made over time for larval *S. purpuratus*,

and hence we compared the effect of pCO₂ on larval ingestion rate using ANCOVA with pH as fixed factor and age as a covariate.

For the swimming metrics, we compared the effects of pCO₂ treatments with an ANCOVA with larval age as a covariate after confirming homogeneity of variance. We confirmed that larval swimming did not vary within the 36 min of observation or between repeated observations, and therefore these factors were not included as random factors in the statistical analysis. Swimming behavior of larval *D. excentricus* differed significantly between maternal lineages under acidified conditions and therefore we did not pool data between populations (Chan *et al.*, 2011). Post-hoc analyses with Bonferroni corrections were conducted for larval *B. lyrifera* and *S. purpuratus*. All statistical analyses were conducted using PASW18.

4.4 Results

*OA reduced survivorship but may be compensated for by budding in *Brissopsis lyrifera**

For both *S. purpuratus* and *A. filiformis* larval density decreased linearly over time (Fig. 4.2, Table 4.2). pCO₂ treatments also had a significant effect on larval survivorship (Table 4.3). There were significant differences between changes in larval density over time between the three populations of *S. purpuratus* observed (ANOVA, $F_{2,410} = 37.26$, $p < 0.001$). Interactions between pCO₂ level and population also had significant effect on the changes in larval density over time (ANOVA, $F_{4,410} = 7.91$, $p < 0.001$).

Abrupt increases in larval density were observed in *S. purpuratus* exposed to high pCO₂ levels. For example, offspring of female 1 reared in 1000 μ atm increased to 190% of the initial density 7 days post fertilization (Fig. 4.2). This sudden increase in larval density suggested individuals underwent budding and was confirmed by direct observation of bud formation (Fig. 4.2; see Chan *et al.*, in review for details). However, these individuals disintegrated over 24-48 h, such that the net mortality over the course of the 27 days experiment was not affected by these sporadic events.

Larval *B. lyrifera* underwent budding under low pH conditions. Unlike those of the *S. purpurta*s, individual buds survived and developed into functional, prism-shaped larvae. The frequency of budding differed between populations, demonstrated by the difference in larval survivorship among the two populations. Size of population 1 decreased linearly over time (Fig 4.2) and pCO₂ treatments had no significant impact on larval survivorship over time (Table 4.3). For population 2, larval density dropped over the first 24 hours in all pCO₂ treatments. Larval density subsequently remained stable in the control but increased linearly with age in the high pCO₂ treatments (Fig. 4.2). Larval densities at the end of the experiment were higher in the high pCO₂ treatments compared to the controls.

Reduced ingestion rate under acidified conditions

Larval *A. filiformis* had significantly lower ingestion rates when reared under acidified conditions: 1.20 ± 0.257 ng C individual⁻¹ hr⁻¹ at 380 μatm compared to 0.0006 ± 0.0005 ng C individual⁻¹ hr⁻¹ at 1000 μatm (Student's t test, $F_{1,3} = 12.99$, $p = 0.037$, Fig 4.3).

Larval *B. lyrifera* also had significantly lower ingestion rates in the acidified treatments (0.947 ± 0.353 and 0.432 ± 0.159 ng C individual⁻¹ hr⁻¹ for 1000 and 2000 μatm respectively) than in the control (3.53 ± 0.532 ng C individual⁻¹ hr⁻¹, Student's t-test, $F_{2,6} = 19.51$, $p = 0.02$). However, the two high pCO₂ treatments did not significantly differ from each other.

Ingestion rate of larval *S. purpurta*s increased with larval age. The increases were linear for larvae reared in 1000 μatm and 380 μatm (Regression, $F_{1,8} = 27.35$, $p = 0.001$ and $F_{1,8} = 23.12$, $p = 0.001$ respectively). The regression coefficients suggested that larvae reared at lower pH have a smaller change in ingestion rate over time ($B = 0.394$ for 1000 μatm and 0.506 for 380 μatm). At 27 days post fertilization, larvae in the 2000 μatm treatment had lower ingestion rates than the two other treatments. However, ANCOVA suggests that age had a significant effect on ingestion rate ($F_{1,25} = 39.95$, $p < 0.001$) but pCO₂ level did not ($F_{2,25} = 1.49$, $p = 0.243$).

Increased oxygen consumption under acidification

Due to the high mortality rate, oxygen consumption rates of larval *A. filiformis* could not be measured. For larval *B. lyrifera*, oxygen consumption rate was measured 6 days post fertilization for population 1 and at three time points for population 2 (Fig 4.4). For population 1, larvae in the acidified treatment had an average oxygen consumption rate of 24.07 ± 3.42 pmol O₂ individual⁻¹ hr⁻¹. Larvae in the control had an average oxygen consumption rate of 31.96 ± 4.09 pmol O₂ individual⁻¹ hr⁻¹. These rates were not significantly different between the two pCO₂ treatments in population 1 (Student's t-test, $F_{1,2} = 2.18$, $p = 0.214$). For population 2, age and pCO₂ treatments had significant effects on oxygen consumption rate (ANCOVA, $F_{1,18} = 28.23$, $p < 0.001$ and $F_{2,18} = 3.37$, $p = 0.005$) but post-hoc test did not generate any grouping. Only larvae reared under 1000 µatm had a significant linear relationship between oxygen consumption rates and larval age ($F_{1,6} = 92.48$, $p < 0.001$). The slopes of the regression lines suggest that the rate of increase in oxygen consumption rate was faster in the 1000 µatm treatment than that of 380 µatm control (Fig. 4.4).

Oxygen consumption rates were measured for all three populations of larval *S. purpurta*. Oxygen consumption rates were measured for larvae in the mixed population reared only in 380 and 1000 µatm 4 days post-fertilization. Oxygen consumption rates were not significantly different between the two pCO₂ treatments (380 µatm: 16.25 ± 11.49 pmol O₂ individual⁻¹ hr⁻¹; 1000 µatm: 3.28 ± 2.32 pmol O₂ individual⁻¹ hr⁻¹; Student's t-test, $F_{1,2} = 0.765$, $p = 0.474$). Multiple measurements were made for larvae from the two maternal half-sib groups. Age had a significant positive effect on oxygen consumption rates (ANCOVA, female 1: $F_{1,13} = 10.99$, $p = 0.006$; female 2: $F_{1,17} = 9.935$, $p = 0.006$) but pCO₂ treatments did not (ANCOVA, female 1: $F_{2,13} = 1.72$, $p = 0.218$; female 2: $F_{2,17} = 0.089$, $p = 0.915$). There were significantly linear relationship between oxygen consumption rates and age for some of the pH treatments. Larvae of female 1 in the 380 µatm treatment had a significantly linear increase in oxygen consumption rate over time (Regression, $F_{1,6} = 11.49$, $p = 0.02$, $r^2 = 0.657$). Whilst larvae of female 2 in the 2000 µatm treatment had a significantly linear increase in oxygen consumption rate over time (Regression,

$F_{1,6}=10.38$, $p = 0.02$. $r^2 = 0.634$). Though not significantly linear, the slope of the regression lines suggest that the increase in rate of oxygen consumption over time was higher in the 1000 μatm treatment than the other two treatments with female 1.

Species-specific behavioral responses

Both larval age and pCO_2 treatments had significant effects on some of the swimming metrics. However, responses differed between populations and species (Table 4.4, Fig. 4.5).

A. filiformis was the only species whose larvae did not show significant increases in total and oscillatory speeds over development (i.e. larval age had no effect on swimming speeds). However, larvae had significantly higher vertical speeds over time and swam in wider helices with taller pitches. Larvae in the acidified treatment had significantly slower swimming speeds (total, oscillatory, horizontal, and vertical speeds) and their paths had lower pitches.

For larval *B. lyrifera* from population 1, observations were made on days 4 and 10 post-fertilization. However, there were not enough individuals in the 1000 μatm treatment at the second time point so we made comparisons only between pCO_2 treatments on 4 days post-fertilization. Similar to *A. filiformis*, larvae in the high pCO_2 treatment had significantly slower speeds but no changes in helical shape. Interestingly, larvae in population 2 of *B. lyrifera* showed different responses. Swimming speeds increased significantly with age. However, we did not perform a regression analysis because there were only 2 time points. pCO_2 treatments had significant effects on vertical speeds and marginally significant effects on total and oscillatory speeds. Larvae in the high pCO_2 treatments swam faster than those in the control. However, there were no significant differences in horizontal speeds or helical shape.

Larvae from the two half-sib groups of *S. purpurtaus* both showed significant increases in swimming speeds and the dimensions of the helical paths over time. pCO_2 treatments had significant effect on all swimming metrics for offspring of female 2 but only on total, oscillatory, and vertical speeds

for offspring of female 1. In both groups, larvae in the high pCO₂ treatments had faster speeds than their counterparts in the control.

4.5 Discussion

Ocean acidification has been determined in previous studies to have deleterious impacts on many marine invertebrates (Fabry *et al.*, 2008). However, these studies often focus on single function. Our assessment of OA impacts on multiple ecological functions (survival, growth, feeding, respiration, and swimming) highlighted both inter- and intra-specific variations in OA sensitivity between larval echinoderms. In particular, larvae of *A. filiformis* were most negatively impacted, suffering an average mortality of 11% day⁻¹ at the pCO₂ level of 1000 µatm. The two echinoids observed, *S. purpurtaus* and *B. lyrifera*, underwent budding. The latter species produced viable clones under OA stress, which could compensate for increased mortality or metabolic cost. Larval movement can significantly impact dispersal (Metaxas & Saunders, 2009) and larval nutrition can significantly impact post-settlement success (Pechenik *et al.*, 1998). Our observations suggest tradeoffs between these two ecological functions: larval echinoids maintained, if not enhanced, their swimming performance measured by swimming speeds but had lower ingestion rates. Therefore, though the larval echinoids appeared to be more resilient to OA stress in terms of mortality. Our observed sub-lethal physiological and behavioral responses could have population- and community-level implications.

Reduced survival of *Amphiura filiformis* under OA

Previous studies on OA impacts on marine invertebrate larvae often reported increased mortality at high pCO₂ treatments (Byrne, 2011). Larval *A. filiformis* experienced the highest larval mortality rate per day among the three species in 1000 µatm, with an average of 20% survivorship after 6 days compared to 25% for *S. purpurtaus* after 27 days. *A. filiformis* also has a longer planktonic duration, estimated to be 88 days (Sköld *et al.*, 1994), compared to 30 – 43 days for *S. purpurtaus* raised at comparable temperature in laboratory culture (Strathmann, 1987). Such high larval mortality over a short

duration suggests the hypothesis that successful recruitment is improbable. *A. filiformis* is highly abundant in the muddy substratum of the North Sea, plays important roles in bioturbation and hence biogeochemical cycling, and is an important food source for flat fishes and crabs (O'Connor *et al.*, 1983). OA-induced larval mortality in *A. filiformis* could therefore significantly impact benthic community structure and energy transfer.

A previous study on another brittlestar, *Ophiothrix fragilis*, also demonstrated extreme sensitivity to changes in pCO₂ level. Larval *O. fragilis* experienced 100% mortality after 6 days exposure to pCO₂ level of 1000 μ atm (Dupont *et al.*, 2008). Further study is needed to test the hypothesis that sensitivity to OA differs between echinoderm classes and that ophiuroids are more sensitive to OA stress compared to echinoids.

Possible short-term ecological benefits from OA-induced larval budding

Two of three species studied underwent larval budding in the elevated pCO₂ treatments. This response may mitigate deleterious physiological and demographic changes. Larval cloning has been observed in a wide range of echinoderms. However, the mechanisms that induce cloning are not well understood (Eaves & Palmer, 2003). Previous studies demonstrated that high or abrupt changes in food concentration or the presence of predator cues can trigger cloning (McDonald & Vaughn, 2010, Vaughn & Strathmann, 2008, Vickery & McClintock, 2000). Larval cloning could be a result of budding or fission and the frequency of cloning could vary between populations (Vaughn, 2009, Vaughn, 2010). Our observations show that reduction in pH can induce highly-synchronous, high-frequency ($\geq 90\%$) larval budding in *S. purpuratus* (Chan *et al.*, in review). However, buds of larval *S. purpuratus* in our observations were not viable and subsequently disintegrated. In contrast, active budding and sustained increase in larval density over time were observed in both populations of larval *B. lyrifera*. Unlike larval urchins, some of the released blastula-like particles of *B. lyrifera* successfully developed into plutei and contributed to the high survival rates in the acidified treatments (Fig. 4.1, 4.2). Consistent with the

observations on larval sand dollars, the frequency of cloning differed between the two populations of *B. lyrifera* observed. Future study should address the potential for the buds to reach competency and if they do so at a smaller size. Larval cloning has been previously reported in ophiuroids (Eaves & Palmer, 2003), however, we did not observe active budding among *A. filiformis*. Consistent with an earlier study on larval sand dollars (Vaughn, 2009), the frequency and timing of larval budding differed between observed populations of *S. purpurtaus* and *B. lyrifera* (Fig. 4.2). Our findings indicate that there are both inter- and intra-specific variations in potential of larval budding under OA stress.

Larval budding may confer ecological benefits under OA stress in several ways. First, production of viable clones could be a means to increase cohort size and thereby mitigate the elevated mortality rate (Fig. 4.2). Second, individuals are smaller after shedding tissues, which may lower metabolic costs on a per individual basis under OA stress. Oxygen consumption rates of larval *B. lyrifera* reared in 2000 $\mu\text{atm pCO}_2$ were significantly lower than in the other two treatments, and the frequency of budding was highest (Fig. 4.2). Observations on other larval echinoids also suggest that impacts of elevated pCO_2 on growth and respiration rates are size-dependent, such that smaller larvae were relatively less impacted (Dupont et al., unpub). Budding could therefore help compensate for increased metabolic cost imposed by changes in pCO_2 level. Third, smaller individuals also enjoy size-escape from visual predators (Vaughn, 2010). Physiological changes, such as increased oxygen consumption and reduced ingestion rates, were suggested to limit the larval scope of growth under OA stress (Stumpp et al., 2011b). Delays in larval growth could result in an increase in planktonic larval duration and exposure to predators. If this is the case and if budding results in metamorphic competences at smaller size (Vaughn, 2009), budding related size reduction may enhance short-term larval survivorship.

The ecological benefits that larval budding provides are only short-term. Growth and development are needed for individuals to achieve competency for settlement. Prolonging planktonic larval duration while regenerating tissue lost through budding could ultimately lead to higher larval mortality (Rumrill, 1990). Observations on larval sand dollar *D. excentricus* suggested that cloned larval

sand dollar settle at a smaller size (Vaughn & Strathmann, 2008). If this is the case for larval *B. lyrifera* and *S. purpurtaus*, OA-induced budding could also affect post-settlement performance.

Effects of larval age on swimming performance

Larval age had a significant effect on larval swimming performance as indicated by total, oscillatory, horizontal, and vertical speeds (Fig. 4.4, Table 4.4). Age-dependent increase in swimming speeds was consistent with the lengthening of ciliated bands due to increase in larval size, addition of pairs of ciliated arms, and the development of epaulets for *S. purpurtaus*. Similar age effects have been reported for larval sand dollars (Chan *et al.*, 2011). However, in *A. filiformis* age did not have a significant effect on total and oscillatory speeds. Swimming speeds of larvae reared in 1000 μatm initially increased with age, but subsequently decreased between 9 and 13 days post fertilization. Survivorship and ingestion rate were consistently low for *A. filiformis* under OA stress. The observed changes in swimming speed may have been a consequence of stressed individuals failing to maintain their metabolic demands. Reduced motility is likely a generalized stress response, and has been used as an indicator of other environmental stresses such as pollution in other species (Bellas, 2006).

Swimming-feeding tradeoff

Larvae of all three echinoderm species had lower ingestion rates under elevated pCO_2 conditions when food concentration was at satiating level. Despite the fact that the same ciliated bands are used for both feeding and swimming, we did not observe negative impacts of acidification on swimming for population 2 of *B. lyrifera* and for both half-sib groups of *S. purpurtaus*. This observation is consistent with the hypothesis of Chan *et al.* (2011) that larval sand dollars maintained swimming performance at the cost of reduced feeding under OA stress.

While increased swimming speeds suggest a higher particle encounter rate, acidified larvae observed consumed fewer particles. One hypothesis is that the changes in larval morphology under acidified conditions benefit swimming but not feeding. Morphological changes such as smaller overall

size through budding and less calcified skeleton (here and Stumpp et al. 2011) can reduce excess weight of an individual. Assuming an insignificant loss or rapid regeneration of cilia, these changes could increase swimming speeds (Grünbaum & Strathmann, 2003). Previous studies on urchin embryos and larvae suggest that individuals possess a pool of ciliary protein. After deciliation by hypertonic shock, larval cilia regrow to their original length within hours (Auclair & Siegel, 1966). Because larval ingestion rates scale with the length of the ciliated bands, reduction in larval size could negatively impact feeding (Hart & Strathmann, 1994). Another hypothesis is that changes in pCO₂ level affect ciliary motions such as reducing frequency of ciliary reversals or the sensitivity in particle detection. Because ciliary motion is controlled by ionic pumping, changes in surrounding pH could affect ion availabilities and action potentials. Chan and Grünbaum (2010) observed rapid adjustment in swimming trajectories in larval sand dollars in response to temperature reduction that were not associated with changes in larval morphology. If ciliary reversal in response to particles is reduced under acidified conditions, it could explain a reduction in ingestion rate associated with increase in swimming speeds.

Faster swimming speeds under acidified conditions could help individuals more rapidly locate depth strata with more favorable conditions, providing immediate advantages for survival. Though ciliary motion is estimated to account for a small portion (less than 2%) of the energy generated from respiration of marine invertebrate larvae (Sprung, 1984), an increase in swimming speed and hence metabolic demand could pose an additional toll to the acidified larva contributing towards the increased respiration rate (Fig. 4.4). Changes in larval swimming behaviors affect individuals' ability to regulate depth, hence the advective current an individual experiences, and ultimately dispersal (Metaxas & Saunders, 2009). Together with the poor nutritional state, the enhanced swimming performance likely comes at the cost of delayed impacts to subsequent development stages.

Short-term solutions for chronic stressors

Both larval budding and the observed behavioral responses suggest that larval echinoids are capable of coping with short-term, acute exposure to elevated pCO₂ conditions through navigating the water column and reducing their sizes. Larval echinoids in their natural habitat could encounter low pH conditions, e.g. upwelling (Yu *et al.*, 2011), and may therefore be pre-adapted to such acute exposure. However, these physiological and behavioral responses come at long-term ecological cost e.g., reduced feeding and longer pelagic larval duration. OA, a chronic stress, could therefore be deleterious to these species. However, intra-specific variations we observed in this study suggest that there are inherent genetic variations within populations that could be the sources of future adaptive traits towards OA stresses. Further studies need to focus on the potential of organisms to evolve under long-term, multi-generation exposure.

Elevated pCO₂ levels likely negatively impact larval echinoderms through changes in survival, physiologies, and behaviors. Sensitivity differed significantly between species, even though they are found in similar habitats. Further comparative studies are needed to address the question whether evolutionary history or timing of life history events rather than native habitats are more predictive of an organism's ability to cope with acidification stress. Difference in resilience between species could also influence community structure and therefore ecological functions of the marine ecosystems.

Figure 4.1

Micrographs of the representative larvae reared under present-day and elevated pCO₂ levels. Larvae from the same species were of the same date of age. Scale bar represents 100 μm.

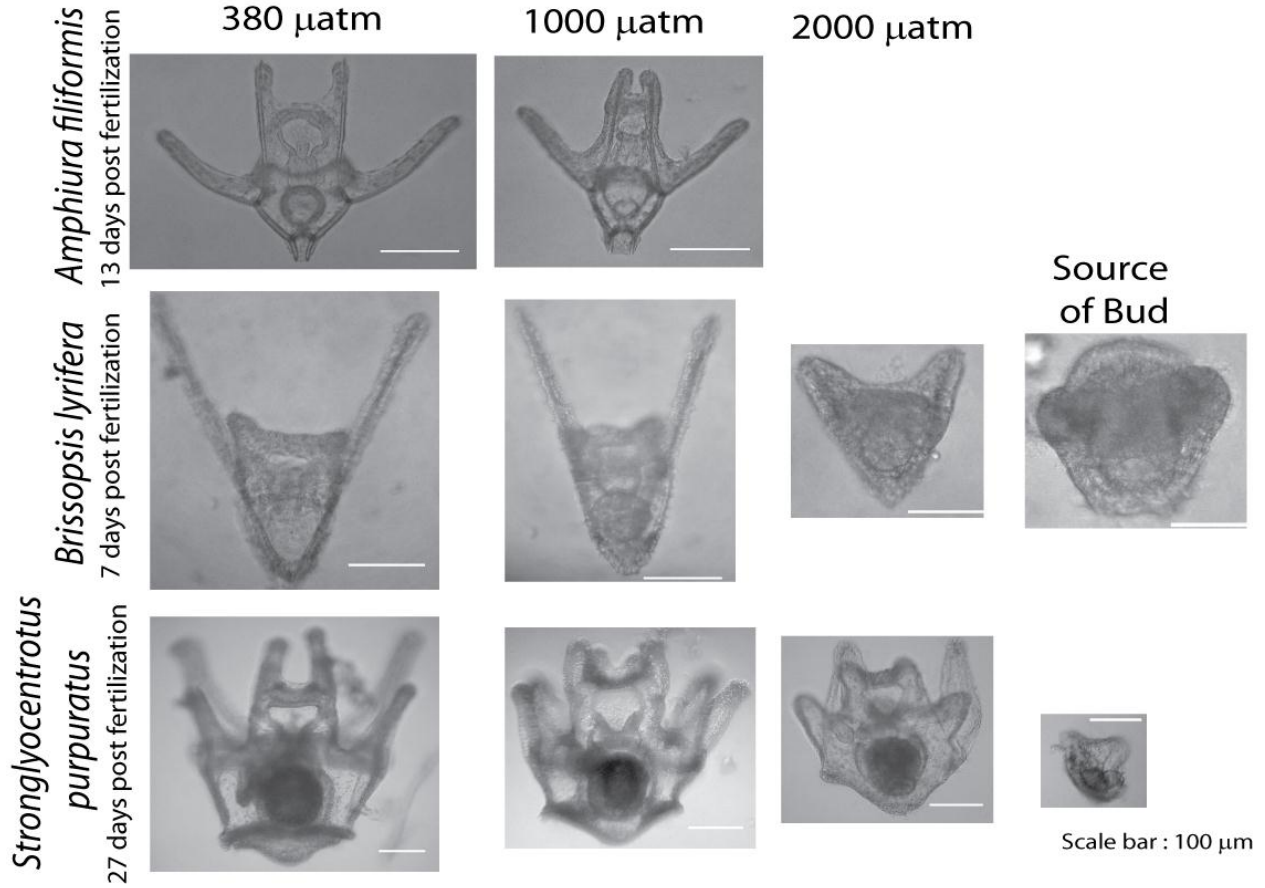


Figure 4.2

Larval density (percentage of the initial density) over time for a) *Amphiura filiformis*, b) and c) *Brissopsis lyrifera* population 1 and 2, and d, e, f) *Strongylocentrotus purpuratus*. Shapes of symbols denote the lineage (mixed population or maternal half-siblings). The colors of the symbols denote the different pCO₂ treatments (black for 380 μ atm, gray for 1000 μ atm and open symbols for 2000 μ atm).

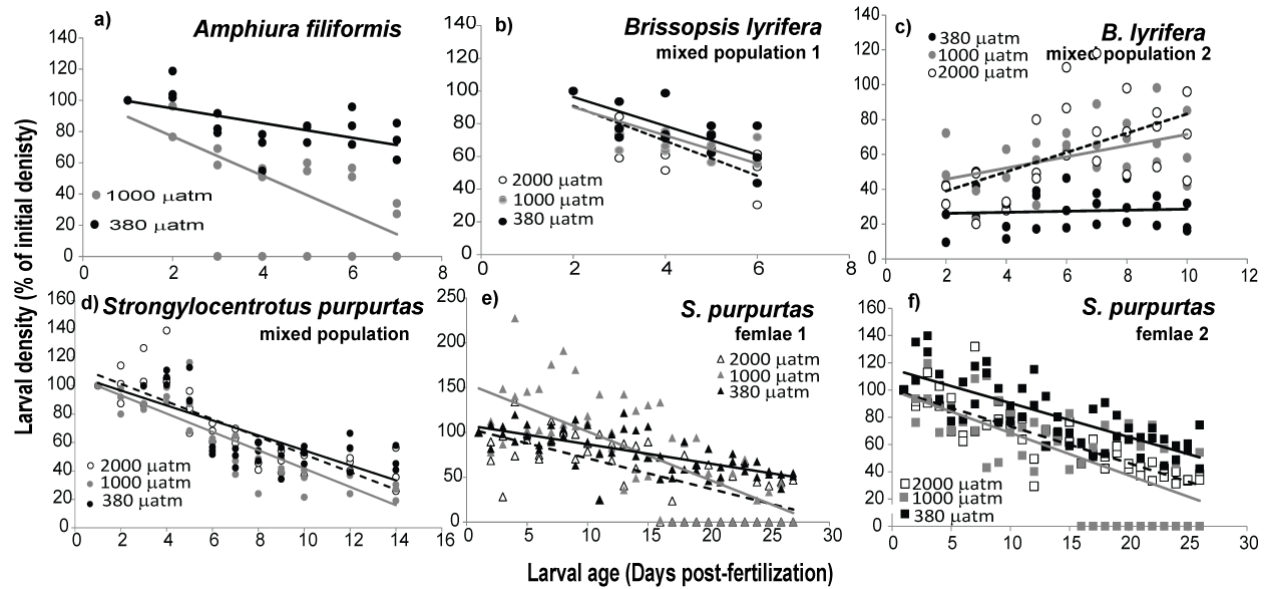


Figure 4.3

Ingestion rates of larval a) *Amphiura filiiformis*, b) *Brissopsis lyrifera*, and c) *Stronglyocentrotus purpuratus*.

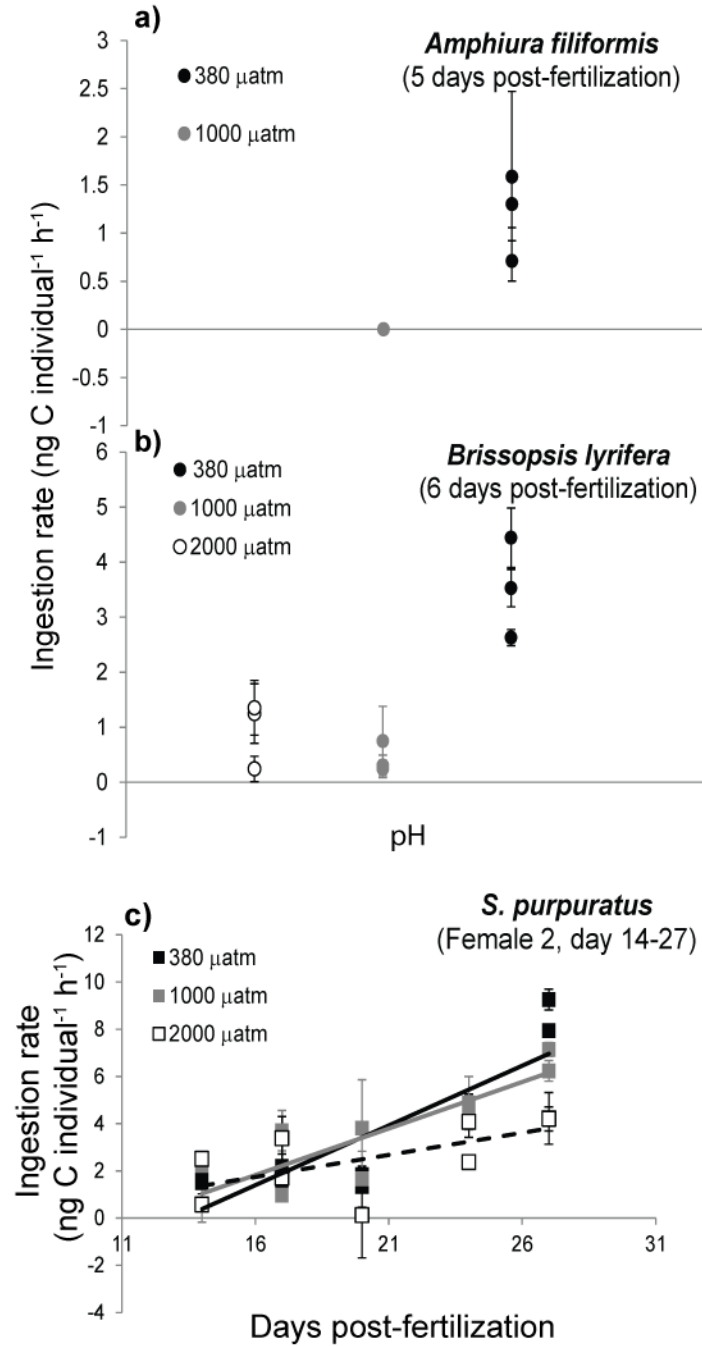


Figure 4.4

Oxygen consumption rates of larval a) and b) *Brissopsis lyrifera* and c, d and e) *Stronglyocentrotus purpuratus*. Shapes of symbols represent lineage and colors of symbols represent different pCO₂ treatment. Asterisk denotes significant linear regression of respiration rate with days post-fertilization.

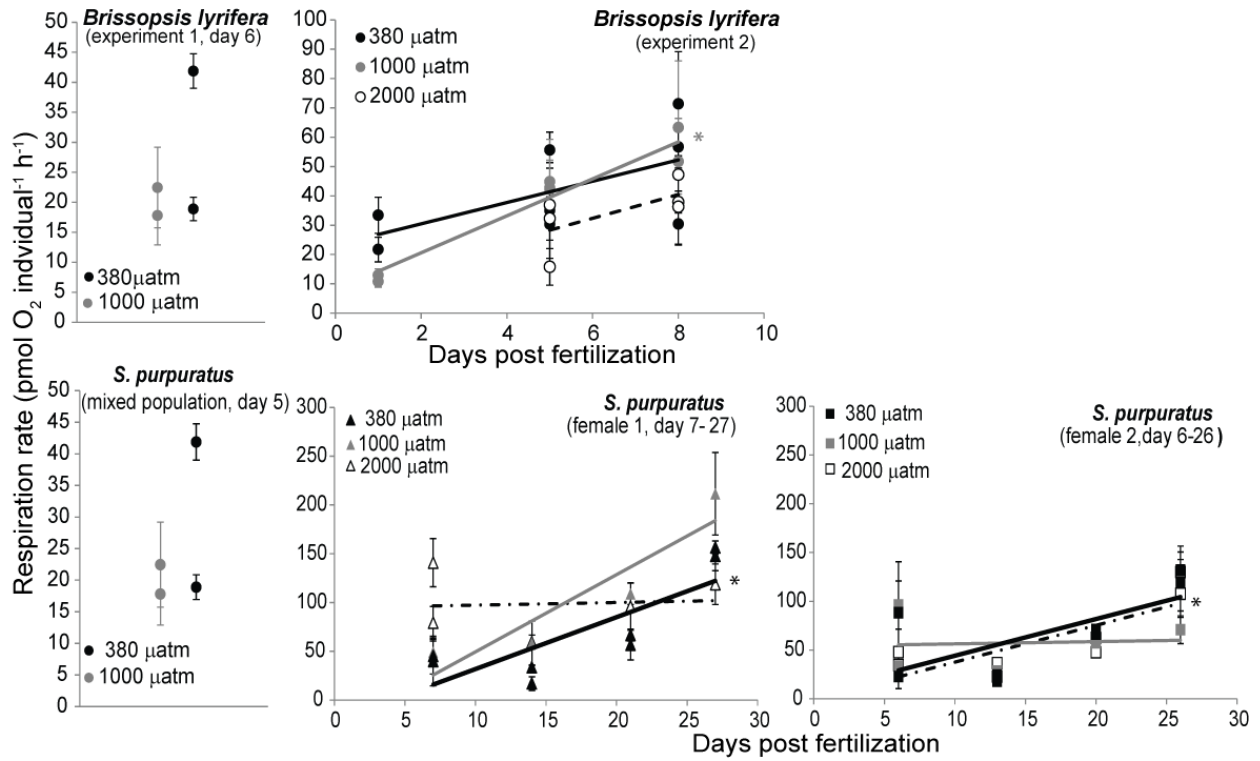


Figure 4.5 Swimming metrics (mean \pm standard error) of larval echinoderms under control and acidified conditions.

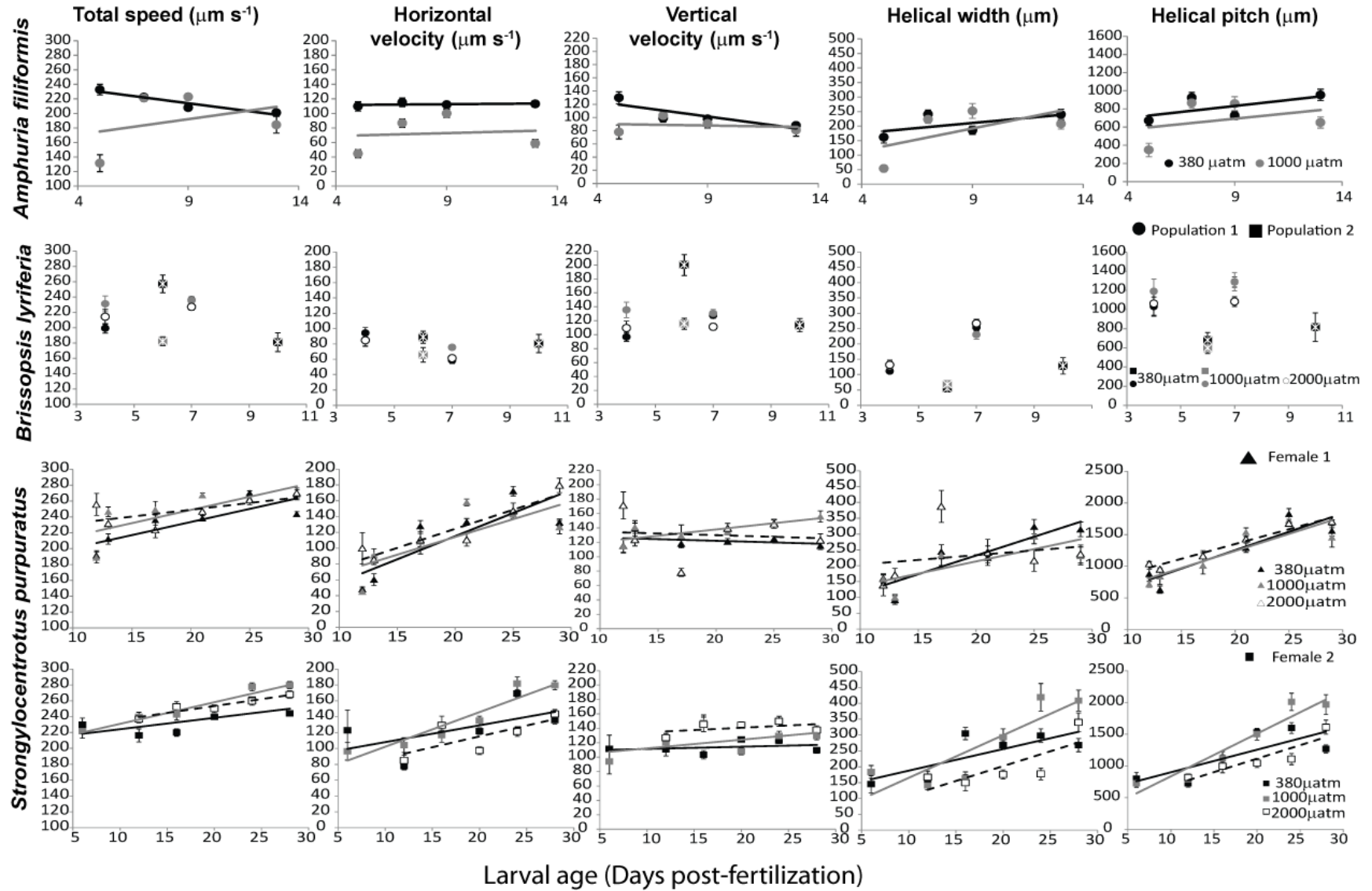


Table 4.1

Carbonate system speciation in the experimental treatments. Total dissolved inorganic carbon (C_T), pCO_2 and calcium carbonate saturation state for aragonite and calcite (Ω_{Ca} , Ω_{Ar}) were calculated from total scale pH (pH_T) and total alkalinity (A_T).

Nominal	pH_T	A_T ($\mu\text{mol/kgSW}$)	C_T ($\mu\text{mol/kgSW}$)	pCO_2 (ppm)	Ω_{Ca}	Ω_{Ar}
pCO_2 (ppm)						
2000	7.42±0.06	2185.13±43.82	2204.73±48.85	2392.04±269.14	1.22±0.28	0.78±0.18
1000	7.63±0.04	2141.09±41.97	2100.48±48.85	1324.65±255.55	1.51±0.14	0.96±0.09
380	8.04±0.02	2186.64±40.024	2002.59±41.22	408.52±22.56	3.29±0.09	2.09±0.06

Table 4.2

Mortality rate (m) is the standardized coefficient (slope divided by the standard deviation of the data) of the regression line.

		380 μ atm				1000 μ atm				2000 μ atm			
		m	F	p	R ²	m	F	p	R ²	m	F	p	R ²
<i>A. filiformis</i>	Mixed population	-0.62	11.91	0.003	0.35	-0.72	19.96	<0.001	0.49				
	Mixed population 1	-0.82	31.87	<0.001	0.65	-0.88	56.64	<0.001	0.77	-0.86	44.88	<0.001	0.72
<i>B. lyrifera</i>	Mixed population 2 (all days included)	-0.45	7.20	0.012	0.18	0.012	0.004	0.951	0.04	0.20	1.21	0.281	0
	Mixed population 2 (excluding day 1)	0.08	0.16	0.693	0.01	0.47	7.19	0.13	0.22	0.56	11.41	0.02	0.31
<i>S. purpuratus</i>	Female 1	-0.7	51.06	<0.001	0.49	-0.72	55.16	<0.001	0.51	-0.69	48.04	<0.001	0.5
	Female 2	-0.78	77.75	<0.001	0.6	-0.68	42.53	<0.001	0.45	-0.85	131.8	<0.001	0.7
	Mixed population	-0.8	62.13	<0.001	0.64	-0.88	113.1	<0.001	0.76	-0.85	85.11	<0.001	0.7

Table 4.3

Analysis of covariance (ANCOVA) for larval density with pH as fixed factor and larval age as covariate.

		ANCOVA for larval density					
		pH			Age		
		df	F	p	df	F	p
<i>A. filiformis</i>	Mixed population	1	32.45	<0.001	1	26.934	<0.001
<i>B. lyfierisa</i>	Mixed population 1	2.00	2.67	0.08	1.00	65.63	<0.001
	Mixed population 2	2	14.43	<0.001	1	0.426	0.52
<i>S. purpuratus</i>	Female 1	2	8.011	<0.0001	1	126.08	<0.001
	Female 2	2	23.01	<0.001	1	190.2	<0.001
	Mixed population	2	4.403	0.015	1	217.23	<0.001

Table 4.4. Analysis of covariance (ANCOVA) of swimming metrics for larval *Amphiura filiformis*, *Brissopsis lyrifera*, and *Strongylocentrotus purpuratus*. Only data from paths there were tracked for more than 5 s were included in the analysis. Weighted means were computed based on the duration of the path recorded and only video clips with at least 5 or 10 paths (10% of the individuals put into the tanks) were included. * indicates statistically significant differences.

Source		<i>Amphiura filiformis</i>				<i>Brissopsis lyrifera</i> (population 1)				<i>Brissopsis lyrifera</i> (population 2)						
		df	MS	F	p	df	MS	F	p	df	MS	F	p			
Age	Total speed	1	960.98	0.32	0.57					1	48752.79	16.23	0.00	*		
	Oscillatory speed	1	326.29	0.12	0.73	Comparison between pCO2				1	44824.60	16.99	0.00	*		
	Horizontal speed	1	7028.37	3.30	0.07	treatments was only made at one				1	63976.71	26.96	0.00	*		
	Vertical speed	1	39825.16	12.72	0.00	*	time point (6 days post-				1	14105.36	4.05	0.05	*	
	Helical width	1	469992.09	20.93	0.00	*	fertilization)				1	1784987.76	143.58	0.00	*	
	Helical pitch	1	3392739.65	13.41	0.00	*					1	1976715.61	3.11	0.08		
pH	Total speed	1	68056.60	22.96	0.00	*	1	104020.48	45.95	0.00	*	2	8313.90	2.77	0.06	
	Oscillatory speed	1	56253.30	20.57	0.00	*	1	88034.14	44.77	0.00	*	2	7116.26	2.70	0.07	
	Horizontal speed	1	147408.33	69.11	0.00	*	1	27152.07	13.77	0.00	*	2	466.18	0.20	0.82	
	Vertical speed	1	37664.97	12.03	0.00	*	1	93167.51	23.80	0.00	*	2	23711.18	6.80	0.00	*
	Helical width	1	17689.11	0.79	0.38		1	2914.48	2.12	0.15		2	19972.19	1.61	0.20	
	Helical pitch	1	1146637.99	4.53	0.03	*	1	115129.46	0.76	0.39		2	949489.19	1.50	0.23	
Error	Total speed	498	2964.83			69	2263.63			438	3003.33					
	Oscillatory speed	498	2734.90			69	1966.22			438	2638.08					
	Horizontal speed	498	2132.98			69	1972.55			438	2372.93					
	Vertical speed	498	3129.81			69	3915.45			438	3486.97					
	Helical width	498	22455.75			69	1373.65			438	12431.90					
	Helical pitch	498	253007.73			69	151607.87			438	635248.66					

		<i>Stronglyocentrotus purpuratus</i> 0					<i>Stronglyocentrotus purpuratus</i>				
		(female 1)					(female 2)				
Source		df	MS	F	p		df	MS	F	p	
Age	Total speed	1	233984.07	175.17	0.00	*	1	136340.16	118.67	0.00	*
	Oscillatory speed	1	201609.49	172.94	0.00	*	1	117050.15	116.75	0.00	*
	Horizontal speed	1	600488.63	283.80	0.00	*	1	391448.45	189.14	0.00	*
	Vertical speed	1	11835.83	6.38	0.01	*	1	8824.68	4.81	0.03	*
	Helical width	1	1264299.53	52.87	0.00	*	1	2517065.44	105.10	0.00	*
	Helical pitch	1	62270000.00	159.38	0.00	*	1	64790000.00	190.03	0.00	*
pH	Total speed	2	8347.82	6.25	0.00	*	2	23423.61	20.39	0.00	*
	Oscillatory speed	2	6853.18	5.88	0.00	*	2	19898.11	19.85	0.00	*
	Horizontal speed	2	4430.01	2.09	0.12		2	41066.26	19.84	0.00	*
	Vertical speed	2	15376.33	8.28	0.00	*	2	44339.63	24.19	0.00	*
	Helical width	2	51433.24	2.15	0.12		2	345168.07	14.41	0.00	*
	Helical pitch	2	426753.38	1.09	0.34		2	5606345.10	16.44	0.00	*
Error	Total speed	611	1335.73				715	1148.89			
	Oscillatory speed	611	1165.75				715	1002.61			
	Horizontal speed	611	2115.87				715	2069.59			
	Vertical speed	611	1856.53				715	1833.22			
	Helical width	611	23911.98				715	23950.47			
	Helical pitch	611	390716.82				715	340962.48			

CHAPTER 5: ADVANCES IN BIOMECHANICAL ANALYSIS OF FUNCTIONAL MORPHOLOGY IN PLANKTONIC LARVAE: A CASE STUDY OF STARVED AND FED LARVAL SAND DOLLARS

5.1 Abstract

Larval morphologies are complex and highly variable. Often, larval morphological changes are induced by variations in environmental conditions. Previous modeling studies have suggested that slight changes in morphologies could significantly impact larval swimming, a key ecological function. Larval sand dollars, *Dendraster excentricus*, are known to be phenotypically plastic and grow longer arms when starved. This morphological change has been shown to enhance clearance rate. However, the impacts of starvation-induced morphological changes on swimming are not understood. Using video motion analysis, we quantified larval swimming of starved and fed larval sand dollars. Starved 4-arm larval sand dollars had higher oscillatory speeds and swam in wider helices. Such differences in swimming could be a behavioral response or due to biomechanical effects of changes in morphologies. To distinguish these two mechanisms, we developed a protocol to extract detailed outlines of larval bodies and skeletal rods based on laser confocal micrographs and used these outlines to generate finite element meshes. We used the resulting meshes as the bases for hydrodynamic models of larval swimming. The model starved larva had a higher skeleton volume to tissue volume ratio and had higher passive sinking speed in still water than the model control. In vertical shear, without active swimming, both model larvae preferential moved towards upwelling current and hence experienced net upward transport. This result highlights the importance of considering morphology-flow interactions in assessing larval distributions. This novel reconstruction approach to quantify morphology when combined with hydrodynamic modeling, allows us to investigate the biomechanical implications of coordinated morphological changes, providing context for future investigations of the evolution of larval form.

5.2 Introduction

Planktonic larvae of many marine invertebrates have complex and highly variable morphologies. Larval physiologies impose developmental constraints on morphologies. Within these developmental constraints, past and on-going selective pressures determine which combinations of morphological characteristics are favorable for survival. Selection likely plays key roles in the evolution of larval form because larval morphologies are tightly coupled with performance in key ecological functions.

One key ecological function for planktonic larvae is swimming. Larvae are typically denser than seawater and use swimming to navigate the vertically-structured water column. Changes in swimming behaviors have significant implications for larval survival and dispersal (Chan, 2012). Echinoplutei use long ciliated extensions called arms for both swimming and feeding. Previous observational and modeling studies suggested that variations in larval morphology, for example arm lengths and positions, can significantly impact both feeding and swimming performance. For example, Clay and Grünbaum (2011) compared the swimming performance assessed by vertical speeds of model plutei from three hypothetical morphological families. Their modeling results suggest that upward swimming (positive performance) is restricted to a small morphospace, such that slight changes in larval morphology can compromise larval ability to maintain directed swimming in moving water (stability).

Despite such sensitivity, larval morphology is highly variable and often changes in response to environmental conditions. For example, larval sand dollars had narrower bodies under elevated pCO₂ conditions at 1000 μ atm but their swimming performance did not significantly differ from that of their siblings under present-day conditions (Chan *et al.*, 2011). This observation of changing larval morphology but not swimming performance suggest two non-mutually exclusive hypotheses: 1) observed morphological changes are coordinated such that biomechanical constraints imposed by

swimming requirements are met; 2) larvae exhibit behavioral adjustments, such as changes in ciliary beat pattern, to compensate for morphological changes so as to maintain swimming performance.

Echinoplutei are phenotypically plastic and are therefore good model organisms in which to study the functional implications of morphological variations. Under food-limited conditions, both in the laboratory and in the field, echinoplutei develop longer ciliated arms and have smaller stomachs (Fenaux *et al.*, 1994, Paulay *et al.*, 1985). These larvae capture particles through localized ciliary reversal (Strathmann, 1971). Clearance rate (volume of water cleared of particles per unit time) is proportional to the length of ciliated bands. Hence, longer larval arms increase feeding performance (Hart & Strathmann, 1994). Because the ciliated bands are used for both propulsive force generation and feeding, changes in larval morphology likely impact swimming (Strathmann & Grünbaum, 2006). If the increase in arm length is isometric, starved plutei with longer arms are predicted to have higher swimming speeds in still water. However, individuals with longer arms have lower stability, i.e., they are more likely to tumble or move towards downwelling water when exposed to shear and turbulence (Grünbaum & Strathmann, 2003). Here, we applied non-invasive video motion analysis to test some of these predictions by comparing the swimming performance of starved and well-fed larval sand dollars *Dendraster excentricus* in still water.

In addition to describing the swimming behaviors of starved larval sand dollars, this study also aimed to distinguish between the biomechanical implications of the observed morphological changes and behavioral adjustment. In earlier models, plutei were approximated by ciliated rods representing arms and by non-ciliated rods extending to the bases of the larvae representing larval bodies (Clay & Grünbaum, 2010, Grünbaum & Strathmann, 2003). Using laser confocal micrographs, we developed a protocol to create finite element meshes that represents accurate three-dimensional larval morphology. The resulting distributions of tissue and calcite skeleton can then be used to compute buoyancy and gravitational forces in Stokes' flow. Our new approach allows investigation of

the biomechanical implications of observed morphological variations in more detail than previously possible.

5.3 Materials and Methods

Larval rearing

Adult sand dollars *Dendraster excentricus* were collected in East Sound, Washington, USA in April 2009 and kept in outdoor flow through tanks at Friday Harbor Labs until spawning. Individuals were induced to spawn by injecting 0.5 – 1 ml of 0.55M KCl into the coleomic cavity (Strathmann, 1987). Collected eggs were washed through a 200 μm sieve, placed in a beaker with 1000 mL of 0.22 μm -filtered seawater, and fertilized with 10 drops of sperm. Ten minutes after fertilization, the eggs were examined under a microscope for the presence of fertilization envelopes to confirm fertilization success. Two maternal lineages were created by fertilizing eggs from two females with sperm from a single male.

Larvae were reared under continuous stirring at $16 \pm 1.5^\circ\text{C}$ in 1 L glass jars in 0.45 μm filtered seawater at a density of $\sim 2 \text{ ind. ml}^{-1}$. Larvae were fed with *Rhodomonas lens*, with algal concentrations determined by haemocytometer counts. Larvae were assigned randomly to one of the two food treatments: individuals in the control were fed *ad libitum* at 5000 cells ml^{-1} (“fed”) and individuals in the starved treatment were at 500 cells ml^{-1} (“starved”). Water was changed and food was added every other day. Each dietary treatment had four replicate jars, arranged in a Latin square.

Video motion analysis

Using the video motion analysis techniques detailed in Chan *et al.* (2011), we compared the swimming behaviors of 4-arm larval sand dollar reared under different food concentrations 2 days post fertilization. In brief, approximately 300 larvae from each maternal lineage of each food treatment (~ 75 larvae from each replicated culturing jar) were pipetted into one of four Plexiglas® chambers (3.5 cm x 3.5 cm x 30 cm) containing 0.45 μm filtered sea water submerged in a common

water bath at a constant temperature (16°C). Larvae were allowed to acclimate for ten minutes, and then were gently stirred. After five additional minutes for transient water movement to dissipate prior to filming, movements of individuals were recorded under infrared illumination with digital camcorders (Panasonic DS400) at 15 frames per second. 180s long video clips were captured sequentially from two fields of view (near bottom, 0– 14.4 cm and near surface, 11.6 – 25 cm). We repeated six of these vertical profiles over the period of 1 hour.

We used a customized version of the open source video editing software Avidemux 2.4 to analyze the video clips by equalizing lighting, removing background variations, distinguishing moving larvae based on brightness and size, and extracting the pixel coordinates of larvae. Pixel coordinates were converted to physical positions and assembled into larval swimming trajectories using Tracker3D, an in-house Matlab program.

We computed six swimming metrics for larval trajectories. To exclude detritus and poorly resolved trajectories, only those that are longer than 15 s and having horizontal acceleration $> 0.06 \text{ mm s}^{-2}$ in magnitude were included in the statistics. Details of the swimming metrics are provided in Chan et al. (2011). Briefly, we used cubic smooth splines to remove frame rate noise and to differentiate the overall direction of travel from the oscillatory components of the helical swimming trajectories. We computed total speed as the time derivative of the smoothed track. We computed the net horizontal and vertical velocities as the displacement between the starting and ending points of each track divided by the track duration. We computed the oscillatory speed as the time derivative of the distance between the axis and smoothed track. To describe the helical paths, we identified points where the oscillatory component and the axis intersect (zero-crossings). Helical pitch is the distance between two consecutive zero crossings. Helical width is the maximum distance between the actual path and the axis within the bounds of two consecutive zero crossings.

Statistical analysis

To account for different durations in which individuals were tracked, we computed weighted means of all the swimming metrics by sampling at 5 s time intervals and averaging trajectories intersecting each time point. We assessed the effects of maternal lineages, food concentration, and their interaction on swimming metrics with an ANOVA. All the statistical analyses were conducted in PASW 18.0.

Sample preparation and laser confocal microscopy

On the day of the behavioral observations, random individual larvae were taken from each culturing jar for laser confocal microscopy. Individuals were first relaxed in 0.35M MgCl₂ for 5 minutes and fixed by adding sodium borate buffered paraformaldehyde (pH 8.0) drop by drop until reaching 2% final concentration. Samples were fixed for 1 hour and transferred into 0.45 µm filtered seawater with 0.01% sodium azide until staining. 10-15 individuals were picked from the fixed samples. Individuals were rinsed with 0.01M phosphate buffered solution (PBS) and subsequently stained with the DNA stain propidium iodide at 2 µg/ml in PBS for 1 hour. Rinsed samples were then mounted on glass slides in PBS and sealed with Vaseline to avoid evaporation. Larval skeletons were also visualized with polarized light. Imaging was conducted with a laser scanning confocal microscope (MRC-600; Bio-Rad Laboratories) on a microscope (E800; Nikon) with a 16x objective (Nikon) using LaserSharp image acquisition software (Bio-Rad Laboratories).

To visualize ciliary band placement of larval sand dollar, we spawned additional adults in June 2011 and labeled the larval cilia with α-tubulin antibody. Larvae were relaxed and fixed with the previously described protocol, except that PBT was used in place of PBS. PBT is PBS with 0.1% Triton X-100 used to remove surface proteins. Larvae were washed three times with PBT and incubated with 1/2500 anti-α-tubulin rabbit antibody for 4-6 hours at room temperature. Larvae were then washed with PBS for three times for 5 minutes over 3 hours, then the rabbit antibody was labeled

with the Alexa 568-conjugated goat anti-rabbit IgG phorophore at 1/1000 for 3 hours (Molecular Probes Inc). Larvae were then washed three times with PBT and stained with propidium iodide for 1 hour. Confocal imaging was conducted with a Leica TCS SP5 II laser scanning confocal microscope at the University of Washington Biology Imaging Facility.

5.4 Model parameterization

To distinguish between impacts of morphological changes and behavioral adjustments, we developed a protocol to create finite element meshes that reflect realistic larval morphologies using these confocal micrographs. The dense columnar cells at the base of the ciliated bands stained with propidium iodide denote the boundary of the tissue (Fig. 5.2); larval skeletal rods were illuminated with polarized light (Fig 5.6); and the cilia were labeled with the tubulin antibody (Fig. 5.2). However, there was background noise due to the lack of blocking with goat serum during the staining procedure.

For each micrograph taken in the z-direction (horizontal cross-sections, Fig. 5.3a), we applied a 2 μm Gaussian blur and threshold for brightness using the software Fiji (Schindelin *et al.*, 2012) (Fig. 5.3b). We then traced the outline using the free-hand point tool (Fig. 5.3c). The extracted x-y coordinates were then used to create cubic smoothing splines (Fig. 5.3d). Denser and more spatially uniform coordinate points were extracted from these splines. Using a combination of customized python scripts and the open source software Gmsh (Geuzaine & Remacle, 2009), we manually specified boundary representations using line segments and line loops. The cubic spline could not be directly read into Gmsh because the software could not accommodate extrusions e.g., the beginning of an arm. In these cases, we defined additional line segments such that the meshes were connecting only the correct portion (e.g., excluding the red segment of posterodorsal arm from the rest of the larval body, Fig. 5.4 b).

The completed lists of boundary representations or geometric elements were then imported into Gmsh to create meshes using specified scales (Fig. 5.5). We completed reconstruction of the

external layers for two selected individuals. The starved individual was 2 days old while the fed individual was 3 days old. The surfaces created provide the basis for further hydrodynamic modeling. Details of the low-Reynolds' number slender body model are described in Grünbaum and Strathmann (2003) and Grünbaum (1995).

We also described the calcite skeleton of larval plutei because this dense material contributes significantly towards the gravitational forces, especially stabilizing forces that larvae experience (Pennington & Strathmann, 1990). We approximated the larval skeleton with cylinders (Figure 5.6a, b) and parameterized their spatial distributions and widths based on the polarized light micrograph (Table 5.2). Because larval skeletal rods were only part calcite (CaCO_3), we modified the density of the skeletal rods to 2.66 g cm^{-3} to reflect the presence of approximately 5% MgCO_3 (Okazaki & Inoue, 1976). Larval sand dollars have two kind of skeletal rods: simple and fenestrated (Emler, 1982). To account for the tri-radiate nature and fenestration (pores) on the postoral and posterodorsal rods, we applied a 68% discount on the nominal volume of these rods (Fig 5.6 c, d, Table 5.2). This estimate was based on measuring the average size of fenestration to be $2 \times 5 \text{ }\mu\text{m}$ and the inner diameter of the fenestrated rod reported in Emler (1982, 1983) to be approximately $2 - 2.5 \text{ }\mu\text{m}$.

5.5 Observational results and discussion

Starved larvae had higher oscillatory speeds

Two days post-fertilization, mean swimming metrics of the 300 4-arm larval sand dollars observed did not differ significantly among the two maternal lineages (Table 5.1). Larvae from the two food treatments had similar total speeds. However, starved individuals had significantly higher oscillatory and horizontal speeds (Fig. 5.1). Starved individuals also swam in helices with larger width and pitch. There was no significant interaction between maternal lineage and food treatment.

Higher oscillatory speeds and wider helices but not higher total speeds imply that starved larval sand dollars traversed a relatively longer total distance in a given depth range. These

differences in swimming metrics could be a form of biased random walk – individuals swam in more tortuous paths to increase encounter rate in food rich environments and reduce turning rate in food poor environments (Grünbaum, 1998). Larval echinoids have been shown to respond to the presence and aggregate in algal food patches (Metaxas & Young, 1998). Therefore, starved individuals could be exploring a relatively larger spatial scale by directing more of their movement in the oscillatory components.

Observed differences in swimming metrics could also be a result of the change in weight distribution due to morphological changes or difference in ciliary beat pattern. Because the ciliated arms are rigidly attached to the body at this early stage of development, the change in helical swimming could not have resulted from larval arm movement. Instead, it is possible that increases in arm lengths for the starved individuals affected the relative portion of anterolateral arms and postoral arm thereby disrupting the front-back symmetry of an individual (Clay & Grünbaum, 2011). Alternatively, it is possible that food treatments affect larval ciliary beat patterns. Chan and Grünbaum (2010) reported that larval sand dollars swam in narrower helices when exposed to a temperature drop without any commensurate morphological changes, suggesting that rapid behavioral adjustments can occur at the ciliary level.

5.6 Modeling results and discussion

Trajectories of the model larvae (starved and fed) were simulated in still water and in vertical shear (i.e., horizontal gradients in vertical velocities) while larvae were passively sinking (i.e., no traction velocity was applied to approximate ciliary motion). Sinking speeds in still water were measured at the end of 64 s long simulations and these simulations were repeated 16 times with model larvae starting with random orientations (Fig. 5.7). Both model fed and starved larvae passively reoriented themselves with their arms pointing upwards within the first 5 s of the simulations regardless of the initial positions. The model starved larva sank at a faster speed (587 μm

s^{-1}) than the model fed larva ($460 \mu m s^{-1}$). This difference in sinking speed could be explained by at least two mechanisms. First, the model fed larva was parameterized based on a developmentally more advanced individual. The longer arm lengths (Table 5.3) and presence of the additional pair of arms (posterodorsal arm, Fig. 5.5) may have increased drag, reducing sinking speed (Emler, 1983, Emler, 1991). Second, the model starved larva had a larger skeletal volume to tissue volume ratio (Table 5.3), and therefore, a larger total excess density. Our model results suggest that individuals reared under different food concentrations have intrinsic biomechanical differences, and thus, are likely to differ in still water swimming performance.

When exposed to shear levels ranging from 0.2 to $16 s^{-1}$ at $0.4 s^{-1}$ increments for 250s, both model larvae exhibited biased horizontal movement towards upwelling water, and experienced net upward transport at intermediate and high shear levels ($\geq 1.0 s^{-1}$, Fig. 5.8). Previous observations suggest that many actively up-swimming algae and other plankton, including larval sand dollars, are tilted towards downwelling water when exposed to shear (Clay & Grünbaum, 2010, Strathmann & Grünbaum, 2006). This non-vertical inclination causes swimming organisms to cross streamlines and to be transported downwards at a speed faster than passive sinking alone. Our observation that larval sand dollars passively sinking in vertical shears can reduce downward movement, or even have net upward movement, by sinking with a biased horizontal movement is to our knowledge unique and may have significant implications for larval functional morphology. It is possible that the ventral-dorsal asymmetry or other aspects of morphological details affect the weight distribution, and hence, location of the center of gravity relative to the center of buoyancy for these model larvae. This shift in centers of forces could result in an upwelling biased tilt. In nature, larval sand dollars likely experience turbulence as shear with changing directions over time. Therefore, it is not clear whether this upwelling bias would persist if the direction of shear changes over time. It is also important to note that larvae were modeled as passive sinkers. Future studies should address the question of how incorporation of ciliary motion would affect larval movement in shear.

5.7 Conclusions

Larval morphologies impose biomechanical constraints on ecological functions such as feeding and swimming. However, morphologies often vary with environmental conditions, suggesting the hypothesis that these variations reflect functional tradeoffs to maximize functional performance. Larval sand dollars are phenotypically plastic and develop longer ciliated arms under food limited conditions. Our results suggest that in addition to previously reported effects on clearance rate, such changes in larval morphology also impact larval swimming. Starved 4-arm larval sand dollars had higher oscillatory speeds and travelled in wider helices. Using a detailed biomechanical model, we demonstrated that the morphological differences affected the sinking behaviors of larvae differed in age and feeding regimes. Therefore, it is possible that environmentally-induced morphological variations are coordinated to maintain swimming performance. Laser confocal microscopy allows detailed three dimensional reconstructions of detailed morphologies and can easily be applied to other swimming planktonic organisms. Our modeling approach, therefore, not only provides a novel means to investigate the role of coordinated morphological changes for a single species but also provides a tool to compare the performance of multiple complex larval morphologies in realistic flow fields. Combining such theoretical studies with experimental observations will help better understand the functional constraints that larval morphology imposes and ultimately the evolution of larval forms.

Figure 5.1

a and e) Micrographs of representative 4-arm larval sand dollars in fed and starved food treatments. b, c, d, f, g, h) Swimming metrics of larvae from the two food treatments (Mean \pm Standard errors). * denotes statistically significantly differences (see Table 5.1). Note that the y-axes have different scales.

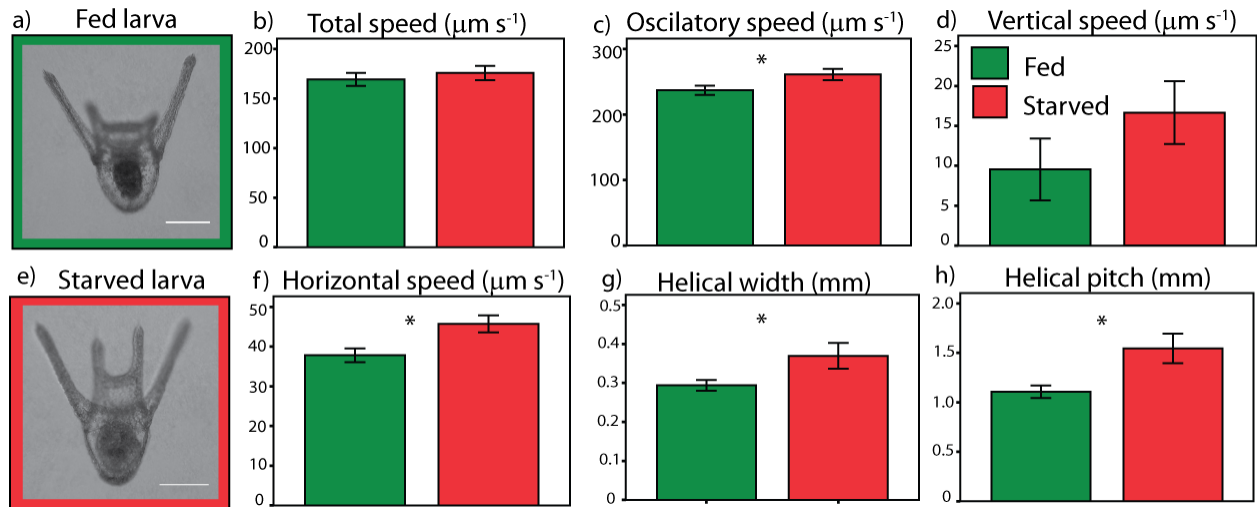


Figure 5.2

Laser confocal micrographs of an 8-arm larval sand dollar as illustration for the use of immune-staining. b) the result of DNA stain; c) the result of tubulin antibody labels. a) The composite of both channels, reflecting the DNA stain and antibody labels. Scale bars represent 100 μm .

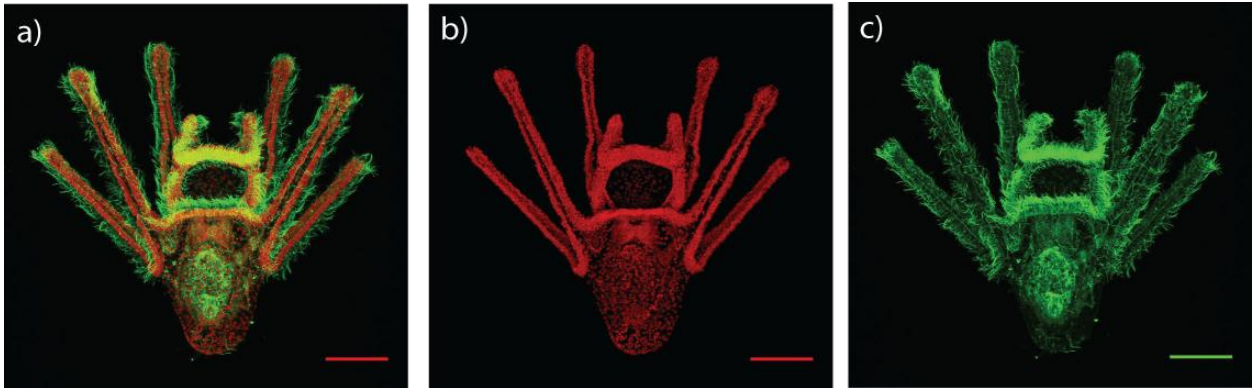


Figure 5.3

Steps in extracting tissue outline based on confocal micrographs.

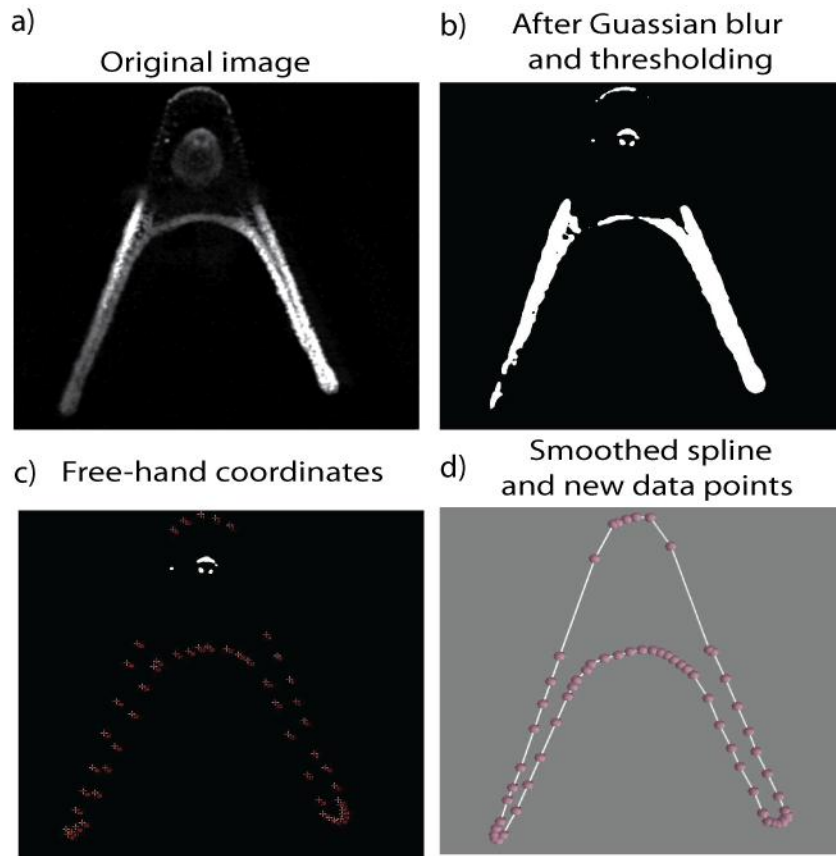


Figure 5.4

Defining geometric elements for meshing using smoothing splines. a) A simple case where two line loops can be joined with two line segments. b) A special case where part of the original line loop (red) needs to be excluded and meshed separately. c) A completed stack of line loops after splining and editing.

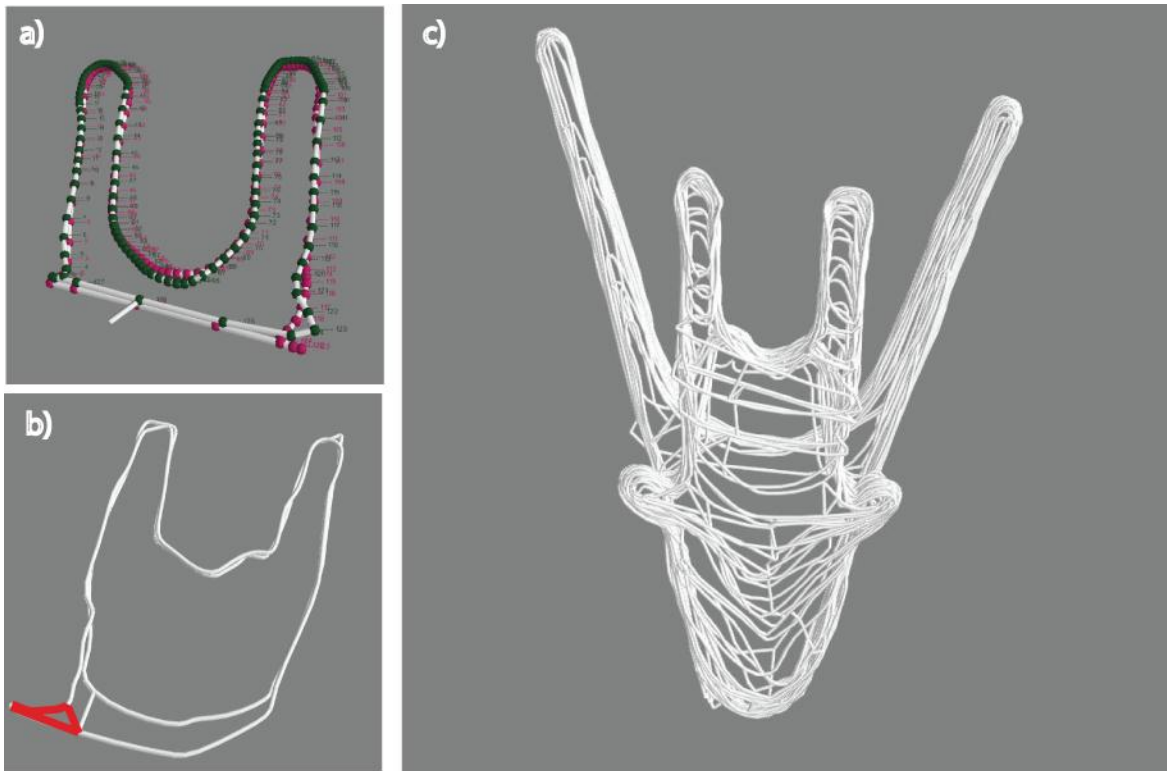


Figure 5.5

Results of the finite element mesh generation for fed and starved larvae.

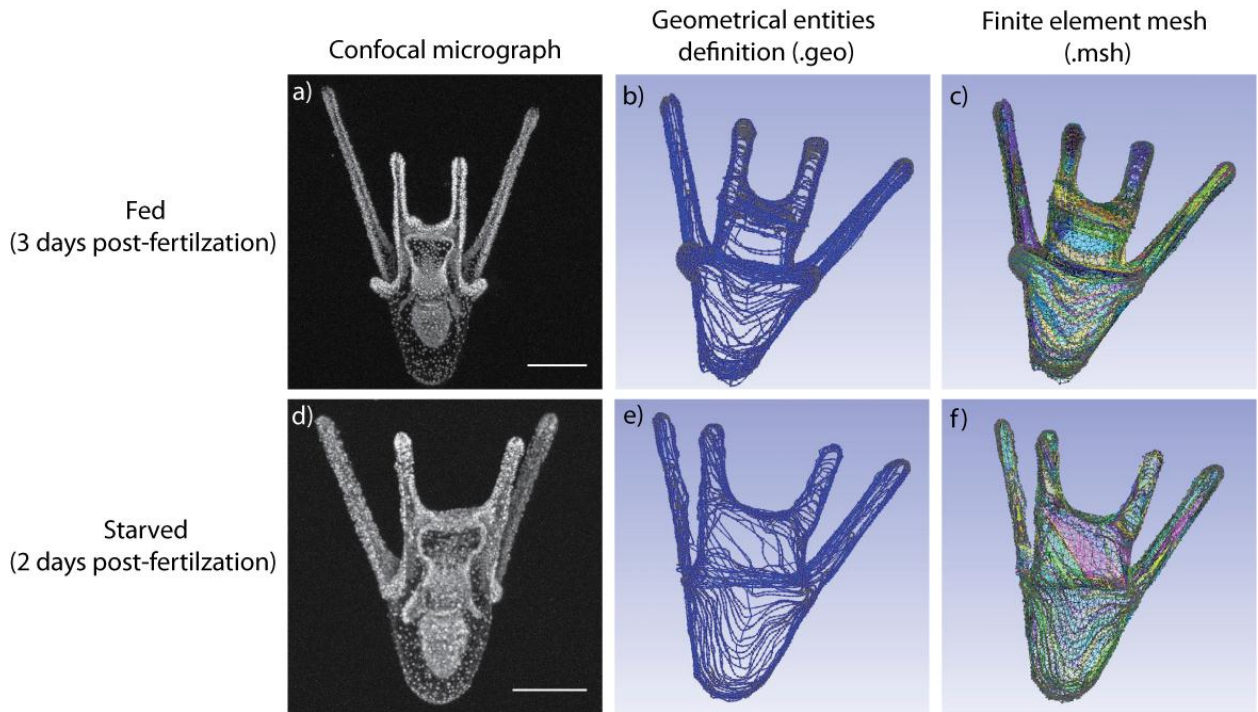


Figure 5.6

Model representation of larval skeleton. a) Cylinders representing the skeleton shown in b). AL refers to anterolateral arm, PO refers to postoral arms, PD refers to posterodorsal arm, B1 refers to body rod 1, B2 refers to body rod 2 and B3 refers to the basal body rod. Fenestrations on skeletal rods were represented by a discount in skeletal density c). Further discount was applied to account for the tri-radiated nature of these fenestrated rods (e, f).

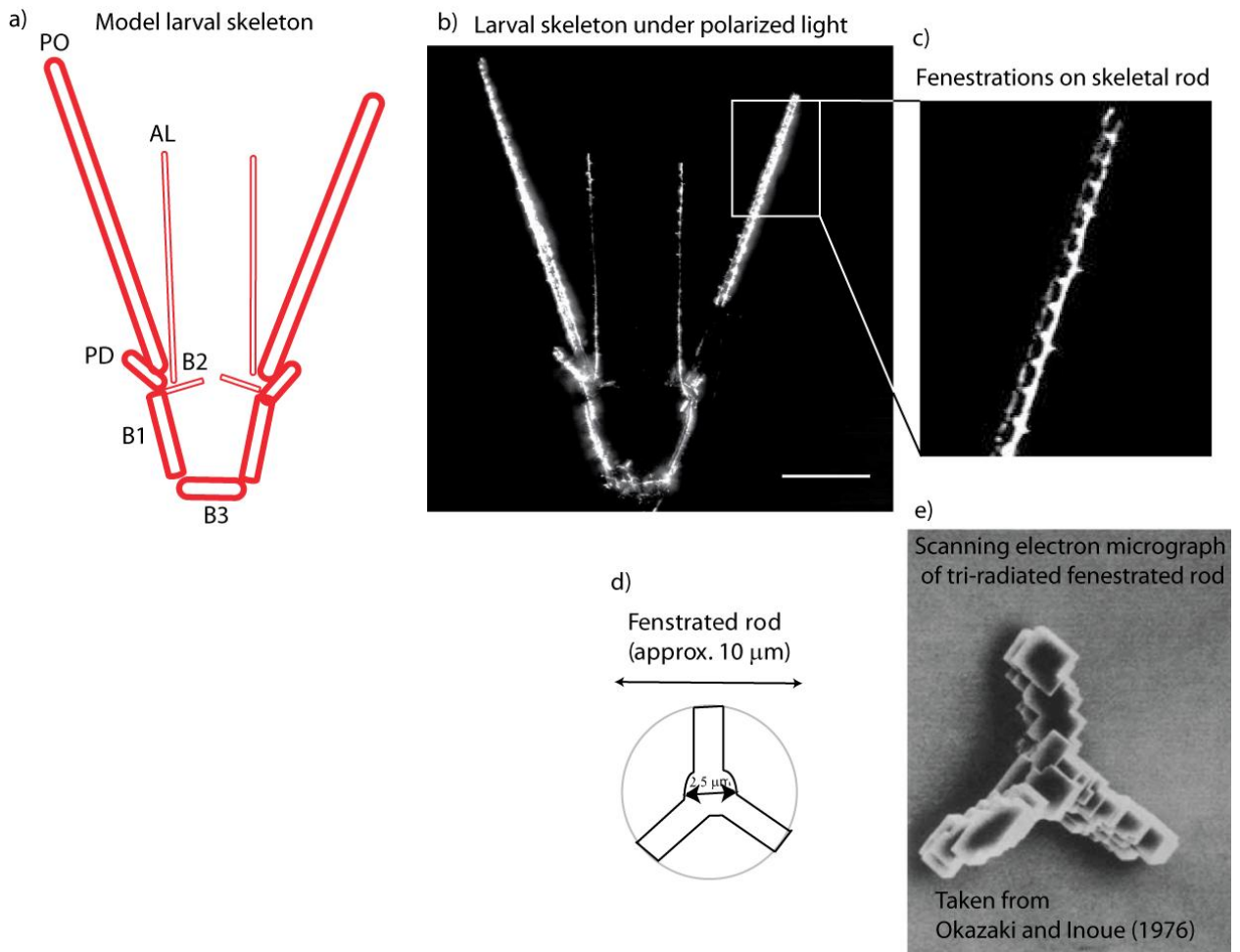


Figure 5.7

Sequence of position of model fed larva passively sinking in still water. a) Model larva started at the origin (0,0,0), sinks, and reorients itself to upright position passively, b) and c) model larva sinks in still water at $460 \mu\text{m s}^{-1}$, d) schematic illustration of larval movement over time.

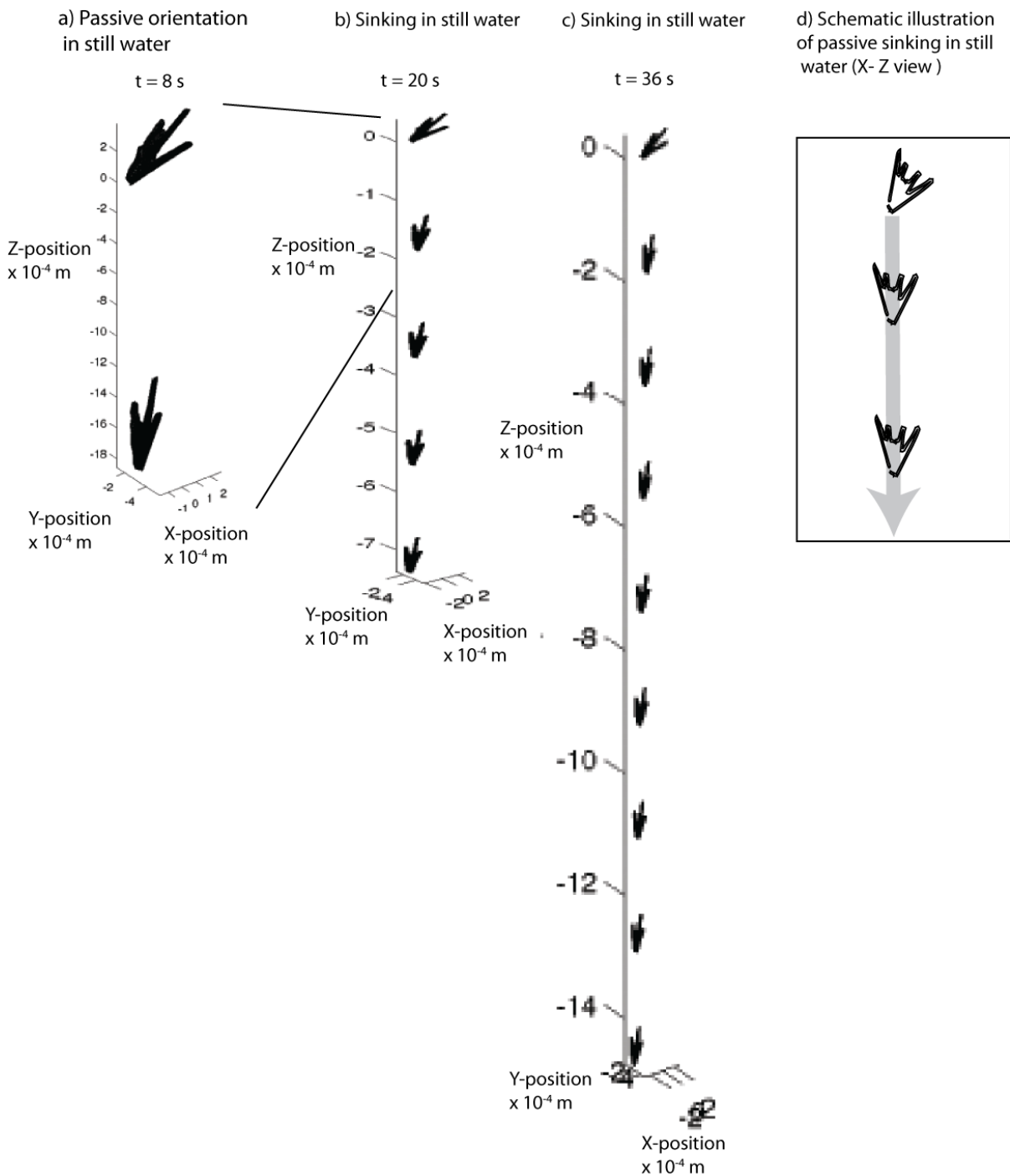


Figure 5.8

Sequence of position of model fed larva passively sinking in vertical shear (2.0 s^{-1}). a) Model larva starting at the origin (0,0,0), sinks, and reorients itself to upright position passively, b) model larval sinks with a horizontal bias towards upwelling water, and c) model larva tumbles but experiences net upward transport, d) schematic illustration of larval movement over time.

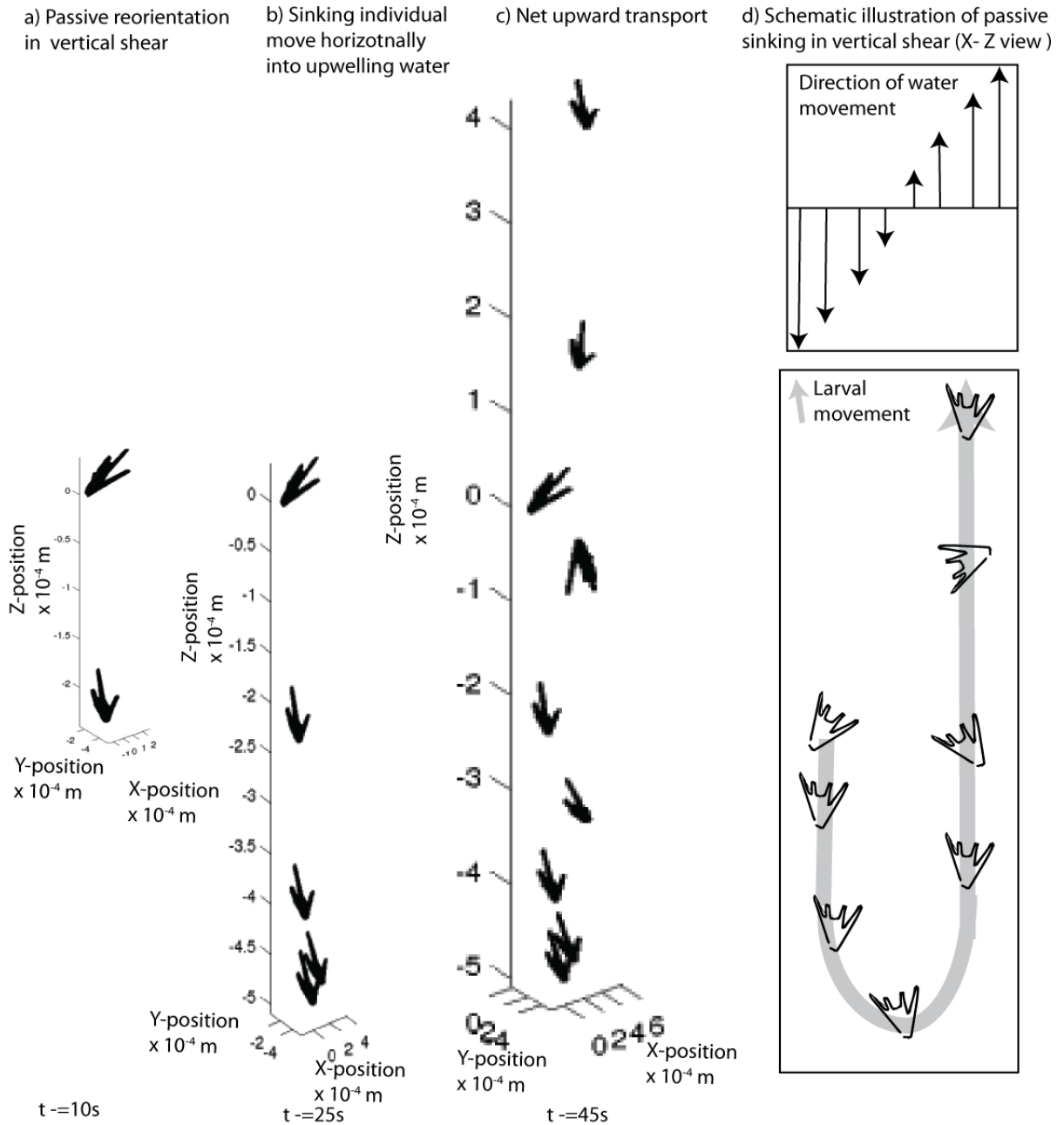


Table 5.1

2-way ANOVA on the effect of maternal lineages and food treatments on swimming metrics of larval sand dollars. * denotes significant difference ($p < 0.005$).

Source		df	Mean Square	F	p	
Female	Total speed	1	.005	1.063	.304	
	Oscillatory speed	1	.012	2.166	.143	
	Horizontal speed	1	.000	.104	.748	
	Vertical speed	1	.003	2.371	.125	
	Helical Pitch	1	.398	.322	.571	
	Helical Width	1	.040	.656	.419	
Food	Total speed	1	.002	.370	.544	
	oscillatory speed	1	.023	4.062	.045	*
	Horizontal speed	1	.002	8.745	.004	*
	Vertical speed	1	.003	1.907	.169	
	Helical Pitch	1	9.027	7.293	.008	*
	Helical Width	1	.263	4.354	.038	*
Female x Food	Total speed	1	.000	.042	.837	
	oscillatory speed	1	.000	.033	.857	
	Horizontal speed	1	.000	1.212	.272	
	Vertical speed	1	.002	1.622	.204	
	Helical Pitch	1	.002	.002	.965	
	Helical Width	1	.001	.015	.902	
Error	Total speed	182	.005			
	oscillatory speed	182	.006			
	Horizontal speed	182	.000			
	Vertical speed	182	.001			
	Helical Pitch	182	1.238			
	Helical Width	182	.060			

Table 5.2

Parameters of larval skeleton used in the hydrodynamic model.

	Arm	Rod Type	Centroids of end discs (μm)						Measured diameter (μm)	Model diameter (μm)	Volume correction factor	Calcite Correction Factor		
			x1	y1	z1	x2	y2	z2						
Fed	AL	Simple	L	68.22	495.00	14.00	185.11	160.39	20.00	2.42	1.21		2.83	1
			R	411.17	460.00	24.00	297.00	157.72	30.00	2.44	1.22		2.83	
	PO	Fenestrated	L	288.44	385.80	124.93	286.20	145.05	70.96	8.00	4.00	0.32	2.83	
			R	182.84	395.45	127.36	192.50	145.24	40.00	8.00	4.00	0.32	2.83	
	PD	Fenestrated	L	148.29	177.75	80.70	190.16	142.91	49.40	7.10	3.55	0.32	2.83	
			R	328.60	175.76	64.53	292.22	145.96	56.28	6.60	3.30	0.32	2.83	
	B1	Simple	L	19.59	135.77	36.00	21.72	28.56	28.00	8.22	4.11			2
			R	294.51	157.65	43.00	267.84	30.56	44.78	8.76	4.38			2
	B2	Simple	L	182.56	147.11	14.00	223.20	149.11	40.00	2.72	1.36		2.83	
			R	282.78	140.16	28.00	267.98	147.36	52.00	2.72	1.36		2.83	
B3	Simple		270.30	25.70	29.84	220.90	23.80	29.84	7.74	3.87		2.83		
Starved	AL	Simple	L	151.56	50.27	143.00	166.29	275.58	76.00	5.25	2.63			
			R	310.28	48.50	128.00	270.60	290.98	68.00	4.01	2.01			
	PO	Fenestrated	L	45.74	23.70	52.00	141.64	281.07	54.00	7.50	3.75	0.32	2.83	
			R	357.12	25.35	2.00	264.02	286.82	46.00	7.62	3.81	0.32	2.83	
	B1	Simple	L	141.08	287.13	68.00	173.05	383.02	74.00	5.03	2.52		2.83	
			R	271.15	290.99	52.00	233.12	385.78	68.00	5.44	2.72		2.83	
	B2	Simple	L	145.86	281.07	54.00	199.50	261.23	50.00	4.68	4.68			2
			R	250.76	287.13	50.00	206.12	257.92	50.00	4.19	4.19			2
	B3	Simple		174.15	380.82	64.00	232.02	387.93	64.00	11.38	5.69		2.42	3

1. Calcite correction Factor (c) was calculated with the following equations

$$M_1 = V_1 (\rho_{\text{calcite}} - \rho_{\text{tissue}}) \quad \text{Excess density is the product between density difference and skeletal volume.}$$

$$M_2 = 0.25 \times V_1 (c \times \rho_{\text{calcite}} - \rho_{\text{tissue}})$$

$$M_1 = M_2 \quad \text{Excess density is conserved despite the volume change.}$$

$$\rho_{\text{calcite}} = 2669 \text{ kg m}^{-3}; \rho_{\text{tissue}} = 1040 \text{ kg m}^{-3}$$

2. Overestimated diameters compared to the literature value of simple rods, probably due to crystal axis affecting reflection of polarized light, and therefore calcite correction factors were not applied.
3. Solid cylinder was an overestimate of skeletal volume. The calcite correction factor was adjusted by considering V_1 as 1.3 times the actual volume.

Table 5.3

Morphometric measurements of starved and fed larval sand dollars, based on which finite element meshes were created.

	Project length from laser confocal micrograph (μm)								Model larva (m^3)		
	AL		PO		BL	AL:BL		PO:BL		Skeletal volume	Tissue volume
	Left	Right	Left	Right		Left	Right	Left	Right		
Fed	382.58	397.10	498.62	530.14	207.59	1.84	1.91	2.40	2.55	5.44×10^{-14}	2.06×10^{-12}
Starved	367.56	373.67	413.60	416.05	190.37	1.93	1.96	2.17	2.19	4.81×10^{-14}	1.34×10^{-12}

CHAPTER SIX: INTERDISCIPLINARY GUIDED INQUIRY ON ESTUARINE TRANSPORT USING A COMPUTER MODEL IN HIGH SCHOOL CLASSROOMS*

6.1 Abstract

The National Science Education Standard has highlighted the importance of active learning and reflection on contemporary scientific methods in K-12 classrooms, including the use of models. Computer modeling and visualization are tools that researchers employ in their scientific inquiry process, and often computer models are used in collaborative projects across disciplines. The goal of this project was to develop and field test a module that used computer model to teach marine sciences content in an applied, inquiry-based, and collaborative manner. Students used an estuarine transport model to explore the question of how circulation patterns affect planktonic organisms, demonstrating the interdisciplinary interaction of physics and biology. Our experience suggests that computer models, when used for inquiry, can help foster students' understanding of the nature of science and critical thinking skills.

* Originally published in the American Biology Teacher in January 2012, Volume 74, Issue 1, pages 26 - 33

6.2 Project motivation:

Calls from the National Research Council (1996) and National Science Foundation (2000) emphasized the importance of providing students with authentic science experiences through active inquiry. They also highlighted the importance of using and understanding the nature of models as conceptual representations that are developed and tested. Computer models and simulations are important tools in modern scientific inquiry, and are cornerstones of many interdisciplinary, collaborative projects. Therefore, introducing students to computer modeling is an important component of understanding modern scientific techniques.

Interactive illustrations are now available for a variety of topics, such as molecular genetics (Marbach-Ad *et al.*, 2008) and chemical bonds (Frailich *et al.*, 2009). These computer modeling tools have been shown to significantly improve students' understanding of abstract ideas by making them more tangible (Harris *et al.*, 2009). However, these examples represent only one of the diverse ways that scientists utilize computer models.

Scientists conduct experiments with computer models to understand phenomena and to generate predictions. For instance, a circulation model of Chesapeake Bay helped scientists to study the variations in flow patterns (Li *et al.*, 2005). This model also enabled scientists to test hypotheses regarding how changes in weather and/or land use would affect these flow patterns, and how organisms are subsequently dispersed (North *et al.*, 2010). Using computer models in an inquiry-based manner requires: i) understanding the concepts on variables and model limitations, ii) formulating testable hypotheses, iii) collecting and analyzing data (model output), and iv) drawing conclusions from the data (de Jong, 2006). Therefore, computer modeling can potentially equip students with scientific process skills essential to understanding scientific concepts.

In addition to being a tool for scientific inquiry, computer models can also provide students the opportunity to work collaboratively and across disciplines. Working collaboratively and in interdisciplinary manner are essential skills for scientists (Sung *et al.*, 2003). To date, several guided inquiry activities that utilize computer models are available (e.g., TELS Center at telscenter.org, Linn *et al.*, 2006). However, these models focus on a single discipline or subject (e.g., Marbach-Ad *et al.*, 2008) and are often designed for individual, independent investigation (e.g., Frailich *et al.*, 2009). Thus, there is an unmet need for well-designed, field tested classroom modeling activities that are both collaborative and interdisciplinary in nature.

We chose to model estuaries because they are good subjects for interdisciplinary learning. First, estuaries are semi-enclosed areas where fresh water and sea water meet, and therefore are good

case studies for physical principles on density and currents. Second, estuaries are important habitats and nursery grounds for many ecologically and economically important organisms (e.g., crabs and salmon), and therefore are places of ecological interest. The rich biological diversity in estuaries also provides a wide array of examples of how organisms adapt to their physical environment (interactions of physics and biology). Finally, estuaries are often heavily populated and threatened by human activities, and are therefore an illustration of how social sciences interact with natural sciences.

6.3 Module Development and Details

The module is developed based on estuarine circulation model (MacCready, 2007) and a particle-tracking algorithm developed by Dr. Grünbaum to study the role of behaviors in particle transport. We simplified and developed a graphical user interface for this model to allow students to investigate how changes in estuarine circulation would affect dispersal outcome. We also designed activities to provide students with background information on density, estuarine circulation and plankton ecology. We consulted three NSF-OACIS (Ocean and Coastal Interdisciplinary Sciences) GK-12 doctoral fellows who have worked in high school classrooms to ensure content relevance and appropriate presentation format (for more information on this program, visit <http://depts.washington.edu/oacis/>). The module was designed to align with National and Washington State Science Education Standard (Table 6.1).

The lesson was delivered in the combined time of a short 50 minute period and a 1 hour 50 minute long period. (See the discussion for how the lesson may be extended.) The lesson plan roughly followed the learning cycle (engagement, concept introduction, application and assessment). Instructors of the classes were two GK-12 doctoral fellows. Their research projects are not related to computer modeling or estuarine transport, so subject expertise is not necessary to teach this lesson. Lesson materials are available at http://www.ocean.washington.edu/people/faculty/grunbaum/education_resources.htm.

Engagement

Students were shown a physical model of an estuary, consisting of a clear box with salt water and freshwater, kept separate by a removable gate (Fig. 6.1). The students were asked to formulate a hypothesis regarding what would happen upon removal of the gate between salt and fresh water. They tested their hypothesis by removing the gate and were asked to draw a conclusion based on their observations. Instructors then led class discussion on students' observations, reviewing the concepts of density and circulation.

Concept introduction

A 20-minute-long, mini-lecture was presented to the students introducing three major concepts: 1) the characteristics of estuaries, 2) variations in estuarine circulation patterns, and 3) the nature of plankton. Students were asked to reflect on how changes in flow pattern would affect plankton, especially larvae of sessile marine invertebrates (Fig. 6.2).

Application

Students integrated the chemical (salinity), physical (density-driven flow), and biological (nature of plankton) concepts that they have learned by addressing the problem: "When and where should an organism release its larvae if the larvae grow best within the nutrient-rich estuary?" To investigate this problem, the students were introduced to the graphic user interface of the Estuary Model (Fig. 3), a Matlab® based program. In groups of two to three, students formulated their own hypotheses to answer the stated problem, explained their rationale, and collected, graphed, and drew conclusions from the model data they collected (Fig. 6.3 & 6.4).

This model simulates how density-driven currents transport passive particles within and out of an estuary. Model flow patterns are based on those of Willapa Bay, Washington, USA (MacCready, 2004). Students can manipulate three variables in this model, namely the volume of river flow (high,

medium and low representing different amounts of snow melt), the date of larval release, and the location of larval release (distance from the mouth of the estuary). Because the particles lack behavior, the distance transported is positively correlated to the duration of the larvae exposed to high river flow (i.e. the overlap between the 14 day larval duration, and the peak of river discharge), and the volume of river flow. Not surprisingly, larvae released closer to the mouth of the estuary are more likely to be washed out of the domain.

Learning Assessment

To assess understanding, students were asked to present to the class: their motivating questions, their data in a graphical format, and their conclusions (Fig. 6.4). The instructors guided the presentations and final discussion in which students reflected upon the lessons learned. In this discussion, the instructors provided real examples of organisms that migrate up and down estuaries that match students' predictions (Forward *et al.*, 2003). Instructors also encouraged students to reflect on the limitations of this simple computer model and potential way it could be enhanced.

6.4 Module Evaluation

The lesson was first pilot tested in a Marine Science classroom with 13 students in tenth to twelfth grade. Based on students' oral and written responses and on teachers' feedback, we modified the worksheets and field tested the current version of the lesson in another high school.

The lesson was presented by a GK-12 doctoral fellow to a total of 107 ninth through eleventh graders, enrolled into four different periods of a Marine Science class. Students filled in worksheets in class before and after the lesson to gauge their learning gain. The two tests contained six paired questions that were identical. The worksheets consisted of multiple choice, true or false, and short answer questions (Fig. 6.5). All short answer questions were graded on a 2 point scale (see Table 6.2). To gauge students' preconception, the pre-test contained a question asking student to name a plankton and explain how currents may affect plankton. The post-test had additional questions focusing on

students' understanding of the estuarine model and how currents affect particle transport. Identifiers were removed and replaced with randomly generated numbers, and graded by the same person in one sitting for objective assessment. Prior to administration, the tests were presented to five independent experts (doctoral candidates in Oceanography at University of Washington) for content validation. We did not have a control group that did not receive any instruction to confirm the reliability of the assessment. However, our goal is to assess whether student's understanding improved after the module. We, therefore, compared an individual's scores on the pre- and post- lesson worksheets for each question were compared with a paired t-test using the statistical package PSAW 18.0. Only students who turned in both the pre- and post- lesson worksheets in class were included in the statistics (n = 56).

6.5 Results

Students lack prior exposure to computer models

Of the 107 students in the Marine Biology Class, 23.1% responded that they had used a computer model prior to this lesson. They were asked in a follow-up question to describe the model. Four models were identified by the students: the star dome in physics, changes in carbon dioxide levels over time in biology, the relationship between temperature and respiration in biology, and natural selection/evolution in biology. Of these models, the first three were visualization of ideas; only the evolution model was used as a tool for inquiry (AVIDA is available at <http://avida-ed.msu.edu/>). In the evolution model, students manipulated traits of model organisms (microbe color) and observed how the population changed over time. Our survey shows that the large majority of students have little understanding of applying computer models in an inquiry manner.

Students' understanding of estuary and computer models improved significantly

In the six paired questions, students' scores significantly increased by the end of the lesson (Fig. 6.6). We note that students performed well, with averages >1.5 out of 2, in the pre-lesson

survey in most areas (concepts on density, making and explaining predictions for the physical model, estuarine characteristics, and estuarine circulation patterns). The lessons nonetheless helped students to reinforce their understanding, and hence to obtain significantly higher scores.

Students' lowest scored question on the pre-test addressed their understanding of why scientists use computer models. A majority of students thought scientists use computer models because "computers do not make mistakes" and "computers can give answers quickly". Responses like these indicated poor understanding of how computer models are designed, and a lack of awareness of modeling limitations. After the lesson, students provided much more sophisticated answers about why scientists use models. Some responses included: "models can help create an idea of possible outcomes without affect[ing] the real system (e.g. oil spill)" and "model[s] can be helpful to study places that [are] too difficult to reach or areas too large to sample".

In addition to better understanding of modeling motivation, students also improved their awareness of model limitations. Students were able to identify missing biological and physical mechanisms that could potentially affect the model outcome. Students were asked in the post test to suggest one feature to add to the model, and to list questions that could be addressed using the proposed feature. Example student responses include: "How would temperature and rainfall affect particle transport?", "I would add death rate because not all larvae survive in nature. Does the change in flow pattern still matter when organisms are dying?", "How would human interaction (e.g. pollution) and predator[s] affect larval transport?" In contrast to the novices' view that models are simply scaled-down replicas that accurately represent nature (Grosslight *et al.*, 1991), students developed a deeper understanding of modeling. They understood that models are often used to test ideas and phenomena, that models reflect the question/intent of the modeler and his/her assumptions, and that models can change through time.

Students' and in-service teachers' feedback

In addition to the worksheets, we also asked a small subset of the students whether they found the lesson interesting and whether they believed they had learned from the experience (n = 23). On a Likert scale of 1- 5, students believed that the lesson was 3/5 interesting and 3/5 useful. One student commented that s/he liked this lesson and learned from it because it was very clear and simple. Another commented that the lesson helped him/her put concepts from different subjects together.

Because the lessons in both the marine science classrooms were taught by GK12 fellows, their partner in-service teachers were able to observe the class. We held short debriefing sessions with the teachers to solicit their impressions of the lesson:

“The students were really impressed by the dynamic model and were engaged in the activities... I think this lesson is a valuable opportunity for my students to be exposed to and to conduct an experiment with an actual research tool that scientists use.” -- Marine Science Teacher 1.

“At first I was a little skeptical about this modeling lesson but now I think it is worth the effort. Students were really engaged and learned new concepts. This lesson provided a good transition between physical components and biological components in an environmental science class like ours.” -- Marine Science Teacher 2.

6.6 Discussion

The high school students we studied had had very little exposure to computer models – over 70% of them stated they had never used a computer model. Of those who had used a computer model, very few of them had used a model as a tool to conduct inquiry. It is also possible that teachers have introduced computer model but the activities did not make an impression. During our lesson, some student commented that “to win” they had to figure out the combination of parameters for which most particles were retained. Comments as such reflected students were treating the model as a computer game and failed to appreciate the scientific questions behind it. Despite widespread access to

computers, the applicability of computers to developing and testing scientific ideas has not been conveyed to the vast majority of high school science students. Our survey results emphasize the importance of making user-friendly, guided inquiry computer models more available to teachers and students. Our modeling lesson is an example illustrating how to move beyond using computer models as a visualization tool, and encourage students to actively and collaboratively conduct inquiries.

Beyond introducing students to using computer models for inquiry, our lesson also exposed students to interdisciplinary learning. Clay *et al.* (2008) pointed out that students failed to transfer their knowledge from one subject area to another, based on field tests of their interdisciplinary biology/physics lesson on plankton. Similar to their approach, our module encouraged student to connect large-scale physical phenomenon (estuarine flow) to biological concepts (maintaining population) through a real-life problem (larval dispersal in an estuary). In addition to biophysical interactions, estuaries can also be used to discuss human-nature interactions. For example, teachers can lead a follow-up discussion on human impacts on estuarine transport (e.g., how damming of rivers might interfere with river flow and the implications for larval transport). Alternatively, teachers may go more deeply into plankton biology by collecting plankton samples to illustrate diversity, by studying the morphology of plankton and understanding their life history adaptations (see Clay *et al.*, 2008), or by discussing how swimming behaviors such as vertical migration may affect dispersal patterns.

While computer labs in the high school classroom require advanced planning (such as reserving computer labs or carts), we believe conducting modeling activities in class could better facilitate group interactions and thus aid student learning. In our classes, students were actively engaged in discussion and were able to help each other overcome technical problems very quickly. Students were initially unfamiliar with the computer model and the graphical user interface, yet within- and between-group interactions allowed the students to make forward progress through the exercise. Students were also motivated to explore different aspects of the model so that they could

compare and contrast their findings with their classmates. Different modeling outcomes and conclusions between groups also stimulated in-depth discussion of the modeled systems. Therefore, group exploration of a new computer model was an effective approach in our classrooms.

Students' understanding of estuary and computer models improved after our lesson, suggesting that we achieved our project goal of making a lesson available that effectively delivers specific content and skills knowledge. Our experience showed that computer models are teaching tools with great potential as means of inquiry, venues of interdisciplinary learning, and intellectual challenges for student groups. We encourage teachers to use computer models both for visualization and inquiry to supplement existing lesson plans, so that high school classrooms better emulate and stimulate students' interests in real-world scientific research.

Figure 6.1

Physical model of an estuary

Created from a plastic container, the estuary model is divided into two compartments by a “flood gate.” The “flood gate” is a piece of plexiglass with a slit (approx. 1/2” x 1”) cut in the middle. An acetate sheet held in place with Vaseline closes off this slit and when removed allows the blue and yellow water to interact. Details of how to construct the model can be found at http://fermi.jhuapl.edu/student/currents/waterfall_apparatus.htm

- a) Salt water (blue) and fresh water (yellow) were poured into each compartment.
- b) When the flood gate was released, the denser, saline water sank to the bottom of the fresh water compartment, displacing the fresh water on top
- c) A stratified water column was formed.

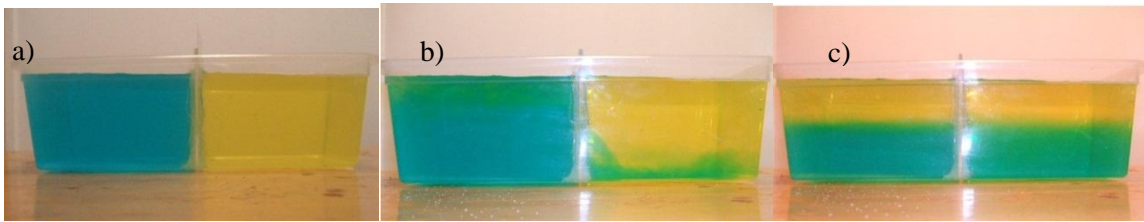


Photo credits: Elizabeth Tobin

Figure 6.2

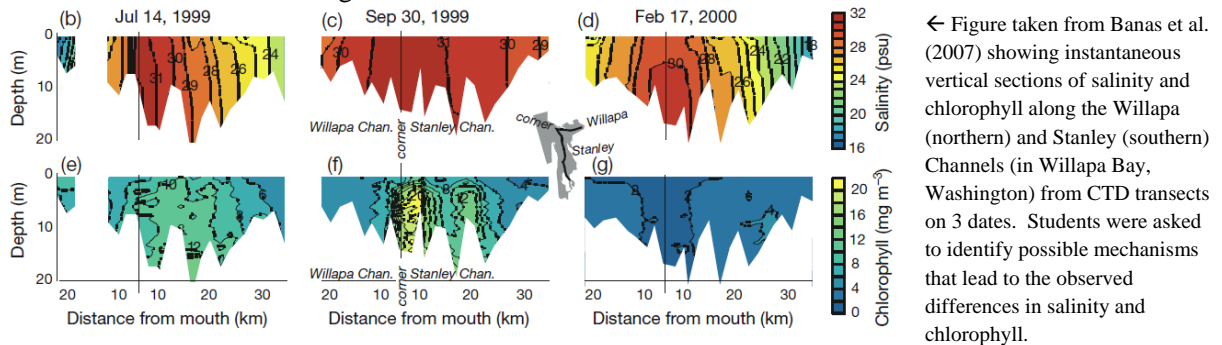
Key concepts introduced during the mini lecture

Characteristics of estuaries:

Students studied aerial photographs and maps of estuaries and discussed similarities between geographic locations.

Estuaries are coastal, semi-enclosed, well protected areas, often strongly influenced by human activities (as indicated by the number of cities and buildings).

Estuarine circulation and changes with time:



Students were asked to think about how flow pattern within an estuary changed across different time scales using different figures as clues (above). Circulation patterns are affected by tides (daily - monthly variation), rainfall (daily - seasonal variation), and snowfall (seasonal - yearly variations).

Plankton:

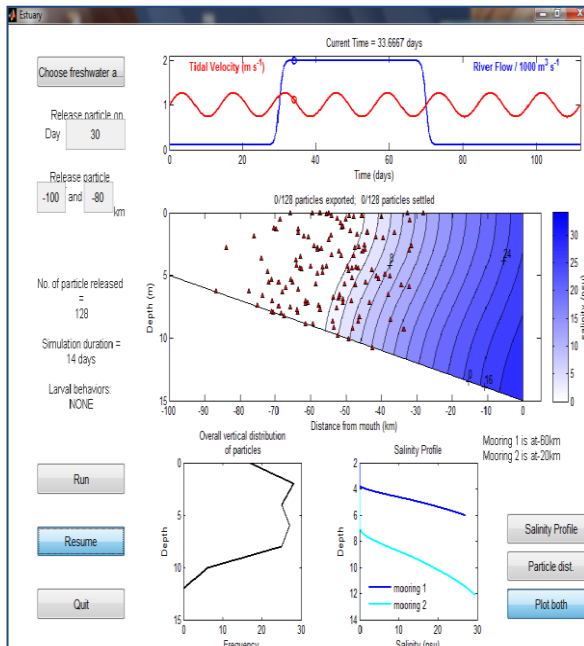


← Images of meroplanktonic invertebrate larvae (meroplankton are organisms that spend only a part of their life in the water column): a) a geoduck veliger ©Karen Chan, b) a crab zoea ©Richard Kirby, c) a sea star bipinnaria ©Fernanda Oyarzun, and d) a sand dollar pluteus ©Karen Chan

Students were shown a series of pictures of plankton (above). Students were introduced to the concept that some marine invertebrates spend part of their life in the plankton through a matching game to pair larval stages with adults.

To provide context of for the Estuary model, instructors illustrated the concept that for weakly swimming larvae, timing and locations of release and their behaviors could significantly affect where they are dispersed. The study by North et al. (2008) was an easy to understand example. Movies of North et al.'s computer model are available at http://northweb.hpl.umces.edu/videos_animations/Oyster_Larvae_Animations.htm

Figure 6.3
Computer model of estuarine model



Screen shot of the graphical user interface of the particle transport model used in this lesson (left).

Top panel: Volume of river flow (blue), and tidal cycle (red)

Middle panel: Cross section of estuary with contours showing salinity. Dots represent transported particles (model larvae)

Bottom panel: Vertical distribution of transported particle (left) and vertical salinity profile (right)

Students can manipulate 3 variables in this model: 1) volume of river flow (high, middle and low); 2) location of particle release; 3) timing of particle release.

In groups of 2-3, students formulated hypotheses about how changes in one or more of these variables affect particle transport. They reported their findings in a graph and orally to their peers at the end of the lesson.



Figure 6.4

Examples of students' responses on the guided inquiry worksheet

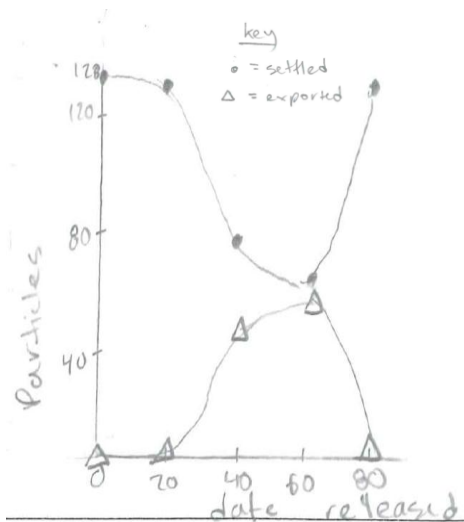
Your motivating statement:

We wonder what would happen if we change the release date of the particles to a low river flow period. We think dates with higher river flows will export more particles.

Your expected outcome and rationale:

We predict less particle[s] will be exported because there will be less flow to carry the particles away.

Sketch a graph to present your data:



Your conclusion:

We conclude that releasing the particle during the high river flow period caused more particles to be exported and not settled.

Your assumptions:

This model has many limitations such as carrying currents in different spots, presence of other organism[s] and the unsteady depth of the river bed.

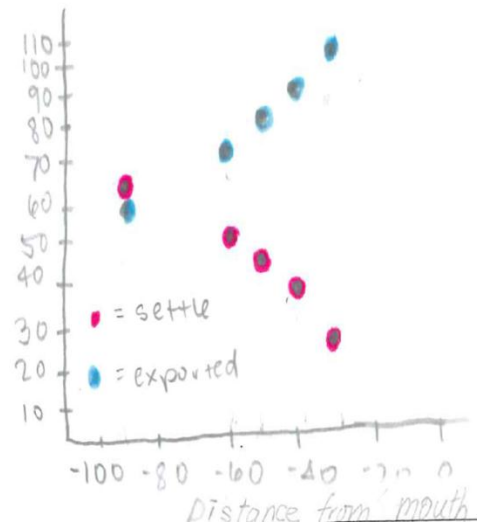
Your motivating statement:

We wonder what would happen if we change the release particle site [towards the mouth of the estuary]. We think less larvae would settle because there would be less time to mature and settle.

Your expected outcome and rationale:

Less larvae will settle when the release site is moved closer to the mouth of the estuary because they will have less time to mature.

Sketch a graph to present your data:



Your conclusion:

The higher the salinity (closer to the mouth) at the release site, the fewer particles that settle.

Your assumptions:

We assumed that no other organism[s] would be affecting the larvae and there is no human effect.

Figure 6.5

Example of assessment questions

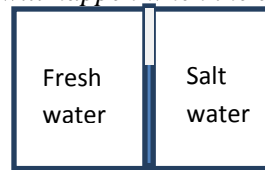
1: Water Density

Which of the following things can make fresh water at room temperature denser?

Cooling the water Adding more salt Heating the water Adding freshwater

2: Applying density concepts to physical models

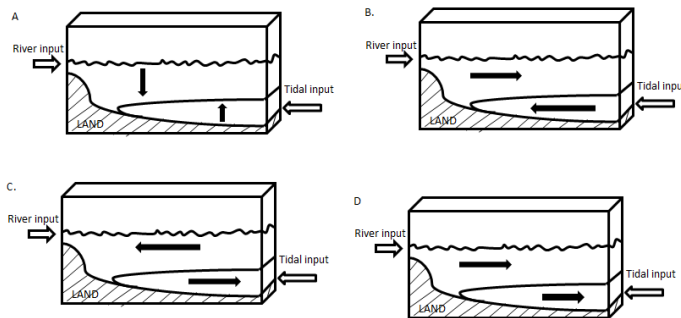
Based on your understanding of water density and density-driven water currents, what would you predict to happen in the model estuary shown? Mark on the following cross section (i.e. a slice of the box cut along the dotted line) using arrows of what will happen when the acetate is removed.



Explain your reasoning for the above prediction.

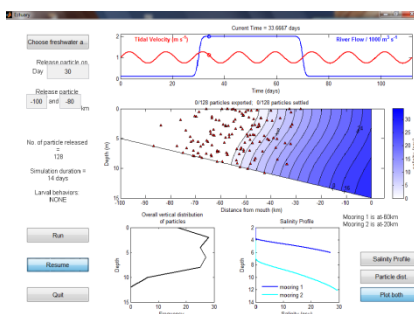
3: Characteristics of estuaries

The flow inside an estuary can be affected by the density of the freshwater input from the rivers and saline water from the sea. Based on your understanding of density-driven currents, which of the following pictures shows the overall direction of flow within an estuary most accurately?



4: Particle transport in estuary

One of the ways that scientists study estuary is using computer models to simulate flow patterns within the estuary. These models are also used to study how changes in flow patterns affect organism living in the estuary. Below is a screenshot of a model estuary within a normal year.



- What do you think will happen to the amount of freshwater input to the estuary in a year with intense rainfall such that the river flow doubled between Day 30 and 70?
- What do you predict would happen to the water flow within the estuary in the wet year described in part a) of this question? You can use drawings or describe in words.
- What would happen to the number of particles swept out of the estuary if the release date, location, and simulation duration remain unchanged? Give your reasons.

5: Modeling motivation and limitations

One of the ways that scientists study estuaries is using computer models to simulate flow patterns within an estuary and how these patterns would affect organisms living in the estuary.

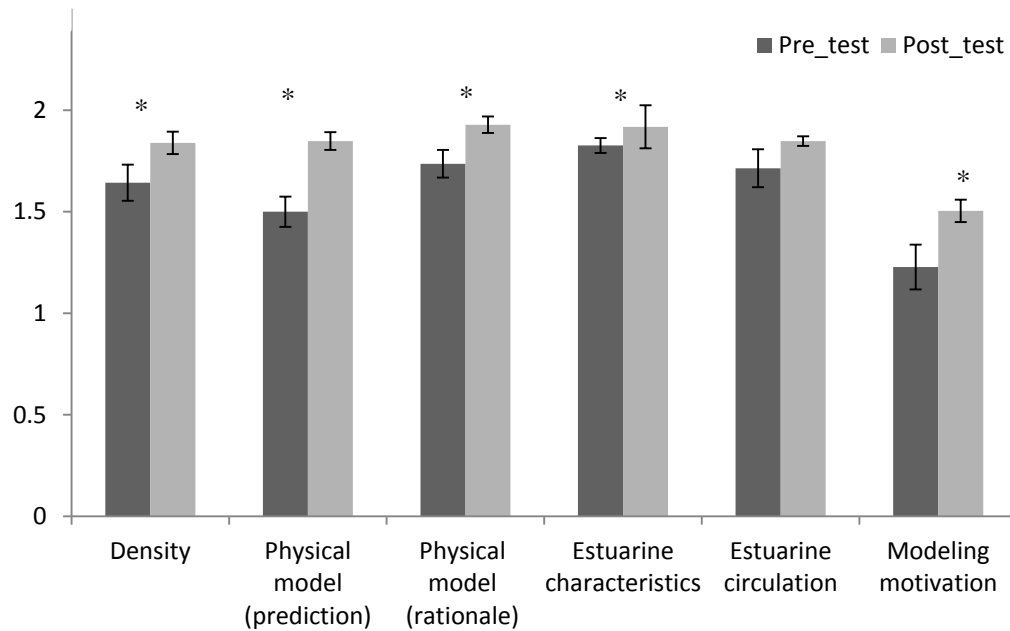
- Give two reasons why you think scientists use computer models in their research?
- Name one limitation of modeling estuaries on a computer.

Figure 6.6

Students' learning gain

Average scores and standard errors of students' responses in the pre- and post- lesson worksheet. Short answer questions were graded on a 2 point rubric. All questions are normalized to a 2-point scale. The table shows *t* and *p*-value for paired *t*-test. * represents significant difference.

Scoring rubric for short answer questions (0-2 point)	
Score	Criteria
0	No response
0.5	Incorrect answer
1	Correct answer but wrong logic
1.5	Correct answer with incomplete explanation
2	Correct answer with logical explanation



$T_{1,55}$	-2.281	-4.172	-2.619	-1.992	-1.218	-3.716
P	0.013	>0.001	0.006	0.026	0.114	0.0002

Table 6.1.

List of National and Washington State Science Education Standards met by this module

<u>National Science Education Standards</u>	<u>Washington State Science Education Standards</u>
<u>Level 9-12</u> <i>Science as inquiry Standards</i> Abilities necessary to do scientific inquiry Understanding about scientific inquiry	<u>Grade 9-12</u> EALR* 2 ~ Inquiry (Conducting analysis and thinking logically) The essence of scientific investigation involves the development of a theory or conceptual model that can generate testable predictions. EALR 3 ~ Application (Science, Technology and Society) The ability to solve problems is greatly enhanced by use of mathematics and information technologies. EALR 4 ~ Life Sciences (Maintenance and Stability of Population) Scientists represent ecosystems in the natural world using mathematical models.
<i>Physical Science Standards</i> Structure and properties of matters Motion and forces	
<i>Life Science Standards</i> Mass, energy and organization of living systems Behaviors of organisms	<u>Grade 6-8</u> EALR 2 ~Inquiry (Questioning and Investigating) Models are used to represent objects, events, systems, and processes. Models can be used to test hypotheses and better understand phenomena, but they have limitations. EALR 4~ Physical Sciences (Atoms and Molecules) Substances have characteristic intrinsic properties such as density, solubility, boiling point, and melting point, all of which are independent of the amount of the sample.
<i>Science and Technology Standards</i> Understanding about science and technology	
* EALR stands for Essential Academic Learning Requirement; Core concepts is stated in the ().	

BIBLIOGRAPHY

- Abramoff, M. D., Magelhaes, P. J. and Ram, S. J. (2004) Image Processing with ImageJ. *Biophotonics International* **11**, 36-42.
- Auclair, W. and Siegel, B. W. (1966) Cilia regeneration in the sea urchin embryo: evidence for a pool of ciliary proteins. *Science*, **154**, 913-915.
- Barton, A., Hales, B., Waldbusser, G. G., Langdon, C. and Feely, R. (2012) The Pacific oyster, *Crassostrea gigas*, shows negative correlation to naturally elevated carbon dioxide levels: Implications for near-term ocean acidification effects. *Limnology and Oceanography*, **57**, 698-710.
- Bartumeus, F., Peters, F., Pueyo, S., Marrase, C. and Catalan, J. (2003) Helical Levy walks: Adjusting searching statistics to resource availability in microzooplankton. *Proceedings of the National Academy of Sciences, USA*, **100**, 12771-12775.
- Bellas, J. (2006) Comparative toxicity of alternative antifouling biocides on embryos and larvae of marine invertebrates. *Science of the Total Environment*, **367**, 573-585.
- Bertram, D. F. and Strathmann, R. R. (1998) Effects of maternal and larval nutrition on growth and form of planktotrophic larvae. *Ecology*, **79**, 315-327.
- Blackford, J., Allen, J. I., Anderson, T. R. and Rose, K. A. (2010) Challenges for a new generation of marine ecosystem models: Overview of the Advances in Marine Ecosystem Modelling Research (AMEMR) Symposium, 23-26 June 2008, Plymouth UK Preface. *Journal of Marine Systems*, **81**, 1-3.
- Boidron-Metairon, I. F. (1988) Morphological plasticity in laboratory-reared echinoplutei of *Dendraster excentricus* (Eschscholtz) and *Lytechinus variegatus* (Lamarck) in response to food conditions. *Journal of Experimental Marine Biology and Ecology*, **119**, 31-41.
- Bookstein, F. L. (1997) *Morphometric tools for landmark data: Geometry and biology*. Cambridge University Press.
- Botello, G. and Krug, P. J. (2006) 'Desperate larvae' revisited: age, energy and experience affect sensitivity to settlement cues in larvae of the gastropod *Alderia* sp. *Marine Ecology Progress Series*, **312**, 149-159.
- Boudreau, B., Simard, Y. and Bourget, E. (1992) Influence of a thermocline on vertical-distribution and settlement of post-larvae of the American lobster *Homarus americanus milne* (Edwards). *Journal of Experimental Marine Biology and Ecology*, **162**, 35-49.
- Brett, M. T., Muller-Navarra, D. C., Ballantyne, A. P., Ravet, J. L. and Goldman, C. R. (2006) Daphnia fatty acid composition reflects that of their diet. *Limnology and Oceanography*, **51**, 2428-2437.

- Broekhuizen, N., Lundquist, C. J., Hadfield, M. G. and Brown, S. N. (2011) Dispersal of oyster (*Ostrea chilensis*) larvae in Tasman Bay inferred using a verified particle tracking model that incorporates larval behavior. *Journal of Shellfish Research*, **30**, 643-658.
- Brown, M., Jeffrey, S., Volkman, J. and Dunstan, G. (1997) Nutritional properties of microalgae for mariculture. *Aquaculture*, **151**, 315-331.
- Burke, R. D. (1983) Neural Control of Metamorphosis in *Dendraster excentricus* *Biological Bulletin*, **164**, 176-188.
- Byrne, M. (2011) Impact of ocean warming and ocean acidification on marine invertebrate life history stages: vulnerabilities and potential for persistence in a changing ocean. *Oceanography and Marine Biology: An Annual Review*, **49**, 1-42.
- Byrne, M., Soars, N., Selvakumaraswamy, P., Dworjanyn, S. A. and Davis, A. R. (2010) Sea urchin fertilization in a warm, acidified and high pCO₂ ocean across a range of sperm densities. *Marine Environmental Research*, **69**, 234-239.
- Cai, W.-J. and Reimers, C. E. (1993) The development of pH and pCO₂ microelectrodes for studying the carbonate chemistry of pore waters near the sediment-water interface. *Limnology and Oceanography*, **38**, 1762-1773.
- Caldeira, K. and Wickett, M. E. (2003) Anthropogenic carbon and ocean pH. *Nature*, **425**, 365-365.
- Chan, K. Y. K. (2012) Biomechanics of Larval Morphology Affect Swimming: Insights from the Sand Dollars *Dendraster excentricus*. *Integrative and Comparative Biology*.
- Chan, K. Y. K. and Grünbaum, D. (2010) Temperature and diet modified swimming behaviors of larval sand dollar. *Marine Ecology Progress Series*, **415**, 49-59.
- Chan, K. Y. K., Grünbaum, D. and O'Donnell, M. J. (2011) Effects of ocean-acidification-induced morphological changes on larval swimming and feeding. *Journal of Experimental Biology*, **214**, 3857-3867.
- Chia, F. S., Bucklandnicks, J. and Young, C. M. (1984) Locomotion of marine invertebrate larvae - a review. *Canadian Journal of Zoology*, **62**, 1205-1222.
- Clark, D., Lamare, M. and Barker, M. (2009) Response of sea urchin pluteus larvae (Echinodermata: Echinoidea) to reduced seawater pH: a comparison among a tropical, temperate, and a polar species. *Marine Biology*, **156**, 1125-1137.
- Clay, T. W., Fox, J. B., Grünbaum, D. and Jumars, P. A. (2008) How plankton swim: An interdisciplinary approach for using mathematics & physics to understand the biology of the natural world. *American Biology Teacher*, **70**, 363-370.
- Clay, T. W. and Grünbaum, D. (2010) Morphology-flow interactions lead to stage-selective vertical transport of larval sand dollars in shear flow. *Journal of Experimental Biology*, **213**, 1281-1292.

- Clay, T. W. and Grünbaum, D. (2011) Swimming performance as a constraint on larval morphology in plutei. *Marine Ecology Progress Series*, **423**, 185-196.
- Collin, R. (1997) Ontogeny of subtle skeletal asymmetries in individual larvae of the sand dollar *Dendraster excentricus*. *Evolution*, **51**, 999-1005.
- Cowen, R. K., Gawarkiewicz, G., Pineda, J., Thorrold, S. R. and Werner, F. E. (2007) Population connectivity in marine systems: an overview. *Oceanography*, **20**, 14-21.
- Cowen, R. K. and Sponaugle, S. (2009) Larval dispersal and marine population connectivity. *Annual Review of Marine Science*, **1**, 443-466.
- Cox, P. M., Betts, R. A., Jones, C. D., Spall, S. A. and Totterdell, I. J. (2000) Acceleration of global warming due to carbon-cycle feedbacks in a coupled climate model. *Nature*, **408**, 184-187.
- Dai, M., Lu, Z., Zhai, W., Chen, B., Cao, Z., Zhou, K., Cai, W. J. and Chen, C. T. A. (2009) Diurnal variations of surface seawater pCO₂ in contrasting coastal environments. *Limnology and Oceanography*, **54**, 735-745.
- Davis, J. P. and Stephens, G. C. (1984) Uptake of free amino acids by bacteria-free larvae of the sand dollar *Dendraster excentricus*. *American Journal of Physiology: Regulatory, Integrative and Comparative Physiology*, **247**, R733-739.
- De Jong, T. (2006) Technological Advances in Inquiry Learning. *Science*, **312**, 532-533.
- Decker, G. L. and Lennarz, W. J. (1988) Skeletogenesis in the sea urchin embryo. *Development*, **103**, 231.
- Deksheniaks, M. M., Hofmann, E. E., Klinck, J. M. and Powell, E. N. (1996) Modeling the vertical distribution of oyster larvae in response to environmental conditions. *Marine Ecology Progress Series*, **136**, 97-110.
- Dickson, A. and Millero, F. (1987) A comparison of the equilibrium constants for the dissociation of carbonic acid in seawater media. *Deep Sea Research (Part I, Oceanographic Research Papers)*, **34**, 1733-1743.
- Dickson, A. G., Sabine, C. L. and Christian, J. R. (2007) Guide to best practices for ocean CO₂ measurements. *PICES special publication*, **3**.
- Doney, S. C., Fabry, V. J., Feely, R. A. and Kleypas, J. A. (2009) Ocean acidification: the other CO₂ problem. *Annual Review of Marine Science*, **1**, 169-192.
- Doo, S. S., Dworjanyn, S. A., Foo, S. A., Soars, N. A. and Byrne, M. (2011) Impacts of ocean acidification on development of the meroplanktonic larval stage of the sea urchin *Centrostephanus rodgersii*. *ICES Journal of Marine Science*.
- Dupont, S., Dorey, N., Stumpp, M., Melzner, F. and Thorndyke, M. (2012) Long-term and trans-life-cycle effects of exposure to ocean acidification in the green sea urchin *Strongylocentrotus droebachiensis*. *Marine Biology*, 1-9.

- Dupont, S., Dorey, N. and Thorndyke, M. (2010) What meta-analysis can tell us about vulnerability of marine biodiversity to ocean acidification? *Estuarine, Coastal and Shelf Science*, **89**, 182-185.
- Dupont, S., Havenhand, J., Thorndyke, W., Peck, L. and Thorndyke, M. (2008) Near-future level of CO₂-driven ocean acidification radically affects larval survival and development in the brittlestar *Ophiothrix fragilis*. *Marine Ecology Progress Series*, **373**, 285-294.
- Durham, W. M., Kessler, J. O. and Stocker, R. (2009) Disruption of vertical motility by shear triggers formation of thin phytoplankton layers. *Science*, **323**, 1067-1070.
- Eaves, A. A. and Palmer, A. R. (2003) Widespread cloning in echinoderm larvae. *Nature*, **425**, 146-146.
- Emler, R. B. (1982) Echinoderm calcite - a mechanical analysis from larval spicules. *Biological Bulletin*, **163**, 264-275.
- Emler, R. B. (1983) Locomotion, drag, and the rigid skeleton of larval echinoderms. *Biological Bulletin*, **164**, 433-445.
- Emler, R. B. (1986) Larval production, dispersal, and growth in a fjord - a case-study on larvae of the sand dollar *Dendraster excentricus*. *Marine Ecology Progress Series*, **31**, 245-254.
- Emler, R. B. (1990) Flow-fields around ciliated larvae - effects of natural and artificial tethers. *Marine Ecology Progress Series*, **63**, 211-225.
- Emler, R. B. (1991) Functional constraints on the evolution of larval forms of marine invertebrates - experimental and comparative evidence. *American Zoologist*, **31**, 707-725.
- Emler, R. B. (1994) Body form and patterns of ciliation in nonfeeding larvae of echinoderms - Functional solutions to swimming in the plankton. *American Zoologist*, **34**, 570-585.
- Evans, J. P. and Marshall, D. J. (2005) Male-by-female interactions influence fertilization success and mediate the benefits of polyandry in the sea urchin *Heliocidaris erythrogramma*. *Evolution*, 106-112.
- Fabry, V. J., Seibel, B. A., Feely, R. A. and Orr, J. C. (2008) Impacts of ocean acidification on marine fauna and ecosystem processes. *ICES Journal of Marine Science*, **65**, 414-432.
- Feely, R. A., Sabine, C. L., Hernandez-Ayon, J. M., Ianson, D. and Hales, B. (2008) Evidence for upwelling of corrosive "acidified" water onto the continental shelf. *Science*, **320**, 1490-1492.
- Fenaux, L., Strathmann, M. F. and Strathmann, R. R. (1994) Five tests of food-limited growth of larvae in coastal waters by comparisons of rates of development and form of echinoplutei. *Limnology and Oceanography*, 84-98.
- Fiksen, O., Jorgensen, C., Kristiansen, T., Vikebo, F. and Huse, G. (2007) Linking behavioural ecology and oceanography: larval behaviour determines growth, mortality and dispersal. *Marine Ecology Progress Series*, **347**, 195-205.

- Fisher, R. (2005) Swimming speeds of larval coral reef fishes: impacts on self-recruitment and dispersal. *Marine Ecology Progress Series*, **285**, 223-232.
- Ford, M. D., Schuegraf, M. J., Elkink, M. S. and Demont, M. E. (2005) A comparison of swimming structures and kinematics in three species of crustacean larvae. *Marine and Freshwater Behaviour and Physiology*, **38**, 79-94.
- Forward, Tankersley and Pochelon (2003) Circatidal activity rhythms in ovigerous blue crabs *Callinectes sapidus*: implications for ebb-tide transport during the spawning migration. *Marine Biology*, **142**, 67-76.
- Forward, R. B. and Tankersley, R. A. (2001) Selective tidal-stream transport of marine animals. *Oceanography and Marine Biology: An Annual Review*, **39**, 305-353.
- Frailich, M., Kesner, M. and Hofstein, A. (2009) Enhancing students' understanding of the concept of chemical bonding by using activities provided on an interactive website. *Journal of Research in Science Teaching*, **46**, 289-310.
- Fuchs, H. L., Mullineaux, L. S. and Solow, A. R. (2004) Sinking behavior of gastropod larvae (*Ilyanassa obsoleta*) in turbulence. *Limnology and Oceanography*, **49**, 1937-1948.
- Gaines, S. and Roughgarden, J. (1985) Larval settlement rate - a leading determinant of structure in an ecological community of the marine intertidal zone. *Proceedings of the National Academy of Sciences of the United States of America*, **82**, 3707-3711.
- Gallager, S. M. (1993) Hydrodynamic disturbances produced by small zooplankton - case-study for the veliger larva of a bivalve mollusk. *Journal of Plankton Research*, **15**, 1277-1296.
- Gazeau, F., Quiblier, C., Jansen, J. M., Gattuso, J. P., Middelburg, J. J. and Heip, C. H. R. (2007) Impact of elevated CO₂ on shellfish calcification. *Geophysical Research Letters*, **34**.
- George, S. B., Fox, C. and Wakeham, S. (2008) Fatty acid composition of larvae of the sand dollar *Dendraster excentricus* (Echinodermata) might reflect FA composition of the diets. *Aquaculture*, **285**, 167-173.
- Geuzaine, C. and Remacle, J. F. (2009) Gmsh: A 3-D finite element mesh generator with built-in pre- and post-processing facilities. *International Journal for Numerical Methods in Engineering*, **79**, 1309-1331.
- Grosslight, L., Unger, C., Jay, E. and Smith, C. L. (1991) Understanding models and their use in science: Conceptions of middle and high school students and experts. *Journal of Research in Science Teaching*, **28**, 799-822.
- Grünbaum, D. (1995) A model of feeding currents in encrusting bryozoans shows interference between zooids within a colony. *Journal of Theoretical Biology*, **174**, 409-425.
- Grünbaum, D. (1998) Using spatially explicit models to characterize foraging performance in heterogeneous landscapes. *American Naturalist*, **151**, 97-113.

- Grünbaum, D. and Strathmann, R. R. (2003) Form, performance and trade-offs in swimming and stability of armed larvae. *Journal of Marine Research*, **61**, 659-691.
- Hadfield, M. G., Faucci, A. and Koehl, M. A. R. (2006) Measuring recruitment of minute larvae in a complex field environment: The corallivorous nudibranch *Phestilla sibogae* (Bergh). *Journal of Experimental Marine Biology and Ecology*, **338**, 57-72.
- Hall-Spencer, J. M., Rodolfo-Metalpa, R., Martin, S., Ransome, E., Fine, M., Turner, S. M., Rowley, S. J., Tedesco, D. and Buia, M. C. (2008) Volcanic carbon dioxide vents show ecosystem effects of ocean acidification. *Nature*, **454**, 96-99.
- Hall, J. M., Parrish, C. C. and Thompson, R. J. (2002) Eicosapentaenoic acid regulates scallop (*Placopecten magellanicus*) membrane fluidity in response to cold. *Biological Bulletin*, **202**, 201-203.
- Hammond, L. M. and Hofmann, G. E. (2012) Early developmental gene regulation in *Strongylocentrotus purpuratus* embryos in response to elevated CO₂ seawater conditions. *Journal of Experimental Biology*, **215**, 2445-2454.
- Harris, M. A., Peck, R. F., Colton, S., Morris, J., Chaibub Neto, E. and Kallio, J. (2009) A combination of hand-held models and computer imaging programs helps students answer oral questions about molecular structure and function: A controlled investigation of student learning. *CBE Life Sciences Education*, **8**, 29-43.
- Harris, R. J. (1975) *A primer of multivariate statistics*. Vol., Lawrence Erlbaum.
- Hart, M. W. (1990) Manipulating external Ca²⁺ inhibits particle capture by planktotrophic echinoderm larvae. *Canadian Journal of Zoology*, **68**, 2610-2615.
- Hart, M. W. (1991) Particle captures and the method of suspension feeding by echinoderm larvae. *Biological Bulletin*, **180**, 12-27.
- Hart, M. W. and Strathmann, R. R. (1994) Functional consequences of phenotypic plasticity in echinoid larvae. *Biological Bulletin*, **186**, 291-299.
- Havenhand, J. N., Buttler, F. R., Thorndyke, M. C. and Williamson, J. E. (2008) Near-future levels of ocean acidification reduce fertilization success in a sea urchin. *Current Biology*, **18**, R651-R652.
- Hayakawa, K., Handa, N., Kawanobe, K. and Wong, C. S. (1996) Factors controlling the temporal variation of fatty acids in piculate matter during a phytoplankton bloom in a marine mesocosm. *Marine Chemistry*, **52**, 233-244.
- Hettinger, A., Sanford, E., Gaylord, B., Hill, T. M. and Russell, A. D. (2012) Extended Larval Carry-over Effects: Synergisms from a Stressful Benthic Existence in Juvenile Olympia Oysters. *Ecology*.

- Heyland, A. and Hodin, J. (2004) Heterochronic developmental shift caused by thyroid hormone in larval sand dollars and its implications for phenotypic plasticity and the evolution of nonfeeding development. *Evolution*, **58**, 524-538.
- Intergovernmental Panel on Climate Change (2007) Summary for policymakers. In: S. Solomon (ed) *Climate Change 2007: The Physical Science Basis. Contribution of Working Group I to the Fourth Assessment Report of the Intergovernmental Panel on Climate Change*. pp. 1-18.
- Irisson, J. O., Guigand, C. and Paris, C. B. (2009) Detection and quantification of marine larvae orientation in the pelagic environment. *Limnology and Oceanography: Methods*, **7**, 664-672.
- Kjørboe, T. and Visser, A. W. (1999) Predator and prey perception in copepods due to hydromechanical signals. *Marine Ecology Progress Series*, **179**, 81-95.
- Klein Breteler, W., Schogt, N., Baas, M., Schouten, S. and Kraay, G. (1999) Trophic upgrading of food quality by protozoans enhancing copepod growth: role of essential lipids. *Marine Biology*, **135**, 191-198.
- Kleypas, J. A., Buddemeier, R. W., Archer, D., Gattuso, J. P., Langdon, C. and Opdyke, B. N. (1999) Geochemical consequences of increased atmospheric carbon dioxide on coral reefs. *Science*, **284**, 118-120.
- Klingenberg, C. P. (2011) MorphoJ: an integrated software package for geometric morphometrics. *Molecular Ecology Resources*, **11**, 353-357.
- Koehl, M. A. R. (2007) Mini review: Hydrodynamics of larval settlement into fouling communities. *Biofouling*, **23**, 357-368.
- Kurihara, H. (2008) Effects of CO₂-driven ocean acidification on the early developmental stages of invertebrates. *Marine Ecology Progress Series*, **373**, 275-284.
- Kurihara, H. and Shirayama, Y. (2004) Effects of increased atmospheric CO₂ on sea urchin early development. *Marine Ecology Progress Series*, **274**, 161-169.
- Lacalli, T. C. and Gilmour, T. H. J. (1990) Ciliary Reversal and Locomotory Control in the Pluteus Larva of *Lytechinus pictus*. *Philosophical Transactions of the Royal Society of London Series B-Biological Sciences*, **330**, 391-396.
- Levin, L. A. (2006) Recent progress in understanding larval dispersal: new directions and digressions. *Integrative and Comparative Biology*, **46**, 282-297.
- Li, M., Zhong, L. and Boicourt, W. C. (2005) Simulations of Chesapeake Bay estuary: Sensitivity to turbulence mixing parameterizations and comparison with observations. *Journal of Geophysical Research*, **110**, C12004.
- Liao, J. C. (2007) A review of fish swimming mechanics and behaviour in altered flows. *Philosophical Transactions of the Royal Society B-Biological Sciences*, **362**, 1973-1993.
- Linn, M. C., Lee, H.-S., Tinker, R., Husic, F. and Chiu, J. L. (2006) Teaching and assessing knowledge integration in science. *Science*, **313**, 1049-1050.

- Logue, J. A., Howell, B. R., Bell, J. G. and Cossins, A. R. (2000) Dietary n-3 long-chain polyunsaturated fatty acid deprivation, tissue lipid composition, ex vivo prostaglandin production, and stress tolerance in juvenile Dover sole (*Solea solea* L.). *Lipids*, **35**, 745-755.
- Maccready, P. (2004) Toward a unified theory of tidally-averaged estuarine salinity structure. *Estuaries and Coasts*, **27**, 561-570.
- Maccready, P. (2007) Estuarine adjustment. *Journal of Physical Oceanography*, **37**, 2133-2145.
- Machemer, H. and Braucker, R. (1992) Gravireception and graviresponses in ciliates. *Acta Protozoologica*, **31**, 185-214.
- Marbach-Ad, G., Rotbain, Y. and Stavy, R. (2008) Using computer animation and illustration activities to improve high school students' achievement in molecular genetics. *Journal of Research in Science Teaching*, **45**, 273-292.
- Marsh, A. G. and Manahan, D. T. (1999) A method for accurate measurements of the respiration rates of marine invertebrate embryos and larvae. *Marine Ecology Progress Series*, **184**, 1-10.
- Mayali, X., Franks, P. J. S., Tanaka, Y. and Azam, F. (2008) Bacteria-induced motility reduction in *Lingulodinium polyedrum* (Dinophyceae). *Journal of Phycology*, **44**, 923-928.
- McDonald, K. A. (2004) Patterns in early embryonic motility: Effects of size and environmental temperature on vertical velocities of sinking and swimming echinoid blastulae. *Biological Bulletin*, **207**, 93-102.
- McDonald, K. A. and Grünbaum, D. (2010) Swimming performance in early development and the “other” consequences of egg size for ciliated planktonic larvae. *Integrative and Comparative Biology*, **50**, 589-605.
- McDonald, K. A. and Vaughn, D. (2010) Abrupt change in food environment induces cloning in plutei of *Dendraster excentricus*. *Biological Bulletin*, **219**, 38-49.
- McEdward, L. R. (1985) Effects of temperature on the body form, growth, electron transport system activity, and development rate of an echinopluteus. *Journal of Experimental Marine Biology and Ecology*, **93**, 169-181.
- McHenry, M. J., Azizi, E. and Strother, J. A. (2003) The hydrodynamics of locomotion at intermediate Reynolds numbers: undulatory swimming in ascidian larvae (*Botrylloides* sp.). *Journal of Experimental Biology*, **206**, 327-343.
- McManus, M. A. and Woodson, C. B. (2012) Plankton distribution and ocean dispersal. *Journal of Experimental Biology*, **215**, 1008-1016.
- Mehrbach, C., Culberson, C., Hawley, J. and Pytkowicz, R. (1973) Measurement of the apparent dissociation constants of carbonic acid in seawater at atmospheric pressure. *Limnology and Oceanography*, 897-907.
- Melzner, F., Gutowska, M., Langenbuch, M., Dupont, S., Lucassen, M., Thorndyke, M. C., Bleich, M. and Pörtner, H. O. (2009) Physiological basis for high CO₂ tolerance in marine ectothermic

- animals: pre-adaptation through lifestyle and ontogeny? *Biogeosciences Discussions*, **6**, 2313-2331.
- Menden-Deuer, S. (2008) Spatial and temporal characteristics of plankton-rich layers in a shallow, temperate fjord. *Marine Ecology Progress Series*, **355**, 21-30.
- Menden-Deuer, S. and Grünbaum, D. (2006) Individual foraging behaviors and population distributions of a planktonic predator aggregating to phytoplankton thin layers. *Limnology and Oceanography*, **51**, 109-116.
- Metaxas, A. (2001) Behaviour in flow: perspectives on the distribution and dispersion of meroplanktonic larvae in the water column. *Canadian Journal of Fisheries and Aquatic Sciences*, **58**, 86-98.
- Metaxas, A., Mullineaux, L. S. and Sisson, J. (2009) Distribution of echinoderm larvae relative to the halocline of a salt wedge. *Marine Ecology Progress Series*, **377**, 157-168.
- Metaxas, A. and Saunders, M. (2009) Quantifying the "bio-" components in biophysical models of larval transport in marine benthic invertebrates: advances and pitfalls. *Biological Bulletin*, **216**, 257-272.
- Metaxas, A. and Young, C. M. (1998) Responses of echinoid larvae to food patches of different algal densities. *Marine Biology*, **130**, 433-445.
- Miner, B. G. (2005) Evolution of feeding structure plasticity in marine invertebrate larvae: a possible trade-off between arm length and stomach size. *Journal of Experimental Marine Biology and Ecology*, **315**, 117-125.
- Mogami, Y., Ishii, J. and Baba, S. A. (2001) Theoretical and experimental dissection of gravity-dependent mechanical orientation in gravitactic microorganisms. *Biological Bulletin*, **201**, 26-33.
- Morgan, S. G. (1995) Life and death in the plankton: larval mortality and adaptation. In: L. McEdward (ed.) *Ecology of Marine Invertebrate Larvae*, CRC Press, Boca Raton, Florida. CRC Press, Boca Raton, Florida. , pp. 279-321.
- Mullin, M., Sloan, P. and Eppley, R. (1966) Relationship between carbon content, cell volume, and area in phytoplankton. *Limnology and Oceanography*, **11**, 307-311.
- Natioanl Research Council (1996) *Natioanl Science Education Standards*. Vol., National Academy Press, Washington, D.C. .
- Nawroth, J. C., Feitl, K. E., Colin, S. P., Costello, J. H. and Dabiri, J. O. (2010) Phenotypic plasticity in juvenile jellyfish medusae facilitates effective animal-fluid interaction. *Biology Letters*, **6**, 389-393.
- Naylor, E. (2006) Orientation and navigation in coastal and estuarine zooplankton. *Marine and Freshwater Behaviour and Physiology*, **39**, 13-24.

- North, E. W., King, D. M., Xu, J., Hood, R. R., Newell, R. I. E., Paynter, K., Kellogg, M. L., Liddel, M. K. and Boesch, D. F. (2010) Linking optimization and ecological models in a decision support tool for oyster restoration and management. *Ecological Applications*, **20**, 851-866.
- North, E. W., Schlag, Z., Hood, R. R., Li, M., Zhong, L., Gross, T. and Kennedy, V. S. (2008) Vertical swimming behavior influences the dispersal of simulated oyster larvae in a coupled particle-tracking and hydrodynamic model of Chesapeake Bay. *Marine Ecology Progress Series*, **359**, 99-115.
- O'Connor, B., Bowmer, T. and Grehan, A. (1983) Long-term assessment of the population dynamics of *Amphiura filiformis* (Echinodermata: Ophiuroidea) in Galway Bay (west coast of Ireland). *Marine Biology*, **75**, 279-286.
- O'Donnell, M. J., Todgham, A. E., Sewell, M. A., Hammond, L. T. M., Ruggiero, K., Fanguie, N. A., Zippay, M. L. and Hofmann, G. E. (2010) Ocean acidification alters skeletogenesis and gene expression in larval sea urchins. *Marine Ecology Progress Series*, **398**, 157-171.
- Okazaki, K. and Inoue, S. (1976) Crystal Property of the Larval Sea Urchin Spicule. *Development, Growth & Differentiation*, **18**, 413-434.
- Orr, J. C., Fabry, V. J., Aumont, O., Bopp, L., Doney, S. C., Feely, R. A., Gnanadesikan, A., Gruber, N., Ishida, A. and Joos, F. (2005) Anthropogenic ocean acidification over the twenty-first century and its impact on calcifying organisms. *Nature*, **437**, 681-686.
- Parrish, C. C., Thompson, R. J. and Deibel, D. (2005) Lipid classes and fatty acids in plankton and settling matter during the spring bloom in a cold ocean coastal environment. *Marine Ecology Progress Series*, **286**, 57-68.
- Paulay, G., Boring, L. and Strathmann, R. R. (1985) Food limited growth and development of larvae: experiments with natural sea water. *Journal of Experimental Marine Biology and Ecology*, **93**, 1-10.
- Pearse, J. S. (2006) Ecological Role of Purple Sea Urchins. *Science*, **314**, 940-941.
- Pechenik, J. A. (1987) Environmental influences on larval survival and development. In: A. Giese, J. Pearse and V. Pearse (eds) *Reproduction of marine invertebrates*. Vol. X. Blackwell Scientific, Palo Alto, CA, pp. 511-608.
- Pechenik, J. A., Wendt, D. E. and Jarrett, J. N. (1998) Metamorphosis is not a new beginning. *Bioscience*, **48**, 901-910.
- Pennington, J. T. and Emlet, R. B. (1986) Ontogenic and diel vertical migration of a planktonic echinoid larva, *Dendraster excentricus* (Eschscholtz) - occurrence, causes, and probable consequences. *Journal of Experimental Marine Biology and Ecology*, **104**, 69-95.
- Pennington, J. T. and Strathmann, R. R. (1990) Consequences of the calcite skeletons of planktonic echinoderm larvae for orientation, swimming, and shape. *Biological Bulletin*, **179**, 121-133.

- Pierrot, D., Lewis, E. and Wallace, D. (2006) CO2SYS MS Excel Program program developed for CO₂ system calculations. *ORNL/CDIAC-105. Carbon Dioxide Information Analysis Center, Oak Ridge National Laboratory, US Department of Energy, Oak Ridge, TN.*
- Podolsky, R. D. and Emlet, R. B. (1993) Separating the effects of temperature and viscosity on swimming and water-movement by sand dollar larvae (*Dendraster excentricus*). *Journal of Experimental Biology*, **176**, 207-221.
- Pörtner, H. O. (2008) Ecosystem effects of ocean acidification in times of ocean warming: a physiologist's view. *Marine Ecology Progress Series*, **373**, 203-217.
- Ravet, J. L., Brett, M. T. and M • Ler-Navarra, D. C. (2003) A test of the role of polyunsaturated fatty acids in phytoplankton food quality for *Daphnia* using liposome supplementation. *Limnology and Oceanography*, **48**, 1938-1947.
- Riebesell, U., Zondervan, I., Rost, B. È., Tortell, P. D., Zeebe, R. E. and Morel, F. È. M. M. (2000) Reduced calcification of marine plankton in response to increased atmospheric CO₂. *Nature*, **407**, 364-367.
- Roberts, A. M. (1970) Geotaxis in motile micro-organisms. *Journal of Experimental Biology*, **53**, 687-699.
- Rohlf, F. J. (2010.) Tpsdig2, version 2.16. Department of Ecology and Evolution, State University of New York., Stony Brook, NY. .
- Rumrill, S. (1990) Natural mortality of marine invertebrate larvae. *Ophelia.*, **32**, 163-198.
- Sabine, C. L., Feely, R. A., Gruber, N., Key, R. M., Lee, K., Bullister, J. L., Wanninkhof, R., Wong, C. S., Wallace, D. W. R., Tilbrook, B., Millero, F. J., Peng, T. H., Kozyr, A., Ono, T. and Rios, A. F. (2004) The oceanic sink for anthropogenic CO₂. *Science*, **305**, 367-371.
- Sameoto, J. A. and Metaxas, A. (2008) Interactive effects of haloclines and food patches on the vertical distribution of 3 species of temperate invertebrate larvae. *Journal of Experimental Marine Biology and Ecology*, **367**, 131-141.
- Schindelin, J., Arganda-Carreras, I., Frise, E., Kaynig, V., Longair, M., Pietzsch, T., Preibisch, S., Rueden, C., Saalfeld, S., Schmid, B., Tinevez, J.-Y., White, D. J., Hartenstein, V., Eliceiri, K., Tomancak, P. and Cardona, A. (2012) Fiji: an open-source platform for biological-image analysis. *Nature Methods*, **9**, 676-682.
- Schiopu, D., George, S. B. and Castell, J. (2006) Ingestion rates and dietary lipids affect growth and fatty acid composition of *Dendraster excentricus* larvae. *Journal of Experimental Marine Biology and Ecology*, **328**, 47-75.
- Shanks, A. L. (2009) Pelagic larval duration and dispersal distance revisited. *Biological Bulletin*, **216**, 373-385.

- Sheng, J., Malkiel, E., Katz, J., Adolf, J., Belas, R. and Place, A. R. (2007) Digital holographic microscopy reveals prey-induced changes in swimming behavior of predatory dinoflagellates. *Proceedings of the National Academy of Sciences, USA*, **104**, 17512-17517.
- Sköld, M., Loo, L. O. and Rosenberg, R. (1994) Production, dynamics and demography of an *Amphiura filiformis* population. *Marine Ecology Progress Series*, **103**, 81-81.
- Sleigh, M. A. and Blake, J. R. (1977) Methods of ciliary propulsion and their size limitations. In: P. T.J. (ed) *Scale effects in animal locomotion*. Academic Press, London, pp. p 243-256.
- Sprung, M. (1984) Physiological energetics of mussel larvae (*Mytilus edulis*). *Marine Ecology Progress Series*, **18**, 171-178.
- Strathmann, M. F. (1987) *Reproduction and development of marine invertebrates of the northern Pacific coast: data and methods for the study of eggs, embryos, and larvae*. University of Washington Press, Seattle.
- Strathmann, R. R. (1971) The feeding behavior of planktotrophic echinoderm larvae: Mechanisms, regulation, and rates of suspensionfeeding. *Journal of Experimental Marine Biology and Ecology*, **6**, 109-160.
- Strathmann, R. R. (1975) Larval Feeding in Echinoderms. *American Zoologist*, **15**, 717-730.
- Strathmann, R. R. and Grünbaum, D. (2006) Good eaters, poor swimmers: compromises in larval form. *Integrative and Comparative Biology*, **46**, 312-322.
- Stumpp, M., Dupont, S., Thorndyke, M. and Melzner, F. (2011a) CO₂ induced acidification impacts sea urchin larval development II: Gene expression patterns in pluteus larvae. *Comparative Biochemistry and Physiology, Part A: Molecular & Integrative Physiology*, **160**, 320-330.
- Stumpp, M., Wren, J., Melzner, F., Thorndyke, M. and Dupont, S. (2011b) CO₂ induced seawater acidification impacts sea urchin larval development I: Elevated metabolic rates decrease scope for growth and induce developmental delay. *Comparative Biochemistry and Physiology, Part A: Molecular & Integrative Physiology*, **160**, 331-340.
- Sung, N. S., Gordon, J. I., Rose, G. D., Getzoff, E. D., Kron, S. J., Mumford, D., Onuchic, J. N., Scherer, N. F., Summers, D. L. and Kopell, N. J. (2003) Educating Future Scientists. *Science*, **301**, 1485.
- Tang, K. W. and Taal, M. (2005) Trophic modification of food quality by heterotrophic protists: species-specific effects on copepod egg production and egg hatching. *Journal of Experimental Marine Biology and Ecology*, **318**, 85-98.
- Underwood, A. J. and Fairweather, P. G. (1989) Supply-side ecology and benthic marine assemblages. *Trends in Ecology & Evolution*, **4**, 16-20.
- Vasseur, E. and Carlsen, I. (1949) *Sexual maturity on the sea-urchin *Brissopsis lyrifera* (Forbes) in the Gullmar fjord*. Vol. 41A, Stockholm Almqvist & Wiksell Berlin "Natura".

- Vaughn, D. (2009) Predator-induced larval cloning in the sand dollar *Dendraster excentricus*: Might Mothers Matter? *Biological Bulletin*, **217**, 103-114.
- Vaughn, D. (2010) Why run and hide when you can divide? Evidence for larval cloning and reduced larval size as an adaptive inducible defense. *Marine Biology*, **157**, 1301-1312.
- Vaughn, D. and Strathmann, R. R. (2008) Predators induce cloning in echinoderm larvae. *Science*, **319**, 1503.
- Vickery, M. S. and McClintock, J. B. (2000) Effects of food concentration and availability on the incidence of cloning in planktotrophic larvae of the sea star *Pisaster ochraceus*. *Biological Bulletin*, **199**, 298-304.
- Visser, A. W. (2007) Motility of zooplankton: fitness, foraging and predation. *Journal of Plankton Research*, **29**, 447-461.
- Widdicombe, S. and Spicer, J. I. (2008) Predicting the impact of ocean acidification on benthic biodiversity: What can animal physiology tell us? *Journal of Experimental Marine Biology and Ecology*, **366**, 187-197.
- Wood, H. L., Spicer, J. I. and Widdicombe, S. (2008) Ocean acidification may increase calcification rates, but at a cost. *Proceedings of the Royal Society of London, Series B: Biological Sciences*, **275**, 1767-1773.
- Woodson, C. and McManus, M. (2007) Foraging behavior can influence dispersal of marine organisms. *Limnology and Oceanography*, 2701-2709.
- Wootton, J. T., Pfister, C. A. and Forester, J. D. (2008) Dynamic patterns and ecological impacts of declining ocean pH in a high-resolution multi-year dataset. *Proceedings of the National Academy of Sciences, USA*, **105**, 18848-18853.
- Young, C. M. (1990) Larval Ecology of Marine-Invertebrates - a Sesquicentennial History. *Ophelia*, **32**, 1-48.
- Young, C. M. (1995) Behavior and locomotion during the dispersal phase of larval life. In: L. McEdward (ed) *Ecology of marine invertebrate larvae*. CRC Press, Boca Raton, Florida, pp. 249-277.
- Yu, P. C., Matson, P. G., Martz, T. R. and Hofmann, G. E. (2011) The ocean acidification seascape and its relationship to the performance of calcifying marine invertebrates: Laboratory experiments on the development of urchin larvae framed by environmentally-relevant pCO₂/pH. *Journal of Experimental Marine Biology and Ecology*, **400**, 288-295.
- Zar, J. H. (1996) *Bioestatistical analysis*. Vol., Prentice Hall International (UK) Limited, London.

VITA

Kit Yu Karen Chan (Karen Chan) was born in Hong Kong, SAR. Being born in the Year of the Ox and having Taurus as her horoscope, there is no way Karen could have escaped being determined and stubborn.

In the Precious Blood Kindergarten, located 2 blocks from a famous local bakery, Karen learned fresh baked breads are the best. To date, she still puts this important life lesson into practice and spends a lot of her free time in the kitchen baking. Karen's parents cultivated her love of nature through weekend family hikes. However, being a talkative child, her family was expecting a lawyer or a journalist but not a naturalist. Karen then went onto Sacred Heart Canossian School followed by its sister school, Sacred Heart Canossian College. In high school, Karen fell in love with the subject of biology but realized that she was terrified by human anatomy. With the hope that someday she could work with dolphins, she was drawn to conservation biology and ran the school's conservancy club. High school was bliss for Karen with active participation in debate teams, running the school library, and serving as a secretary for the Hong Kong Outstanding Students' Association.

Karen was early admitted to the University of Hong Kong, and shocked many around her by rejecting their law school offer and opted to study Environmental Life Science. There, she found her first mentor Dr. Benny Chan, who gave her a summer internship to work at Swire Institute of Marine Science and taught her larval rearing. Karen's love for larval biology grew after spending the next summer in ichthyoplankton survey for Dr. Cynthia Yau. As an intern for the World Conservation Society, Karen realized her childhood dream of working with dolphins and took part in the Irrawady Dolphin survey in Cambodia. Sadly, she realized counting charismatic megafauna was not her passion and that she would much prefer hugging a microscope. Funded by the CV Starr Scholarship, Karen spent her senior year aboard at University of California, Davis. Under the advice of Dr. Tessa Hill, Karen ventured into the world of paleoceanography. Using stable isotope signatures of

foraminifera tests, Karen studied the trigger for the Storegga Submarine landslide in her senior thesis. Karen got her Bachelor of Science with first class honors and BSc Class Prize in 2006.

Funded by the Sir Edward Youde Memorial Fellowship from Hong Kong, Karen moved to Seattle after graduating from college for a doctoral degree in Oceanography. At the University of Washington, Karen completed her doctoral dissertation on larval ecology under ocean change conditions under the supervision of Dr. Daniel Grünbaum in 2012.

Karen currently resides in Falmouth, MA, working as a postdoctoral scholar at the Woods Hole Oceanographic Institution.